

European School of Molecular
Medicine (SEMM)

Naples site



Università degli Studi di Napoli “Federico II”

PhD in Molecular Medicine –VI/XXIV cycle

Human Genetics



Unravelling aldolase C moonlighting functions:
a multi-task approach

PhD candidate: Simona Langellotti

Tutor: Prof. Francesco Salvatore

Internal Supervisor: Prof. Stefania Orrù

External Supervisor: Prof. Francisco Ernesto Baralle

Academic Year 2011/2012

TABLE OF CONTENTS

LIST OF ABBREVIATIONS	3
FIGURE INDEX	4
TABLES INDEX	5
ABSTRACT	6
SPECIFIC AIMS	9
Chapter 1	10
INTRODUCTION	10
1.1 The aldolase system.....	10
1.2 Aldolase Isozymes.....	11
1.3 Protein structure.....	15
1.4 The aldolase C isozyme.....	17
1.5 Aldolase C gene expression during development.....	19
1.6 Aldolase “moonlighting” functions and involvement of aldolase C in the physiology of the CNS.....	20
1.7 Aldolase C and the NF-L mRNA: a possible involvement in neurodegeneration.....	24
1.8 Proteomics and the functional proteomic approach.....	27
1.9 Monoclonal antibodies: features and production.....	30
Chapter 2	34
MATERIALS AND METHODS	34
2.1 Standard solutions.....	34
2.2 Enzymes.....	34
2.3 Synthetic oligonucleotides.....	35
2.4 Radioactive isotope.....	35
2.5 Bacterial culture.....	35
2.6 Cell culture.....	35
2.7 DNA preparation.....	36
2.7.1 Small scale preparation of plasmid DNA from bacterial cultures.....	36
2.7.2 Large scale preparations of plasmid DNA from bacterial cultures.....	37
2.8 RNA extraction from cultured cells.....	38
2.9 Estimation of nucleic acid concentration.....	38
2.10 cDNA synthesis.....	39
2.11 PCR amplification of selected DNA fragments.....	39
2.12 Enzymatic modification of DNA.....	44
2.12.1 Restriction enzymes.....	44
2.12.2 T4 DNA ligase.....	44
2.13 Agarose gel electrophoresis of DNA.....	45
2.14 Elution and purification of DNA fragments from agarose gels.....	45
2.15 Preparation of bacterial competent cells.....	46
2.16 Transformation of bacteria.....	46
2.17 Cell culture transfections.....	47
2.18 Anti-FLAG immunoprecipitation (IP) and protein(s) co-immunoprecipitation (co-IP).....	47
2.19 SDS-PAGE and In situ hydrolysis of proteins.....	48
2.20 Protein identification by mass spectrometry and bioinformatics.....	49
2.21 Protein extraction from cells or tissues.....	50
2.22 Western blotting (immunoblotting).....	51
2.23 <i>In vitro</i> transcription.....	52
2.24 Protein-RNA co-immunoprecipitation assay.....	54
2.25 Real Time PCR.....	55
2.26 Expression and purification of fusion proteins.....	56

2.27	RNA EMSA.....	57
2.28	UV cross-linking experiments.....	58
2.29	Elisa assay of biotinylated peptides.....	59
2.30	Aldolase C immunoprecipitation using the 9F mAb.....	61
	Chapter 3.....	62
	RESULTS AND DISCUSSION.....	62
	PART A.....	62
	<i>A functional proteomics approach to identify novel molecular interactors of the aldolase C protein: from a new binding partner of aldolase C to the study of its putative RNA-binding ability.</i>	62
3A.1	Immunoprecipitation of 3xFLAG-tagged aldolase C protein in Neuro2a cells.....	62
3A.2	Mass spectrometry identification of aldolase C interacting proteins.....	66
3A.3	Validation of the interaction between aldolase C and the 14-3-3 γ protein by Western Blotting.....	72
3A.4	The NF-L mRNA: a possible functional link between aldolase C and the 14-3-3 γ protein.....	73
3A.4.1	The NF-L RNA co-immunoprecipitates with aldolase C.....	75
3A.4.2	EMSA and supershift tests confirm the presence of aldolase C within an NF-L mRNA-binding complex but demonstrate that no direct binding occurs between aldolase C and this RNA target.....	77
3A.4.3	The protein-RNA UV cross-linking assay confirm the absence of direct binding between aldolase C and the NF-L mRNA.....	82
3A.5	Evaluation of aldolase C expression response after NGF administration in the PC12 cell line.	84
	PART B.....	88
	<i>Antigenic characterization of monoclonal anti-human aldolase C antibodies.</i>	88
3B.1	Monoclonal antibodies preparation.	89
3B.2	Isozyme specificity of the 9F and 2A mAbs.	89
3B.3	Identification of the aldolase C protein “macrodomain” including the specific antigen recognized by the 9F and 2A mAbs.	91
3B.4	Aldolase A vs aldolase C: sequence alignment of residues 1-100.	95
3B.5	“ElliPro” analysis of the tertiary structure of the human aldolase C protein.	96
3B.6	ELISA screening of biotinylated aldolase C peptides.....	102
3B.7	Epitope mapping in eukaryotic cells confirms specificity of the 9F and 2A mAbs for peptide 85-102.....	105
3B.8	Evaluation of the anti-aldolase C 9F mAb efficiency in the immunoprecipitation application.....	107
3B.9	Epitope mapping of 9F and 2A mAbs: discussion and conclusions.....	108
	Chapter 4.....	112
	CONCLUSIONS.....	112
	BIBLIOGRAPHY.....	117

LIST OF ABBREVIATIONS

aa	amino acid
bp	base pairs
cDNA	complementary DNA
CNS	central nervous system
co-IP	co-immunoprecipitation
ddH ₂ O	double-distilled water
DMSO	dimethylsulfoxide
dNTP	deoxyribonucleoside triphosphate (A, C, G and T)
DTT	dithiothreitol
ECL	enhanced chemiluminescence
EDTA	ethylenediaminetetraacetic acid
EMSA	electrophoretic mobility shift assay
ESI	electrospray ionization
FBS	fetal bovine serum
h	hour
HPLC	high performance liquid chromatography
IP	immunoprecipitation (IP stands also for immunoprecipitated)
IPTG	Isopropyl β -D-1-thiogalactopyranoside
kDa	Kilodalton
LC	liquid chromatography
mAb	monoclonal antibody
min	minute
MS	mass spectrometry
NCBI	National Center for Biotechnology Information
NGF	nerve growth factor
nt	nucleotides
OD ₆₀₀	optical density measured at a wavelength of 600 nm
ORF	open reading frame
pAb	polyclonal antibody
PAGE	polyacrylamide gel electrophoresis
PBS	phosphate buffered saline
PMSF	phenylmethylsulfonyl fluoride
rNTP	ribonucleoside triphosphate (A, C, G and U)
rpm	revolutions per minute
RT	room temperature
SDS	sodium dodecyl sulphate
sec	second
TBE	tris-borate-EDTA (buffer)
UV	ultraviolet
UTR	untranslated region
WB	western blotting (or immunoblotting)

FIGURE INDEX

Fig. 1.1	<i>The enzymatic reaction catalyzed by fructose 1,6-bisphosphate aldolase</i>	10
Fig. 1.2	<i>Sequence alignment between human aldolase isozymes</i>	12
Fig. 1.3	<i>TIM barrel fold</i>	15
Fig. 1.4	<i>The structure of aldolase C monomer</i>	19
Fig. 1.5	<i>Schematization of the method used to produce monoclonal antibodies</i>	33
Fig. 2.1	<i>Schematization of the Electrophoretic Mobility Shift Assay (EMSA) method</i>	58
Fig. 3.1	<i>Workflow of the functional proteomic strategy used in this study</i>	63
Fig. 3.2	<i>Immunoblot analysis of anti-FLAG immunoprecipitation</i>	64
Fig. 3.3	<i>Aldolase tetramers in the CNS</i>	65
Fig. 3.4	<i>Preparative anti-FLAG immunoprecipitation for mass spectrometry analysis</i>	67
Fig. 3.5	<i>Selection of specific bait-interactors</i>	67
Fig. 3.6	<i>Co-immunoprecipitation of the 14-3-3 γ protein with 3xFLAG-aldoc</i> ..	72
Fig. 3.7	<i>Detail of the sequence alignment between mouse and human NF-L mRNA transcripts, showing the sequence of the in vitro-transcribed NF-L fragment (-75; +91 from TGA)</i>	74
Fig. 3.8	<i>Aldolase C-NF-L RNA co-immunoprecipitation</i>	76
Fig. 3.9	<i>EMSA and supershift assay with the ³²P-labeled NF-L RNA probe</i> ...	78
Fig. 3.10	<i>EMSA with the ³²P-labeled NF-L RNA probe and recombinant GST-aldolase C and GST-TDP43 proteins</i>	80
Fig. 3.11	<i>EMSA with (UG)₆ repeats RNA probe and recombinant GST-aldolase C and GST-TDP43 proteins</i>	81
Fig. 3.12	<i>UV-crosslinking using the ³²P-labeled NF-L mRNA fragment and recombinant GST-aldolase C and GST-TDP43 proteins</i>	83
Fig. 3.13	<i>NGF promotes the formation of neurite-like processes in PC12 cells</i>	86
Fig. 3.14	<i>NGF increases the levels of aldolase C in PC12 cells</i>	86
Fig. 3.15	<i>Western blot with the anti-aldolase C 9F and 2A mAbs on mouse tissue extracts</i>	90
Fig. 3.16	<i>Scheme of the three partially overlapping domains of the human aldolase C protein cloned in the 3xFLAG CMV 7.1 vector</i>	91
Fig. 3.17	<i>Western blot analysis, using the 9F mAb, of total protein lysates from Neuro2a cells alternatively transfected with the 3xFLAG tagged full length (Full. L.), clone 1, clone 2 or clone 3 fusion products</i>	92
Fig. 3.18	<i>Scheme of the two additional sub-clones (clones 1A and 1B) produced in the 3xFLAG CMV 7.1 vector</i>	93
Fig. 3.19	<i>Western blot analysis, using the 9F mAb, of total protein lysates from Neuro2a cells alternatively transfected with the 3xFLAG tagged clone 1A and clone 1B fusion products or mock transfected</i>	93
Fig. 3.20	<i>Western blot analysis, using the 2A mAb, of total protein lysates from Neuro2a cells alternatively transfected with the 3xFLAG tagged full length, clone1, clone2, clone 3, clone 1A, clone 1B fusion products or mock transfected</i>	94
Fig. 3.21	<i>Sequence alignment between residues 1-100 of the human proteins aldolase A and aldolase C</i>	96
Fig. 3.22	<i>“ElliPro” analysis of the human aldolase C protein</i>	98
Fig. 3.23	<i>Selection of the 4 putative epitope-containing peptides of the human aldolase C protein</i>	100

Fig. 3.24	<i>Indirect-ELISA method used in this study.....</i>	<i>102</i>
Fig. 3.25	<i>ELISA screening of biotinylated aldolase C peptides.....</i>	<i>104</i>
Fig. 3.26	<i>Western blot analysis of aldolase C peptides expressed in fusion with a GFP tag at the N-term.....</i>	<i>106</i>
Fig. 3.27	<i>Aldolase C immunoprecipitation using the anti-aldolase C 9F mAb.....</i>	<i>107</i>
Fig. 3.28	<i>Sequence alignment between residues 85-100 of the three human aldolase isoforms; the corresponding Protrusion Index scores assigned by ElliPro to each aa of the human peptide are reported..</i>	<i>109</i>

TABLES INDEX

Table A	<i>Cloning of human aldolase C full length protein and fragments in the p3xFLAG CMV 7.1 vector.....</i>	<i>41</i>
Table B	<i>Cloning of human aldolase C peptides in the pEGFP-C2 expression vector.....</i>	<i>43</i>
Table C	<i>Primary antibodies.....</i>	<i>52</i>
Table D	<i>Primers used to amplify the NF-L mRNA fragment (-75; +91 from TGA) from mouse genomic cDNA.....</i>	<i>53</i>
Table E	<i>Real Time PCR primers.....</i>	<i>54</i>
Table F	<i>Biotinylated human aldolase C peptides.....</i>	<i>60</i>
Table G	<i>Identification of aldolase C interactors by LC-MS/MS.....</i>	<i>69</i>
Table H	<i>Human aldolase C peptides.....</i>	<i>101</i>

ABSTRACT

The aldolase C protein is the brain-specific isoform of the glycolytic enzyme fructose 1-6 biphosphate aldolase. It catalyzes the reversible cleavage of fructose-1,6-bisphosphate (Fru 1,6-P₂) to dihydroxyacetone phosphate (DHAP) and glyceraldehyde 3-phosphate (G3P).

Vertebrates express three tissue-specific isoforms of aldolase namely aldolase A, B and C. Aldolase A is ubiquitous and highly expressed in muscle tissues. Aldolase B is mainly expressed in the liver, where it is involved in the utilization of exogenous fructose. Aldolase C is selectively expressed in the central nervous system (CNS) but its physiological role is still unclear. Indeed, although aldolase C is undoubtedly involved in glycolysis within the brain and other tissues of neuronal origin, its glycolytic function is not believed sufficient to account for the selective expression of this isozyme in nervous tissues, for two main reasons:

- 1) In the CNS aldolase C is invariably expressed together with aldolase A, which could be explained as a redundancy function since aldolase A and C catalyze the same reaction in glycolysis.
- 2) Aldolase C is distributed in a peculiar stripe-like pattern in such areas of the human, mouse and rat brain, as the Purkinje cell layer of the cerebellum.

These observations prompted the hypothesis that aldolase C, beside its role in glycolysis, exerts other specific physiological functions (which may be called “moonlighting”) within the CNS.

To date, only a few observations have been reported about the possible association of the aldolase C protein with other functions. These include: an involvement in a sensory pattern of transmission and in cerebellar development; a protective function in Purkinje cells after cerebral trauma and AMPA-mediated excitotoxicity; and the ability to interact with and regulate the stability of the light neurofilament (NF-L) mRNA, whose proper expression is essential since alterations have been associated to neurodegeneration. Moreover, aldolase C is the only isozyme for which no gene variants have been found so far in animals or humans.

Hence, the physiological role of this enzyme isoform is basically unknown and multi-disciplinary studies are required to unravel this complex biological question.

The purpose of my PhD project was to gain insight into the physiology of the aldolase C protein in the CNS, to propose new hypotheses, to investigate further previously reported hypotheses, and to provide novel tools to be applied in research on aldolase C.

To this aim I carried out three main tasks, which were devoted to the:

- 1) Identification of novel aldolase C protein interactors using a functional proteomics approach.
- 2) Study of the putative RNA-binding ability of the aldolase C protein to the NF-L mRNA.
- 3) Antigenic characterization of two new, non-commercial anti-human aldolase C antibodies.

The results of each task are summarized below:

1) The functional proteomic approach led to the identification of the 14-3-3 γ protein as a novel molecular interactor of aldolase C; the 14-3-3 γ protein is involved in a broad spectrum of cellular functions. Although the functional role of this interaction is still unclear, our results might imply it in NF-L mRNA physiology, and preliminary data also suggest a potential involvement in the NGF-mediated differentiation process.

2) The interaction of aldolase C with the NF-L mRNA was proposed by Canete-Soler and colleagues based on their finding that aldolase C interacts with this transcript through direct binding. We verified the presence of the aldolase C protein in a multimeric complex that interacts with this target molecule, thereby confirming the hypothesis that aldolase C is involved in NF-L mRNA physiology. Importantly, however, our experiments also demonstrated that no direct interaction occurs between aldolase C and the NF-L mRNA, thus confuting the previous data concerning direct binding.

3) The complementary methodologies we used to characterize two novel, non-commercial anti-human aldolase C antibodies resulted in their successful epitope mapping: both antibodies were found to target an epitope localized within a short peptidic region of the aldolase C protein, spanning from residue 85 to residue 102. Moreover, we also demonstrated that these antibodies perform well in multiple applications including immunoblotting, ELISA and immunoprecipitation.

Consequently, we have obtained new, effective tools for routine experiments involving aldolase C and that can also be used to design novel approaches for the investigation of the still unclear physiological functions of this brain-specific isozyme.

SPECIFIC AIMS

As described within the “Abstract”, three main tasks were carried out in the present PhD study:

- 1) Identification of novel aldolase C protein interactors using a functional proteomics approach.
- 2) Study of the putative RNA-binding ability of the aldolase C protein to the NF-L mRNA.
- 3) Antigenic characterization of two new, non-commercial anti-human aldolase C antibodies.

The results of this project are reported and discussed in two parts:

Part A, in which points 1 and 2 are grouped in a single topic:

“A functional proteomics approach to identify novel molecular interactors of the aldolase C protein: from a new binding partner of aldolase C to the study of its putative RNA-binding ability” and

Part B, which contains the results concerning point 3:

“Antigenic characterization of monoclonal anti-human aldolase C antibodies”.

Chapter 1

INTRODUCTION

1.1 The aldolase system.

Fructose 1,6-bisphosphate aldolase is an ubiquitous glycolytic enzyme: it is technically known as D-glyceraldehyde-3-phosphate lyase (EC 4.1.2.13) and, often, it is simply referred to as aldolase. This enzyme plays a central role in the glycolytic pathway, catalyzing the reversible cleavage of fructose-1,6-bisphosphate (Fru 1,6-P₂) to dihydroxyacetone phosphate (DHAP) and glyceraldehyde 3-phosphate (G3P) (Fig. 1.1). Glucose phosphorylation and isomerization steps precede aldolase in the glycolytic pathway, thus converting glucose into Fru 1,6-P₂.

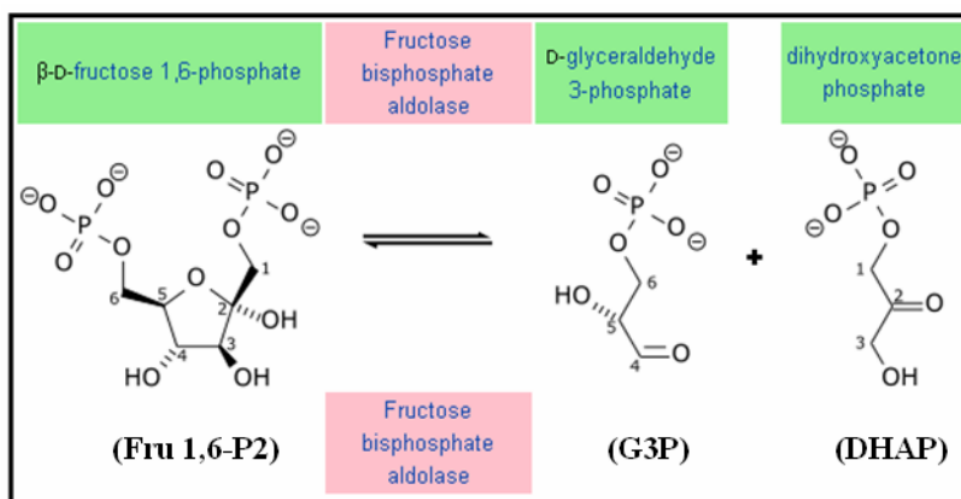


Fig. 1.1. The enzymatic reaction catalyzed by fructose 1,6-bisphosphate aldolase.

Two distinct classes of aldolase exist :

- Class I aldolases, which are present in animals, plants and green algae.
- Class II aldolases, which are present in most bacteria, yeast and fungi.

Aldolases belonging to these two distinct classes are characterized by different catalytic and molecular properties (Rutter, 1964). Particularly, members of class I aldolases use covalent catalysis through a Schiff-based intermediate (Choi et al.,

2006) whereas class II aldolases require a divalent metal cation (Zn^{2+}) in the active site (Rutter, 1960). Interestingly, although class I and class II aldolases differ in their reaction mechanisms and do not show clear sequence similarity, they share a similar quaternary structure, characterized by an alternating (α/β) 8 barrel fold, which will be presented in a following section.

Animal aldolases are all classified under the class I superfamily but it is important to point out that, whereas in invertebrates there are two types of aldolase, neuronal and non-neuronal, which originate from a single gene by alternative splicing, in vertebrates there are three tissue-specific isoforms of aldolase, namely aldolase A, aldolase B and aldolase C (Lebherz and Rutter, 1969), that are encoded by three different genes. The vertebrate isozymes are closely related, have identical molecular weights and subunit structures and catalyze the same overall reactions. However, each constitutes a unique protein species since these three forms are immunologically distinct (Penhoet and Rutter, 1971), have different peptide maps, have distinguishable catalytic activities and different gene sequences (Kukita et al., 1988; Rottmann et al., 1987).

1.2 Aldolase Isozymes.

Aldolases are highly abundant proteins that accounts for up to 7% of soluble protein within the cell (Maughan et al., 2005). Gene sequences for the aldolase isozymes are highly conserved, indicating that they play fundamental roles amongst all species. In mammals and birds, the aldolase genes are composed of nine exons and eight introns and encode for 39 kDa-proteins (Rottmann et al., 1987). The three different isoforms of aldolase expressed in vertebrates (aldolase A, B and C) are encoded by three different genes located, in humans, on chromosome 16 (aldolase A), chromosome 9 (aldolase B) and chromosome 17 (aldolase C) (Izzo et al., 1988; Rocchi et al., 1989; Tolan and Penhoet, 1986).

Phylogenetic studies indicate that they derived by divergent evolution from a common ancestral gene. The comparison of amino acid and nucleotide sequences have shown that aldolase A and C are more closely related to each other. Consequently, it has been proposed that aldolase B diverged from an A/C ancestor (the first duplication produced A and B, while a second more recent event produced C from A) (Kukita et al., 1988). Accordingly, there is a sequence identity of 66% between the human aldolase A and aldolase B proteins, a 71% identity between aldolase B and aldolase C proteins and a 81.4% identity between aldolase A and C proteins (Buono et al., 1990; Rottmann et al., 1987) (Fig. 1.2).

```

aldolaseA      MPYQYPALTPPEQKKEISDIAHRIVAPGKGILAADESTGSIAKRLQSIGTENTEENRRFYR 60
aldolaseC      MPHSPALSAEQKKEISDIALRIVAPGKGILAADESVGSMARRLSQIGVENTEENRRLYR 60
aldolaseB      MAHRFPALTQEQKKEISEIAQSIIVANGKILAADESVGTMGNRLQRIKVENTEENRRQFR 60
               *.: :***: *****:**  *** *****:*.:.:*. * .***** :*

aldolaseA      QLLLTADDRVNPICIGGVILFHETLYQKADDGRPFPQVIKSKGGVVGKIKVDRGVVPLAGTN 120
aldolaseC      QVLFSAADDRVKKCIIGGVIFFHETLYQKDDNGVPPVRTIQDKGIVVGIKVDKGVVPLAGTD 120
aldolaseB      EILFSDVSSINQSIIGGVILFHETLYQKDSQGLFRNILKEKGIVVGIKLDQGGAPLAGTN 120
               :*::.*. :. : *****:***** .:* * .:.* *****:*. * .*****:

aldolaseA      GETTTQGLDGLSERCAQYKKGADFAKWRCVLKIGEHTPSALAIMENANVLARYASICQQ 180
aldolaseC      GETTTQGLDGLSERCAQYKKGADFAKWRCVLKISERTPSALAILLENANVLARYASICQQ 180
aldolaseB      KETTTQGLDGLSERCAQYKKGVDVFGKWRVLRRIADQCPSSLAIQENANALARYASICQQ 180
               *** *****:*****. **.***.*.*.: : **:* ** *****:*****

aldolaseA      NGIVPIVEPEIILPDGDHDLKRCQYVTEKVLAAVYKALSDHHIYLEGTLKPNMVTTPGHAC 240
aldolaseC      NGIVPIVEPEIILPDGDHDLKRCQYVTEKVLAAVYKALSDHHVYLEGTLKPNMVTTPGHAC 240
aldolaseB      NGLVPIVEPEVIEPDGDHDLKRCQYVTEKVLAAVYKALNDHHVYLEGTLKPNMVTAGHAC 240
               **:*****: :*****: :*****:*****.***:*****:*****.****

aldolaseA      TQKFSHEEIAMATVTALRRTVPPAVTGITFLSGGQSEEEASINLNAINKCPLLKPWALTF 300
aldolaseC      PIKYTPPEEIAMATVTALRRTVPPAVPGVTFLSGGQSEEEASFNLMAINRCPLRPWALTF 300
aldolaseB      TKKYTPPEQVAMATVTALHRTVPPAVPGICFLSGGMSEEDATLNLNAINLCPLRPKWLFSF 300
               . *.: *.: *****:*****. **.*: ***** ***:*: ***** ** * :** *:*

aldolaseA      SYGRALQASALKAWGGKKNLKAQEEYVKRALANSIACQKGYTPSGQAGAAAESLFFVS 360
aldolaseC      SYGRALQASALNAWRGQRDNAGAATEEFIKRAEVNGLAAQGRYBGSSEDGGAQAQSLYIA 360
aldolaseB      SYGRALQASALAAMGGKAANKREATQEAFFMGRAMANCQAARKQYVHTGSSGAASTQSLFTA 360
               ***** ** * : * * : * :*** . * *.:* * :* . * .*:***:

aldolaseA      NHAY 364
aldolaseC      NHAY 364
aldolaseB      CYTY 364
               ::*

```

Fig. 1.2. Sequence alignment between human aldolase isozymes.

The alignment was performed using the “ClustalW2-Multiple Sequence Alignment” software (www.ebi.ac.uk/Tools/msa/clustalw2).

Vertebrates aldolases are expressed in a tissue-specific manner. Aldolase A is ubiquitous and highly expressed in muscle tissues (Lebherz and Rutter, 1969). Aldolase B is mainly expressed in the liver, where it is involved in the utilization of exogenous fructose; it is also expressed in kidney cortex and small intestine (Lebherz and Rutter, 1969). Aldolase C is selectively expressed in the central nervous system (CNS) and in tissues of neuronal origin (Penhoet and Rutter, 1975), where its physiological role is still unclear.

The three isozymes catalyze the same overall reactions, although with different kinetics: they are not only involved in glycolysis, but also in gluconeogenesis (catalyzing the reverse reaction of Fig. 1.1, the synthesis of Fru 1,6-P₂ from the two triose phosphates G3P and DHAP) and in fructose metabolism (catalyzing the cleavage of fructose 1-phosphate (Fru 1-P)).

Aldolase A is the most efficient isozyme for glycolysis (Fru 1,6-P₂ cleavage), aldolase B is the most efficient isozyme for both fructose metabolism (Fru 1-P cleavage) and gluconeogenesis (Fru 1,6-P₂ synthesis), whereas aldolase C has catalytic properties intermediate to those of aldolases A and B (Penhoet et al., 1969). Indeed, aldolase C performs the gluconeogenic reaction more efficiently than aldolase A and the glycolytic reaction slightly less efficiently than aldolase A. Notably, the kinetic differences demonstrated by aldolases A and C in the last process are not sufficiently distinct to explain why both isozymes are co-expressed in the brain.

The crucial role of aldolase A in physiology is demonstrated by human diseases that result from mutations in the aldolase A gene. Indeed, most of the mutations so far identified leave the enzyme activity relatively unchanged and therefore are considered mild. Some mutations have been shown to cause nonspherocytic haemolytic anemia (NSHA), a disorder of erythrocytes caused by deficiencies in glycolytic enzymes, the most common of which are in pyruvate

kinase. In NSHA, erythrocytes (which depend on glycolysis as their sole source of energy) are unable to maintain cellular osmolarity via the ATP-powered ion pumps and, consequently, undergo haemolysis. One other aspect of aldolase A-deficient NSHA is myopathy (Kreuder et al., 1996). The known mutations causing aldolase A deficiency are D128G (Beernink and Tolan, 1994; Kishi et al., 1987), E206K (Kreuder et al., 1996), R303X (Yao et al., 2004), C338Y (Yao et al., 2004) and G246S (Esposito et al., 2004). Carriers of the severe mutation R303 were found to be compound heterozygous also for the C338Y mutation. The other mutations were found in individuals who were homozygous for these alleles, except the G246S allele, which was found in compound heterozygosity with the E206K allele. All the mutations that cause NSHA appear to affect protein structure rather than activity (Kishi et al., 1987; Kreuder et al., 1996; Takasaki et al., 1990). For example, the first-described and well characterized human mutation D128G causes an amino acidic substitution in a region of intersubunit contact that destabilizes the oligomeric structure of the enzyme and results in a thermolabile enzyme that falls apart into dimers. Only a little loss in activity is detected for these aldolase A dimers, suggesting that the anemia is caused by the loss in stability rather than in activity (Beernink and Tolan, 1994).

Different mutations have been discovered also in the human aldolase B gene. They result in a reduced enzymatic activity and are associated to an autosomal recessive disease known as hereditary fructose intolerance (HFI). HFI leads to Fru 1-P accumulation, potentially resulting in growth retardation, renal tubular dysfunctions, liver failure, coma and also death if the disease remains undiagnosed and the patient continues to ingest fructose (Lameire et al., 1978; Morris, 1968; Odievre et al., 1978). The most common mutation causing HFI leads to a proline substitution for alanine at position 149 (A149P) of the aldolase B protein which results in a dimeric enzyme that is thermally very unstable (Malay et

al., 2005; Malay et al., 2002). Other common mutations causing HFI are A175D and N335K (Davit-Spraul et al., 2008); moreover, a lot of additional minor mutations in the aldolase B gene have been discovered in HFI patients (Coffee and Tolan, 2010; Esposito et al., 2010; Santer et al., 2005).

On the contrary, no gene variants have been found so far for the aldolase C isoform.

1.3 Protein structure.

At the structural level, aldolase exists as a hetero- or homo- tetramer, whose inter-subunit interactions are very stable, demonstrating one of the strongest known subunit-subunit associations (Tolan et al., 2003).

Vertebrate aldolase monomers have an identical molecular weight of 39 kDa and share a similar subunit structure, characteristic of the so called “TIM barrel” class of proteins, consisting of eight alternating α helices and parallel β strands (Fig. 1.3).

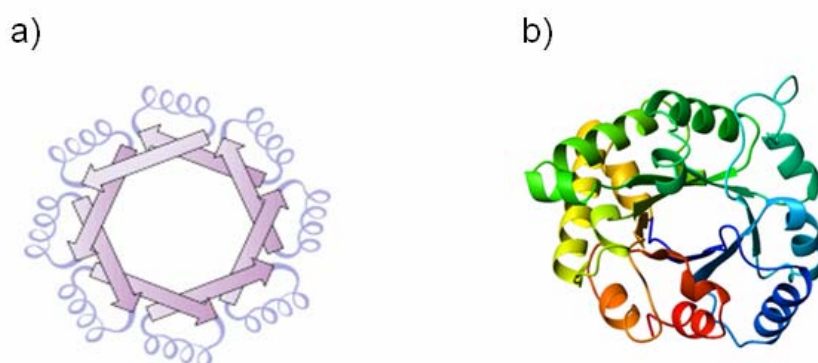


Fig. 1.3. TIM barrel fold.

a) schematization and b) tridimensional view of α -helices and β -strands in the TIM-barrel structure. α -helices are depicted as twisted ribbons; β -strands with broad arrows pointing in the direction of the C-terminal end of the chain.

The active site of each monomer is located at the centre of the α/β barrel (Pezza et al., 2003) and all three isozymes have nearly identical active sites (Arakaki et al., 2004). The highest conserved amino acidic residues in the three isozymes are around Lys 229 in the active site for glycolytic activity (Asp33, Glu34, Lys41, Arg42, Lys107, Lys146, Arg148, Glu187, Ser271, Arg303, Lys229, Gln306, Tyr363), whereas the greatest disparity amongst vertebrate aldolase isozymes typically lies in the carboxyl-terminal tail, where most of the isozyme-specific residues are located (Arakaki et al., 2004; Choi et al., 2001; St-Jean et al., 2007). Due to the preponderance of lysine and arginine residues, the active site has an essentially basic nature. Within the active site there is a hydrophobic pocket, generated by the side chains of Arg42, Arg303 and Gln306, that is often involved in the binding of acidic protein partners including the Wiskott-Aldrich Syndrome Protein (St-Jean et al., 2007) (see paragraph 1.6 for additional details).

The carboxyl terminal region of the protein (particularly the last 18-20 aa) is believed to be flexible, perhaps moving in and out of the active site. Consequently, the real structure for this protein region has not been determined since this portion is able to acquire a variety of conformations, escaping from many x-ray-based structures. Interestingly, the ablation of the C terminus has been found to produce an inactive enzyme (Rose et al., 1965) and it has been implicated in determining the isozyme-specific differences of aldolases, since mutations in this region diminish the kinetic distinctions among isozymes (Berthiaume et al., 1993; Motoki et al., 1993; Pezza et al., 2003). The C terminus of aldolase interact with the active site periphery close to Arg303 and the conserved terminal residue (Tyr363) is essential for proton exchange (at the level of enamine intermediate) in the aldolase catalytic mechanism (St-Jean et al., 2007).

Even though aldolase isozymes have evolved distinct kinetic properties, the structural features that confer the isozyme-specific differences are still unknown.

Aldolase monomers deriving from related as well as from divergent species form hybrid tetramers, indicating that the subunit interfaces are functionally conserved among species (Swain and Lebherz, 1986). Studies on aldolase mutants carrying substitutions in regions of inter-subunit interaction have demonstrated that thermal stability is one crucial role of the quaternary structure whereas the last is not essential for catalysis. Indeed, it has been demonstrated that the major mutations causing HFI (A149P) and NSHA (D128G) affect the quaternary structure of the mutant aldolases rather than their activity: the resulting enzymes are dimeric and not tetrameric and, although they are active at certain temperatures, they are unable to carry out the normal function due to the loss in stability (Beernink and Tolan, 1994; Malay et al., 2002; Swain and Lebherz, 1986).

1.4 The aldolase C isozyme.

The aldolase C protein isoform is expressed selectively within the brain and other tissues of neuronal origin. In the CNS, the aldolase C protein demonstrates a peculiar stripe-like pattern of expression in such areas of the mouse, rat and human brain, including the inferior cerebellar olives, the sensory neurons of the posterior horn of the spinal cord and the Purkinje cell layer of the cerebellum (Ahn et al., 1994; Buono et al., 2001; Hawkes and Herrup, 1995). This stripe-like expression was first demonstrated in mouse cerebellum by Ahn and colleagues, who also proved the aldolase C identity with the previously reported intracellular antigen zebrin II.

Among aldolase isozymes, the strip-like expression is a feature of the aldolase C protein (Buono et al., 2001). The reasons why the expression pattern of aldolase C is organized into alternating bands in such areas of the CNS is far to be clear. It was proposed that the basal metabolic rate of aldolase C-positive cells could be higher than in the negative ones. Accordingly, the expression of

cytochrome oxidase, a mitochondrial enzyme associated with increased rate of oxidative phosphorylation, overlaps the positive aldolase C-stripes expression in rat Purkinje cells (Hess and Voogd, 1986; Leclerc et al., 1990). However, the only glycolytic function is believed not sufficient to explain why aldolase C is expressed in such stripe-like manner nor why aldolase C is always expressed together with aldolase A, since the two isozymes exhibit comparable kinetic properties in glycolysis. For these reasons, it is strongly believed that aldolase C exerts other functions besides its role in glycolysis.

The aldolase C gene sequence is highly conserved in mammals (Buono et al., 1990; Kukita et al., 1988; Paoletta et al., 1986). The human aldolase C gene spans 5198 bp and is shorter than the aldolase A and B genes (Buono et al., 1990). Its coding region, constituted by 1092 bp, consists of eight exons and encodes for a 364 aa protein. DNA sequence alignments demonstrated that exons 4-7 in aldolase A and C are the most highly conserved whereas exons 3 and 9 show the least degree of similarity. Accordingly, most of the aldolase C isozyme-specific residues are located in the C-terminus of the protein.

The X-ray structure of human aldolase C (PDB accession code 1XFB) was published in 2004 (Fig. 1.4) (Arakaki et al., 2004), when the structures of human aldolases A (PDB accession code 1ALD) and B (PDB accession code 1QO5) were already known. Although the three isozymes demonstrate the same overall fold and active site structure, the solved aldolase C crystal structure revealed the existence of a patch of electronegative residues located near the C terminus of the brain-specific isozyme. This negative patch may contribute to determine its still unknown isozyme-specific function.

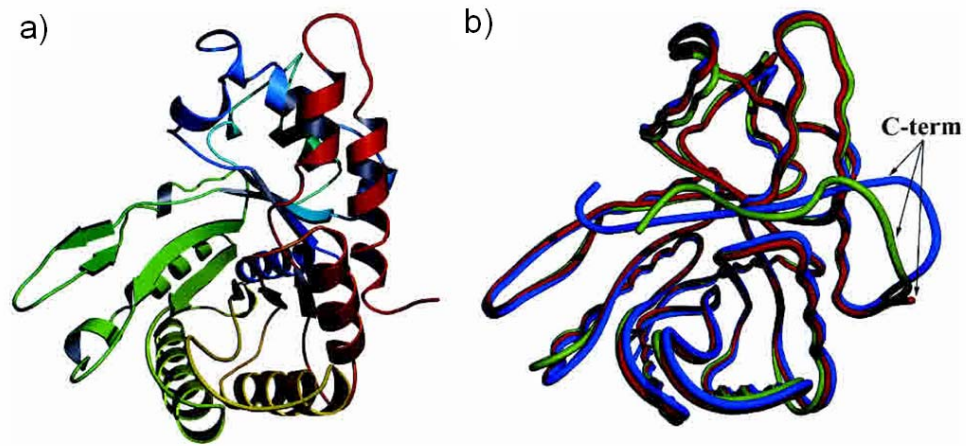


Fig. 1.4. *The structure of aldolase C monomer a) depicted as a ribbon diagram ramped from N terminus (blue) to C terminus (red) and b) depicted as a coil overlay (red) with the structures of human aldolase A (blue) and aldolase B (green).*

1.5 Aldolase C gene expression during development.

In mammalian embryonic tissues, aldolase A is the primary isozyme and in the developing brain it is co-expressed with aldolase C (Lebherz and Rutter, 1969).

In the CNS, aldolase C expression is regulated during development and differentiation. In mouse, aldolase C mRNA appears in all foetal tissues at the late embryonal stage (E17) but, after birth, its levels rapidly decrease in all tissues except for the brain where, instead, they increase till to reach maximum levels in adult (Ahn et al., 1994), particularly in cerebellum, hippocampus and medulla (Mukai et al., 1991; Popovici et al., 1990). It has been found that, during mouse and rat cerebellum development, the aldolase C protein appears at detectable levels from postnatal day 6, is expressed in all Purkinje cells from postnatal day 12 and subsequently, around post-natal day 20, it is suppressed in groups of Purkinje cells thereby resulting in the stripe-like expression (Hawkes and Herrup, 1995; Leclerc et al., 1988; Tano et al., 1992).

Additionally, the aldolase C protein expression follows an antero-posterior gradient, being absent from the motoneurons in the supraorbital cortex, expressed

in some neurons near Rolando's sulcus and in the neurons near the calcarine scissure in the occipital cortex and reaching maximum expression in the Purkinje cells of the cerebellum. This antero-posterior gradient of distribution of aldolase C, considered together with the peculiar stripe-like pattern demonstrated in such areas of the CNS, suggested the intriguing possibility that the different aldolase C expression may result in functional compartments related to a specific sensory transmission (Buono et al., 2001).

1.6 Aldolase “moonlighting” functions and involvement of aldolase C in the physiology of the CNS.

Although the aldolase C protein is undoubtedly involved in glycolysis in the tissues where it is expressed, its physiological role remains elusive.

Many enzymes, including glycolytic enzymes, have been found to “moonlight” (Faik et al., 1988; Lim et al., 2002; Lorenzatto et al., 2012; Watanabe et al., 1996; Xu et al., 1996): they serve additional functions that are generally not enzymatic but, rather, structural or regulatory (Copley, 2003). The multiple functions of moonlighting proteins add higher levels of complexity. The existence of moonlighting for enzymes may be suggested by unusual patterns of expression that are not fully explained by the enzymatic function of the protein in the tissues where it is expressed (Fernandez-Canon et al., 1999). For its tissue-specific and stripe-like distribution, the aldolase C protein demonstrates these features. Nevertheless, little is known about the possible association of aldolase C with functions different than glycolysis since only scattered hypotheses have been reported so far about. Moreover, understanding the isozyme-specific functions is also complicated since some moonlighting functions have been proposed for all of the three isozymes and not for specific aldolase isoforms. For example, several reports define aldolases as “molecular adaptors” that link their interacting partners

to the cytoskeleton since it has been demonstrated, for all three isozymes, an ability to bind the α -subunit of tubulin and actin filaments (Carr and Knull, 1993; Kusakabe et al., 1997; O'Reilly and Clarke, 1993). The functional role of these interactions is still unknown but it has been proposed that aldolase binding contributes to a more efficient supply of chemical energy during cytoskeleton modifications. An involvement of aldolase in modulating the motility and actin dynamics of mammalian cells was also proposed on the basis of its interaction with members of the Wiskott-Aldrich syndrome protein (WASP) family (Buscaglia et al., 2006; St-Jean et al., 2007). In fact, WASP proteins are critical regulators of actin dynamics that bind to actin monomers and that activate the Arp 2/3 complex to promote actin nucleation.

In addition to cytoskeletal proteins, aldolases have also been found to interact with other different partners, including the GLUT4 glucose transporter (Kao et al., 1999), the endocytosis proteins SXN9 and dyn2 (Lundmark and Carlsson, 2004), the vacuolar H⁺-ATPase (V-ATPase) proton pump (Lu et al., 2007; Lu et al., 2001; Lu et al., 2004), phospholipase D2 (Kim et al., 2002) but, in most cases, no data indicate so far if this binding ability is specifically restricted to one form of aldolase or if it is shared among the three isozymes. The functional role for this complex network of aldolase associations is still unclear. It might help in coupling the glycolytic pathway to ATP-hydrolyzing processes, as proposed for the vacuolar H⁺ pump (Lu et al., 2004). However, aldolase seems to be mainly targeted for structural rather than enzymatic purposes, in agreement with the general finding that the additional moonlighting functions of enzymes are not enzymatic (Copley, 2003). For instance, binding of the glucose transporter GLUT4 to aldolase is supposed to provide GLUT4 with an anchorage to F-actin, thus allowing its translocation from intracellular vesicles to the cell surface upon insulin stimulation (Kanzaki and Pessin, 2001; Kao et al., 1999). Moreover, concerning

the interaction of aldolase with SNX9 and dyn2, it was proposed that when these proteins are bound to aldolase in the cytosol, membrane localization of SNX9 is inhibited whereas, upon phosphorylation of SNX9 by an unknown kinase, SNX9/dyn2 are released from the aldolase complex and relocated to the plasma membrane to fulfill their function in endocytosis (Lundmark and Carlsson, 2004).

Interestingly, in addition to all these heterogeneous protein-protein interactions, it has also been reported an RNA-binding ability for aldolase. In particular, an interaction with the light neurofilament (NF-L) mRNA was specifically reported for aldolase A and C but not B proteins, thus introducing the hypothesis of an involvement of the two neuronal aldolases in neurodegeneration (Canete-Soler et al., 2005; Stefanizzi and Canete-Soler, 2007). This aspect will be presented in major details in a following section (paragraph 1.7), since the interaction of aldolase C with the NF-L mRNA was also investigated in this PhD project. However, the involvement of aldolase C in neurodegenerative disorders is further supported by the finding that a specific protein-protein interaction was observed between this enzyme and the human cellular prion protein (PrP^c) in mice brain extract (Strom et al., 2006).

For the aldolase C protein it was also proposed a neurodevelopmental role in the CNS, on the base of multiple findings:

- 1) The analogy between the banding (stripe-like) expression of aldolase C and the one observed for aldehyde dehydrogenase suggested the intriguing possibility that aldolase C, while being an housekeeping metabolic enzyme, could catalyze also the transformation of an unknown substrate with a developmental activity. Indeed, it was demonstrated that the metabolic enzyme aldehyde dehydrogenase, in addition to its main enzymatic activity, was also able to convert retinaldehyde into retinoic acid, a morphogen

whose gradient sets the antero-posterior axis of the developing limb bud (Eichele, 1989; Thaller and Eichele, 1990).

- 2) Following the discovery of a stripe-like distribution of aldolase C in different areas of the CNS, Buono and colleagues demonstrated that the aldolase C gene expression is enhanced by nerve-growth-factor-induced B factor (NGFI-B). Moreover, they also demonstrated that the aldolase C expression parallels that of NGFI-B during rat brain embryo development (Buono et al., 1997; Makeh et al., 1994).
- 3) Based on the observed heterogeneous expression of aldolase C within different cell populations of the neonatal rat forebrain, it was proposed that cells expressing aldolase C at different levels might contribute to drive migration and maturation of surrounding specific cell types (i.e. astrocytes progenitors) during cerebellar development. Indeed, it is believed that a non-random distribution of different cell types, characterized by specific gene expression profiles, might support the formation of microenvironments that stimulate the production of cells with specific potentials at appropriate developmental stages (Staugaitis et al., 2001).

Recently, it was demonstrated that the cerebellum is more vulnerable to global ischemic damage in zones of the Purkinje cell layer lacking aldolase C. Moreover, aldolase C-negative Purkinje cells were found to be more likely to die than the aldolase C-expressing ones after cerebral trauma *in vivo* and following AMPA (Alpha-Amino-3-Hydroxy-5-Methyl-4-Isloxazole Propionic Acid)-mediated excitotoxicity *in vitro* (Slemmer et al., 2007). Therefore, it was proposed that aldolase C might play a protective role to Purkinje cells.

1.7 Aldolase C and the NF-L mRNA: a possible involvement in neurodegeneration.

The light neurofilament (NF-L) mRNA-binding ability was recently reported as a novel activity of aldolase C. It was first described in 2005 by Canete-Soler and colleagues who also proposed, two years later, a possible model to explain its involvement in regulating the expression of NF-L mRNA (Canete-Soler et al., 2005; Stefanizzi and Canete-Soler, 2007). According to the above mentioned studies, both neuronal aldolases A and C, although not possessing classical RNA-binding motifs (Burd and Dreyfuss, 1994), interact specifically with the NF-L mRNA and are components of a neuronal surveillance complex that controls the proper regulation of the transcript stability. It was demonstrated that aldolases A and C, but not B, interact with a 68-nt segment of the NF-L mRNA spanning the translation termination signal. This sequence includes 23 nt of the distal coding region plus 45 nt of the 3'-UTR and was previously shown to be essential for NF-L mRNA stabilization in neuronal cells (Canete-Soler et al., 1998). Interestingly, it was reported that co-expression of NF-L mRNA and aldolase C leads to an increased rate of degradation of the NF-L transcript whereas the degradation was inhibited when both aldolases were co-expressed with a mutant NF-L mRNA lacking the sequence for aldolase binding (Canete-Soler et al., 2005). Subsequently, it was also demonstrated that aldolase C and poly(A)-binding protein (PABP) undergo competitive interactions in cells co-expressing aldolase C and NF-L mRNA suggesting that PABP stabilizes the transcript by shielding it from aldolase attack (Stefanizzi and Canete-Soler, 2007). These findings led to propose that the neuronal aldolase isozymes are ribonucleolytic components of a neuronal surveillance complex that ensure the quality and efficiency of neurofilament expression. These observations might have important consequences for understanding causal mechanism underlying neurodegeneration since it is well

known that the fine regulation of NF-L mRNA stability and expression is essential in maintaining neuronal homeostasis. Indeed, in this context, it is important to remind that neurofilaments (NFs) are major cytoskeletal components of large neurons and are instrumental in maintaining the differentiated state of neurons since they are responsible of axonal growth. NFs are heteropolymers constituted by three different subunits classified, according to their molecular weight, in low molecular weight NF (NF-L, 68 kDa), middle molecular weight NF (NF-M, 160 kDa) and high molecular weight NF (NF-H, 200 kDa). Interestingly, NFs assembly is orchestrated by the NF-L subunit and alterations in NF subunits stoichiometry are often associated to neurodegeneration. Accordingly, a growing body of evidence indicates nowadays that the fine regulation of NF-L subunit expression plays a dominant role in neuronal physiology since its alterations often result in aberrant neurofilament assembly and in the formation of intraneuronal aggregates characteristic of neurodegenerative disorders such as ALS (Amyotrophic Lateral Sclerosis) (Strong et al., 2005). For instance, it has been demonstrated that overexpression of a wild type (wt) NF-L transgene causes motor neuron degeneration (Xu et al., 1993) and that NF-L mRNA levels are selectively reduced in degenerating spinal motor neurons (Bergeron et al., 1994). Moreover, it has also been reported that a severe form of motor neuron degeneration is determined by a mutation within the above-mentioned 68-nt segment, spanning the translation termination signal, of the NF-L mRNA (Canete-Soler et al., 1999).

Since it was found that aldolase C increases the decay rates on NF-L mRNA whereas the PABP stabilizes the molecule by shielding the transcript from aldolase C attack, it was proposed that the modulation of NF-L mRNA stability is affected, at least, by a competing interaction between aldolase C and PABP (Canete-Soler et al., 2005; Stefanizzi and Canete-Soler, 2007). However, since additional proteins were found to bind and modulate the stability of the NF-L

mRNA, a more complex cross-talk between multiple proteins could be actually responsible of the proper regulation of the NF-L mRNA stability. These include mutant SOD1 (Ge et al., 2005), 14-3-3 proteins (Ge et al., 2007), TDP43 (Strong et al., 2007; Volkening et al., 2009) and Rho guanine nucleotide exchange factor (Droppelmann et al., 2013). The 14-3-3 protein family and TDP43 are briefly introduced here, as they were considered with special regard in the present study.

14-3-3 proteins are ubiquitous protein abundant in brain. They are adapter proteins (generally but not exclusively interacting with sites of phosphorylated proteins) involved in a broad spectrum of cellular processes such as apoptosis, cell cycle, proliferation, functioning of ion channels and organization of cytoskeleton (Obsilova et al., 2008; Sluchanko and Gusev, 2010). 14-3-3 proteins are also strongly involved in mediating the NGF-induced neuronal differentiation (Greene and Angelastro, 2005; MacNicol et al., 2000). Recent data indicate that they may play an important role also in neurodegenerative diseases: in fact, 14-3-3 proteins mislocalize in ALS motor neurons in the form of protein aggregates (Kawamoto et al., 2004) and 14-3-3 mRNAs are upregulated in amyotrophic lateral sclerosis spinal cord (Malaspina et al., 2000). In addition, 14-3-3 protein isoforms β , ζ , τ , γ , η were found to interact with the 3' untranslated region (UTR) of the NF-L mRNA and influence its stability since mutations in the 14-3-3 binding motifs result in a stabilized transcript (Ge et al., 2007).

On the contrary, TDP43 was found to bind and act in stabilizing the human NF-L mRNA (Strong et al., 2007). TDP43 is both a DNA and an RNA-binding protein, involved in many crucial cellular processes including transcription and splicing. TDP43 preferentially binds UG repeats but it has also been found to interact with non-UG repeat sequences. Indeed, TDP43 targets a sequence localized within the 3' UTR of the human NF-L mRNA that does not contains (UG) repeats. In normal conditions, TDP43 is almost exclusively nuclear but it was

found to mislocalize into the cytosol in ALS motor neurons, where it is incorporated in ubiquitinated aggregates (Arai et al., 2006; Neumann et al., 2006). As a consequence of its altered cellular localization, it has been proposed that TDP43 contributes to the formation of pathological NF aggregates in ALS, since it is no longer able to stabilize the transcript.

No data are presently available regarding the possibility of an altered aldolase C expression and/or aggregation in ALS motor neurons, but the identification of neuronal aldolases as components of an NF-L mRNA regulatory complex has suggested their possible involvement in the complex pathogenesis of neurodegeneration, through a complex cross-talk with other NF-L mRNA-binding partners.

1.8 Proteomics and the functional proteomic approach.

Most of the current interest of modern biological science is directed toward understanding the function of living cells at the molecular level. For about two decades major efforts were directed at the genome but it became soon clear the necessity to complement the genomic research with the study of all expressed proteins, to achieve a deeper understanding of cellular functions.

The term “proteome” was coined to describe the whole set of proteins encoded by the genome. The study of the proteome is called “proteomics” and comprises nowadays almost everything “post-genomic”, being involved not merely in the description of the set of proteins expressed in any given cell, but in almost all aspects of protein physiology and pathology, i.e. the study of protein isoforms or protein modifications, the investigation of functional interactions occurring between them, the spatial localization of proteins and the elucidation of their involvement in specific pathways *in vivo*. It is not easy to achieve these goals as the dynamic properties of the proteome increase the difficulties of proteomic

research. Proteomics would not be possible without the previous achievements of genomics nor without the tremendous technical progress that allowed the development of powerful scientific tools such as mass spectrometry. Indeed, the ability of mass spectrometry to identify even smaller amounts of protein from increasingly complex mixtures is a primary driving force in proteomic strategies. Of course, it is not enough to identify the proteins expressed in cells, but it is also necessary to understand their functional roles in a specific context since the functional role of a given protein can be strongly dependent on the type of cell in which it is expressed and on the state of that cell. Current proteomic investigations are essentially focused on two major areas: expression proteomics, which aims to measure the up-regulation and down-regulation of protein levels (Marouga et al., 2005), and functional proteomics which aims to characterise protein activities, multiprotein complexes and signalling pathways (Monti et al., 2005). Below, the functional proteomic approach is briefly described in more details, since it was applied in this study in the attempt to shed light on putative moonlighting functions of the aldolase C protein.

Functional proteomics combines classical techniques in protein chemistry to advanced methods of mass spectrometry, aiming to identify the species that participate in molecular networks involving a protein of interest. Understanding protein functions is often made possible by the identification of the interacting proteins: the association of a protein of interest with partners belonging to a complex involved in a specific cellular mechanism would be strongly suggestive of its biological function (Gavin et al., 2002; Ho et al., 2002). The identification of interacting proteins essentially relies on affinity based procedures to fish the specific partners of a protein-bait of interest out of a cellular extract. The isolation of such multi-protein complexes can be accomplished using different possible strategies but, in all cases, the bait is affinity retained on an inert resin that has

been properly derivatized to specifically bind the bait-molecule of interest. The experiment is performed in controlled native conditions, so that the interaction between the bait and its molecular interactors are not disrupted. Subsequently the proteins are eluted from the resin and fractionated by SDS-PAGE. Then, the protein bands are *in situ* enzymatically digested and the resulting peptide mixtures are analysed by mass spectrometry techniques.

The specific strategy used in this work to isolate multi-protein complexes containing aldolase C was based on an immunoprecipitation method; as described in the material and methods section, we took advantage of the availability of a commercial system for the expression and purification of proteins expressed in fusion with the peptidic tag 3xFLAG. Such affinity tag systems generally provide a broad applicability with a large number of proteins without affecting the tertiary structure and the biological activity of the bait. They are usually preferred when it is not available a good antibody to the bait and/or when its use is not desired because it might compete with the interacting proteins for binding to the same bait epitope. The overall experimental strategy applied in this work is summarized in Fig. 3.1

1.9 Monoclonal antibodies: features and production.

A significant part of my thesis work concerned the antigenic characterization of anti-human aldolase C monoclonal antibodies. A clear and effective presentation of the experiments performed in this context requires at least a short introduction about antibodies features and the related specific terminology.

Antibodies are molecules produced by the immune system of vertebrates. They specifically recognize, bind and act to neutralize foreign molecules, called antigens, being therefore essential for the prevention and resolution of infection by invaders, such as viruses. Nowadays, antibodies are extensively produced and commercialized to be used in almost every area of molecular investigation. Concerning the scientific terminology related to antibodies features and production, it is essential to introduce some definitions. First, it is important to distinguish the concept of antigen from that of immunogen. Indeed, an antigen is any molecule that is identified as non-self by the immune system whereas an immunogen is an antigen that is also able to evoke an immune response, including production of antibody. Consequently all immunogens are antigens, but not all antigens are immunogens. There are three characteristics that a substance must have to be immunogenic: 1) foreignness, otherwise the molecule is ignored by the animal; 2) high molecular weight, because small molecules (M.W. less than 1000 Da) as well as many molecules of moderate size (M.W. from 1000 to 6000 Da) are not immunogenic; 3) an at list minimal chemical complexity. Because of their structural complexity and size, proteins are generally strong immunogens whereas peptides may have the complexity necessary to be antigenic, but their small size usually renders them ineffective as immunogens on their own.

The specific site on an antigen to which an antibody binds is called epitope or antigenic determinant. For very small antigens, the entire chemical structure may act as a single epitope. On the contrary, depending on its complexity and size, a

bigger antigen may effect production of antibodies directed at numerous epitopes (Pierce). The interaction between an antibody and its target antigen is characterized by high specificity and affinity. The antibody affinity is defined as the binding strength between an epitope and an antigen-binding site in an antibody; whereas the specificity is defined as the ability of an antibody to selectively bind the target epitope and is a feature depending on the intrinsic structure of antibodies. Indeed, an antibody molecule consists of two identical light chains and two identical heavy chains linked together by disulfide bonds. The N-term domains of both light and heavy polypeptides are highly variable in sequence as well as in number of residues. This variability allows the formation of the specific antigen-combining sites of the antibody. The remaining domains of the light and heavy polypeptides have instead constant sequences, constituting the so called constant region of the antibody (Kumagai, 2001). Even if one of the main features of an antibody is its specificity for a defined antigen, in some cases the binding site of an antibody can accommodate antigens other than the original immunogen. This ability is referred to as cross-reactivity.

Antibodies are distinguished in two categories: polyclonal and monoclonal. Polyclonal antibodies (pAbs) are mixtures of antibodies that collectively bind to multiple epitopes on the same antigen and are produced from several different immune cells. On the contrary, monoclonal antibodies (mAbs) have binding specificity for only one particular epitope and all the molecules of a monoclonal antibody derives from a unique parent cell (Pierce). Both pAbs and mAbs have their own features which make them useful for different applications. Polyclonal antibodies are not as specific as the monoclonal ones and they are basically preferred when the antigen to be recognized is denatured or altered, since they are less sensitive to antigen changes. On the other hand, mAbs are highly specific antibodies, decreasing both background noise and undesired cross-reactivity.

Moreover the quality of results obtained with mAbs is generally more consistent of that derived from pAbs and, therefore, mAbs have to be absolutely preferred when standardization is required (i.e. in clinical tests and therapeutic treatments). Nowadays mAbs are essential tools used by investigators in many areas of scientific research and have applications in virtually all areas of biology and medicine. They are used extensively not only in basic biomedical research but also for diagnosis, and for therapies of infections, cancer, autoimmune disorders and other diseases.

The development of a technique for the production of mAbs has been possible thanks to the genetic engineering revolution. Particularly, it is ascribed to Kohler and Milstein, who developed in 1975 a powerful method to combine the nuclei of normal antibody-forming cells with those of their malignant counterparts (Kohler and Milstein, 1975). Producing mAbs requires the immunization of an animal, usually a mouse, with the desired immunogen. Briefly, mAbs are produced by fusing the immune cells, obtained from the spleen of the immunized animal, with a cancer cell generally deriving from a myeloma (Ward, 1999). A specific chemical agent, the polyethylene glycol, is used to fuse the plasma membranes of the two cells and a selective medium, called HAT medium, allows only fused cells to grow and survive. The resulting fusion cell is called a hybridoma: it is immortal, grow and divide indefinitely and secretes a single type of mAb. An hybridoma cell line must multiply to produce the desired mAb. There are two methods for growing these cells: injecting them into the peritoneal cavity of a mouse or using *in vitro* cell-culture techniques. When injected into a mouse, the hybridoma cells multiply and produce fluid (ascites) in its abdomen; this fluid contains a high concentration of antibody. In the *in vitro* approach, the hybridomas are grown in a suitable cell culture medium that needs to be continuously enriched to favour the growth of hybridoma. After obtaining either a media sample of cultured hybridomas or a

sample of ascites fluid, the desired antibodies are extracted and purified. Although the *in vitro* approach is more expensive, it is usually preferred as the ascites technique is painful to the animal and is considered unethical when alternative techniques exist.

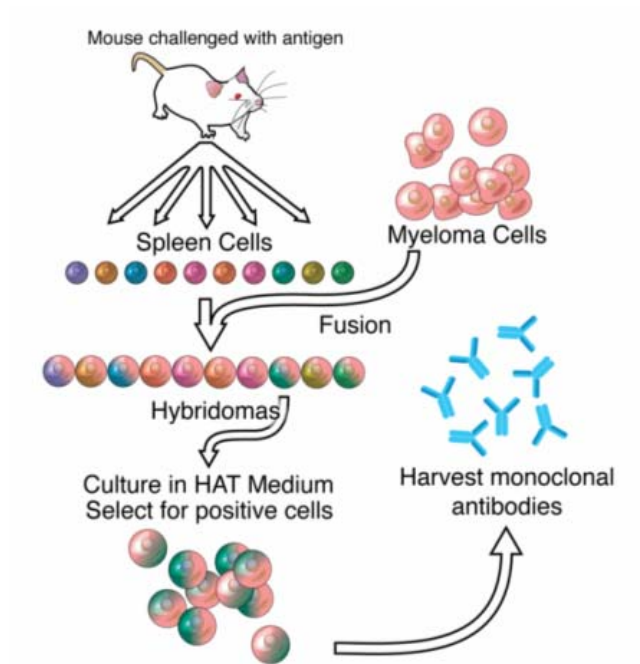


Fig. 1.5. Schematization of the method used to produce monoclonal antibodies.

Chapter 2

MATERIALS AND METHODS

2.1 Standard solutions.

All solutions are identified in the text except for the following:

- a) TE: 10 mM Tris-HCl (pH 7.4), 1 mM EDTA (pH 7.4)
- b) PBS (1X): 137 mM NaCl, 2.7 mM KCl, 10 mM Na₂HPO₄, 1.8 mM KH₂PO₄, pH 7.4
- c) 10X TBE: 108 g/l Tris, 55 g/l Boric acid, 9.5 g/l EDTA
- d) 10X DNA loading buffer: 0.25% bromophenol blue, 20% sucrose in Tris 10 mM, EDTA 1 mM.
- e) 4X protein sample buffer: 8% w/v SDS, 0.4 M DTT, 200 mM Tris-HCl (pH 6.8), 0.4% w/v bromophenol blue, 40% v/v glycerol.

2.2 Enzymes.

Restriction enzymes were from New England Biolabs, Inc. DNA modifying enzymes such as Taq Polymerase, DNase I RNase free, and T4 DNA ligase were obtained from Roche Diagnostic. T7 RNA polymerase was from New England Biolabs, Inc. RNase A was purchased from Sigma Chemicals Ltd. A 10 mg/ml solution of RNase A was prepared in sterile water and boiled for 10 min to destroy trace amounts of DNase activity. M-MLV (Moloney Murine Leukemia Virus) Reverse Transcriptase was purchased from Gibco and Porcine Trypsine from Sigma-Aldrich. All enzymes were used following manufacturer's instructions.

2.3 Synthetic oligonucleotides.

Synthetic DNA oligonucleotides were supplied by CEINGE Biotecnologie Avanzate s.c.a.r.l Napoli, Italy and by IDT Integrated DNA Technologies (IDT) Coralville, United States.

2.4 Radioactive isotope.

Radioactive α -³²P-UTP was from Amersham U.K. Ltd.

2.5 Bacterial culture.

The *E. coli* K12 strain DH5 α was transformed with the plasmids described in this study and used for their amplification. Plasmids were maintained in the short term as single colonies on agar plates at 4°C but for long term storage they were kept on glycerol stocks made by adding sterile glycerol to a final 30% v/v concentration to liquid bacterial cultures. Glycerol stocks were stored at –80°C. When necessary, from the glycerol stocks an overnight culture of bacteria was grown in Luria-Bertani medium [LB medium: per liter: 10 g Bacto Tryptone, 5 g Yeast Extract, 10 g NaCl, (pH 7.5)]. Bacterial growth media were sterilized before use by autoclaving. When appropriate, ampicillin was added to the media at a final concentration of 100 μ g/ml.

2.6 Cell culture.

The cell lines for transfection experiments were Neuro2a (mouse neuroblastoma), and HEK293T (human embryonic kidney). The cell line used for the experiments of NGF-induced neuronal differentiation was PC-12 (rat adrenal pheochromocytoma).

All cell lines used in this study were maintained, sub-cultured and stored following the DSMZ (Deutsche Sammlung von Mikroorganismen und Zellkulturen GmbH, German collection of Microorganisms and Cell Cultures) instructions.

Cell culture media were prepared as following:

- Neuro2a: 87% Dulbecco's modified Eagle's medium (Sigma), 10% FBS (HyClone), 2% ultra-glutamine (Lonza), 1% non-essential amino acids (Gibco).
- HEK293T: 85% Dulbecco's modified Eagle's medium with glutamax (Invitrogen), 15% FBS (HyClone).
- PC12: 85% RPMI 1640 (Sigma), 20% horse serum (Sigma), 10% FBS (HyClone).

For NGF-induced neuronal differentiation experiments, tissue culture plates were coated with collagen type IV (Sigma-Aldrich, Steinheim, Germany) and PC12 cells were seeded one day prior stimulation to obtain a 30% confluence at the time of NGF administration. Stimulation of PC12 cells was performed by addition of NGF- β (Sigma-Aldrich, cat. N1408) at a final concentration of 100 ng/ml and incubating cells at 37°C in a CO₂ incubator for 72 h prior to analysis.

2.7 DNA preparation.

2.7.1 Small scale preparation of plasmid DNA from bacterial cultures.

Rapid purification of small amounts of recombinant plasmid DNA was performed with the method previously described by Sambrook (Sambrook et al., 1989). Briefly, a single colony from a fresh Luria-Bertani agar plate (15 g/L Bacto Agar in LB medium containing 100 μ g/ml ampicillin) was inoculated in 1-10 ml of LB medium (containing the same antibiotic) and incubated 12-16 h at 37°C in a shaking incubator. The bacterial culture was harvested by centrifugation (5 min at

10000xg) and subsequently resuspended in 200 μ l of solution I (10 mg/ml RNase A in ddH₂O). Alkaline lysis of cells was obtained by adding to the bacterial suspension 200 μ l of solution II (0.2 M NaOH, 1% w/v SDS) and incubating them 5 min at RT. Then 300 μ l of solution III (3 M potassium acetate, 11.5% glacial acetic acid, pH 5.2) were added to each tube, mixed by inversion and incubated on ice for 10 min. The bacterial lysate was clarified by centrifugation at maximum speed (16000xg) using an Eppendorf microcentrifuge and the supernatant transferred to a fresh tube. An equal volume of 1:1 v/v phenol:chloroform solution was added to the supernatant. The tube was vortexed and centrifuged as above. The inner aqueous phase, containing the DNA, was transferred to a fresh tube and two volumes of 100% ethanol were added. This mix was incubated at -20°C for 20 min and then centrifuged 20 min at maximum speed. The supernatant was discarded and the resulting DNA pellet was washed with 500 μ l of 70% ethanol. Finally this last DNA pellet was air dried and resuspended in 50 μ l of ddH₂O +3 μ l of RNase A (10mg/ml). For each DNA preparation, 5 μ l of sample were routinely analyzed by performing control endonuclease digests with suitable restriction enzymes.

2.7.2 Large scale preparations of plasmid DNA from bacterial cultures.

Large-scale preparations of plasmid DNA, needed for the transfection experiments, were obtained using the JETStar plasmid purification system (Genomed), following the manufacturer's instructions. In order to get good amounts of plasmid, each purification was performed starting from 50 ml of bacterial culture, obtained as described in the previous paragraph.

2.8 RNA extraction from cultured cells.

Cells were washed twice with PBS and subsequently resuspended in Trifast reagent (EuroGold). Chloroform was added to the suspension and the mixture was incubated for 10 min at RT and then centrifuged for 15 min at 13000 rpm at 4°C. The resulting inner aqueous phase, containing the RNA, was transferred to a fresh tube and precipitated with 100% cold isopropanol. After an additional washing step with 70% ethanol, the RNA pellet was air dried, resuspended in 50 µl of ddH₂O and digested with 1U of DNase RNase-free for 30 min at RT. Following DNase digestion, the RNA was purified again as described above and the final pellet was resuspended in 35 µl of ddH₂O and stored at -80°C. The RNA quality was checked by electrophoresis on 1% agarose gel.

2.9 Estimation of nucleic acid concentration.

Spectrophotometric quantitation of nucleic acids was always performed to determine the average concentrations of DNA or RNA samples, as well as their purity. Using the Beer-Lambert Law, it is possible to relate the amount of UV light absorbed by a sample of nucleic acids to the concentration of the absorbing molecule. An optical density of 1.0 at 260 nm is usually taken to be equivalent to a concentration of 50 µg/ml for double stranded DNA, 40 µg/ml for single stranded DNA and RNA, and approximately 20 µg/ml for single-stranded oligonucleotides samples. The ratio of the absorbance at 260 and 280 nm ($A_{260/280}$) is used to assess the purity of nucleic acids: for pure DNA, $A_{260/280}$ is ~1.8 and for pure RNA $A_{260/280}$ is ~2.

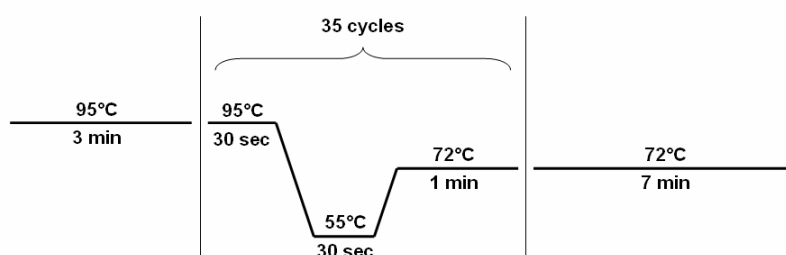
2.10 cDNA synthesis.

In order to synthesize cDNA, 1 μg of total RNA extracted from cells was mixed with 2 μl of a 10 μM polydT primer (IDT) in a final volume of 20 μl . After 30 sec of denaturation at 90°C, this RNA-primer sample was mixed with 20 μl of a solution containing: 1X First Strand Buffer (Invitrogen), 10 mM DTT, 0.5 mM dNTPs, RNase inhibitor 20 U (Ambion) and Moloney murine leukemia virus (M-MLV) reverse transcriptase 100 U (Invitrogen). The resulting reaction mix was incubated for 1 h at 37°C to allow the retro-transcription to proceed. The cDNA was finally stored at -20°C.

2.11 PCR amplification of selected DNA fragments.

The polymerase chain reactions were performed on genomic or plasmid DNA following the basic protocols specified for the Roche Diagnostic Taq DNA Polymerase. For each amplification, the final reaction volume was 30 μl and contained: 1X Taq buffer, dNTP mix 200 μM each, oligonucleotide primers 2 μM each, Taq DNA Polymerase 2.5 U. As DNA template, 0.1 ng of plasmid or 100-500 ng of genomic DNA were used for reaction. When a DNA fragment longer than 2000 bp was amplified, a 3% DMSO (dimethylsulfoxide) solution was also added to the mixture. The amplification reactions were performed using a Gene Amp PCR System (Applied Biosystems).

The general amplification conditions are displayed in the following scheme:



Primer pairs for PCR amplifications were designed to obtain the specific fragments of interest flanked by the appropriate restriction endonuclease sequences, required to clone them in suitable plasmids. In tables A and B all the primer pairs and the main cloning features for all the clones produced in this study are listed. Particularly, Table A shows all the human aldolase C protein clones that were produced using the 3xFLAG CMV 7.1 expression vector (Sigma E4026), which allows the expression of recombinant products characterized by a 3xFLAG tag coupled to their N-terminus; Table B includes clones produced using the pEGFP-C2 plasmid (Clontech, catalog n. 6083-1) that was used to express selected human aldolase C peptides in fusion with an N-terminal GFP tag.

Table A. Cloning of human aldolase C full length protein and fragments in the p3xFLAG CMV 7.1 vector.

Aldolase C PROTEIN DOMAIN (clone name)	PRIMER PAIRS	PCR PRODUCT LENGTH (including primers)	MW of the fusion protein and total number of aa residues	Translation (including the 3xFLAG peptide at the N-term)
aa 1-364 (Full length protein) or 3xFLAG- AldoC)	<i>hAldoC 1-364 aa Kpn1</i> 5'ggggtacctcatATGCCTCACT CGTACC3' <i>hAldoC 1-364aa Xba1</i> 5'tgctctagaTCAGTAGGCATG GTTGGCAA3'	1116 bp	43 kDa 390 aa	MDYKDHDGDYKDHDIDYK DDDDKLEF MPHSYPALSA EQKKELSDIALRIVAPGKGI LAADESVGSMARKLSQIGV ENTEENRRLYRQVLF SAD DRVKKCIGGVIFFHETLYQ KDDNGVPFVRTIQDKGIVV GIKVDKGVVPLAGTDGETT TQGLDGLSERCAQYKKDG ADFAKWRCVLKISERTPSA LAILENANVLARYASICQQN GIVPIVEPEILPDGDHDLKR CQYVTEKVLAAVYKALSDH HVYLEGTLKPNMVTGHA CPIKYTPEEIAMATVTALRR TVPPAVPGVTFLSGGQSE EEASFNLNAINRCPLRPW ALTFSYGRALQASALNAW RGQRDNAGAATEEFIKRAE VNGLAAQGGKYEGSGEDGG AAAQSLYIANHAY
aa 1-210 (clone 1)	<i>hAldoC 1-100aa Hind3-EcoR1</i> 5'actaagcttgaattcATGCCTCAC TCGTACCCAGCCCTTT3' <i>hAldoC 101-210aa NotI-XbaI</i> 5'tgatctagaggcggccgctcaCAA GACCTTCTCTGTAACTACT GACA3'	666 bp	26 kDa 236 aa	MDYKDHDGDYKDHDIDYK DDDDKLEF MPHSYPALSA EQKKELSDIALRIVAPGKGI LAADESVGSMARKLSQIGV ENTEENRRLYRQVLF SAD DRVKKCIGGVIFFHETLYQ KDDNGVPFVRTIQDKGIVV GIKVDKGVVPLAGTDGETT TQGLDGLSERCAQYKKDG ADFAKWRCVLKISERTPSA LAILENANVLARYASICQQN GIVPIVEPEILPDGDHDLKR CQYVTEKVL
aa 1-100 (clone 1A)	<i>hAldoC 1-100aa Hind3-EcoR1</i> 5'actaagcttgaattcATGCCTCAC TCGTACCCAGCCCTTT3' <i>hAldoC 1-100aa NotI-XbaI</i> 5'tgatctagaggcggccgctcaATCC TGGATGGTTCGGACGAAGG GAA3'	336 bp	15 kDa 126 aa	MDYKDHDGDYKDHDIDYK DDDDKLEF MPHSYPALSA EQKKELSDIALRIVAPGKGI LAADESVGSMARKLSQIGV ENTEENRRLYRQVLF SAD DRVKKCIGGVIFFHETLYQ KDDNGVPFVRTIQD

<p>aa 101-210 (clone 1B)</p>	<p><i>hAldoC 101-210aa Hind3-EcoR1</i> 5'actaagcttgaattcAAGGGCATCGTCGTGGGCATCAAGGT3'</p> <p><i>hAldoC 101-210aa NotI-XbaI</i> 5'tgatctagaggcggccgctcaCAAGACCTTCTCTGTAACATACTGACA3'</p>	366 bp	16 kDa 136 aa	<p>MDYKDHDGDYKDHDIDYK DDDDKLEFKGIVVGIVDK GVVPLAGTDGETTTQGLD GLSERCAQYKKGADFAK WRCVLKISERTPSALAIEN ANVLARYASICQQNGIVPIV EPEILPDGDHDLKRCQYVT EKVL</p>
<p>aa 101-300 (clone 2)</p>	<p><i>hAldoC 101-210aa Hind3-EcoR1</i> 5'actaagcttgaattcAAGGGCATCGTCGTGGGCATCAAGGT3'</p> <p><i>hAldoC 210-300aa NotI-XbaI</i> 5'tgatctagaggcggccgctcaGAAGGTAAGCGCCAGGGTCGGGAA3'</p>	636 bp	25 kDa 226 aa	<p>MDYKDHDGDYKDHDIDYK DDDDKLEFKGIVVGIVDK GVVPLAGTDGETTTQGLD GLSERCAQYKKGADFAK WRCVLKISERTPSALAIEN ANVLARYASICQQNGIVPIV EPEILPDGDHDLKRCQYVT EKVLAAYKALSDHHVYLE GTLLKPNMVTPGHACPIKY TPEEIAMATVTALRRTVPP AVPGVTFLSGGQSEEEAS FNLNAINRCPLPRPWALTF</p>
<p>aa 210-364 (clone 3)</p>	<p><i>hAldoC 210-300aa Hind3-EcoR1</i> 5'actaagcttgaattcGCTGCTGTGTACAAGGCCCTGAGTGA3'</p> <p><i>hAldoC 299-364aa NotI-XbaI</i> 5'tgatctagaggcggccgcTCAGTAGGCATGGTTGGCAATGTAGA3'</p>	504 bp	20 kDa 182 aa	<p>MDYKDHDGDYKDHDIDYK DDDDKLEFAAVYKALSDHH VYLEGTLLKPNMVTPGHAC PIKYTPEEIAMATVTALRRT VPPAVPGVTFLSGGQSEE EASFNLNAINRCPLPRPWA LTFTFSYGRALQASALNAW RGQRDNAGAATEEFIKRAE VNGLAAQGGYEGSGEDGG AAAQSLYIANHAY</p>

Table B.

Cloning of human aldolase C peptides in the pEGFP-C2 expression vector.

Aldolase C peptidic residues (clone name)	PRIMER PAIRS	Recombinant product
aa 2-17 (pEGFP-C2 +Aldolase C aa 2-17)	<p><i>AldoC_2-17s</i></p> <p>5'TCGAGCGGGAGTGGGAGTGGACCTCACTCGT ACCCAGCCCTTTCTGCTGAGCAGAAGAAGGAGT TGTCTTGAG 3'</p> <p><i>AldoC_2-17as</i></p> <p>5'GATCCTCAAGACAACCTCCTTCTTGCTCAGC AGAAAGGGCTGGGTACGAGTGAGGTCCACTCC CACTCCCGC 3'</p>	<p>GFP-GSGSG- PHSYPALSAEQKKELS</p>
aa 41-58 (pEGFP-C2 +Aldolase C aa 41-58)	<p><i>AldoC_41-58s</i></p> <p>5'TCGAGCGGGAGTGGGAGTGGAGCCAAGCGG CTGAGCCAAATTGGGGTGGAAAACACAGAGGA GAACCGCCGGCTGTGAG3'</p> <p><i>AldoC_41-58as</i></p> <p>5'GATCCTCACAGCCGGCGGTTCTCCTCTGTGTT TTCCACCCCAATTTGGCTCAGCCGCTTGGCTCC ACTCCCACTCCCGC3'</p>	<p>GFP-GSGSG- AKRLSQIGVENTEENRRL</p>
aa 60-75 (pEGFP-C2 +Aldolase C aa 60-75)	<p><i>AldoC_60-75s</i></p> <p>5'TCGAGCGGGAGTGGGAGTGGACGCCAGGTC CTGTTCACTGCTGATGACCGTGTGAAAAAGTGC ATTGGATGAG3'</p> <p><i>AldoC_60-75as</i></p> <p>5'GATCCTCATCCAATGCACTTTTTTACACGGTC ATCAGCACTGAACAGGACCTGGCGTCCACTCC CACTCCCGC3'</p>	<p>GFP-GSGSG- RQVLFSADDRVKKCIG</p>
aa 85-102 (pEGFP-C2 +Aldolase C aa 85-102)	<p><i>AldoC_85-102s</i></p> <p>5'TCGAGCGGGAGTGGGAGTGGATACCAGAAAG ATGATAATGGTGTTCCTTCGTCCGAACCATCC AGGATAAGGGCTGAG3'</p> <p><i>AldoC_85-102as</i></p> <p>5'GATCCTCAGCCCTTATCCTGGATGGTTCCGGAC GAAGGGAACACCATTATCATCTTTCTGGTATCC ACTCCCACTCCCGC3'</p>	<p>GFP-GSGSG- YQKDDNGVPFVRTIQDKG</p>

2.12 Enzymatic modification of DNA.

2.12.1 Restriction enzymes.

Restriction endonucleases were used for the construction and analysis of recombinant plasmids. For each restriction enzyme the best working conditions were ensured by using suitable buffers characterized by specific optimal ionic strengths. All buffers were supplied by the same company that supplied the enzymes and were used according to the manufacturer's instructions. For analytical digests 100-500 ng of DNA were digested using 5U of the appropriate restriction enzyme, in a final reaction volume of 20 μ l. The reaction was incubated for 2-3 h at 37°C. For preparative digestions 5-10 μ g of DNA were processed by using 5U of restriction enzyme for μ g of DNA, in a final reaction volume of 200 μ l (the incubation conditions were the same above specified).

2.12.2 T4 DNA ligase.

T4 DNA ligase catalyses the formation of a phosphodiester bond between adjacent 3' hydroxyl and 5' phosphoryl termini in DNA, requiring ATP as a cofactor. This enzyme was used to join double stranded DNA fragments with compatible sticky or blunt ends, during generation of recombinant plasmid DNAs. 20 ng of linearized vector were ligated with a 5-10 fold molar excess of insert in a total volume of 20 μ l containing 1X ligase buffer and 1U of T4 DNA ligase. Reactions were incubated 12-16 h at 16°C for both sticky and blunt ends ligations. A sequence analysis of the plasmid DNA was always carried out as the final control step of the cloning procedure. Sequence analyses were performed at CEINGE Biotecnologie Avanzate s.c.a.r.l Napoli, Italy or samples were sent to Macrogen Inc. Seoul, Korea.

2.13 Agarose gel electrophoresis of DNA.

DNA samples were size-fractionated by electrophoresis in agarose gels ranging in concentrations from 0.8% w/v (for large fragments) to 2% w/v (for small fragments). The gels contained ethidium bromide (0.5 µg/ml) and 1X TBE. This type of horizontal gels were routinely used for: fast analysis of DNA restriction enzyme digests, estimation of DNA concentration, isolation of DNA fragments, fast quality control of both RNA and DNA samples. Samples were loaded into gel wells in the presence of 1X DNA loading buffer and electrophoresed at 50-80 mA in 1X TBE running buffer, for a time depending on both the fragment length and the agarose concentration. DNA bands were finally visualized by UV transillumination and the results recorded by digital photography.

2.14 Elution and purification of DNA fragments from agarose gels.

To purify small amounts (less than 1 µg) of DNA fragments for sub-cloning, DNA samples were electrophoresed onto an agarose gel as above described. The DNA fragment of interest was visualized with UV light and the corresponding gel slice was excised from the gel. The DNA was solubilised and purified from gel using the EuroGold Gel Extraction Kit (Euroclone), following the manufacturer's instructions. The final DNA recovery was approximately estimated evaluating the UV fluorescence of the ethidium bromide intercalated in a test DNA sample electrophoresed on agarose gel.

2.15 Preparation of bacterial competent cells.

Bacterial competent cells were prepared following the method described by Chung and Niemela (Chung et al., 1989). Briefly, *E. coli* strains were grown 12-16 h in 3 ml of LB at 37°C. Subsequently, the bacterial culture was transferred into 300 ml of fresh LB and the cells were grown for 4-5 h at RT until the OD₆₀₀ was 0.3-0.4. Cells were then put on ice and centrifuged at 4°C and 1000g for 15 min. The resulting pellet was resuspended in 30 ml of cold TSS solution (10% w/v PEG 4000 molecular weight, 5% v/v DMSO, 35mM Mg Cl₂, pH 6.5 in LB medium). Cells were aliquoted, rapidly frozen in liquid nitrogen and stored at -80°C. Competence was assessed by transformation with 0.1 ng of pUC19 and deemed satisfactory if this procedure resulted in more than 100 colonies.

2.16 Transformation of bacteria.

Transformations of ligase reaction products were performed using 1/2 of the total ligase reaction volume whereas transformations of clones were carried out using 1 ng of plasmid DNA. In both cases, the DNA was incubated with 60 µl of competent cells for 20 min on ice followed by a heat shock step at 42°C for 2 min. Subsequently, 60 µl of LB were added to each tube and incubated for 45 min at 37°C, to allow bacteria the expression of antibiotic resistance. Finally cells were spread onto agar plates, supplemented with the appropriate antibiotic, and incubated for 12-15 h at 37°C. When DNA inserts were cloned into β-galactosidase-based virgin plasmids, 30 µl of IPTG (Isopropyl β-D-1-thiogalactopyranoside) 100 mM and 20 µl of X-Gal (5-bromo-4-chloro-indolyl-β-D-galactopyranoside 4% w/v in dimethylformamide) were spread onto the agar surface before plating, aiming to facilitate the identification of positive clones (blue-white screening technique).

2.17 Cell culture transfections.

One day before transfection, cells were plated in growth medium (without antibiotics) to obtain a 70-90% confluence at the time of transfection. Cells were transfected with the Lipofectamine 2000 transfection agent (Invitrogen), according to the manufacturer's instructions, and incubated at 37°C in a CO₂ incubator for 48 h prior to testing for transgene expression. The culture medium was always changed 6-12 h after transfection.

2.18 Anti-FLAG immunoprecipitation (IP) and protein(s) co-immunoprecipitation (co-IP).

Following transfection of plasmids expressing FLAG-tagged protein(s), total protein extracts were obtained lysing cells in a specific IP lysis buffer (10% Glycerol, 50 mM Tris HCl pH 8, 150 mM NaCl, 0.1-1% NP40, 1X Complete Roche Protease inhibitors, 0.5 mM PMSF). Starting from cell lysis, all the steps were performed at 4°C, unless the procedure specifies otherwise. For the immunoprecipitation of each 3xFLAG-fusion protein, 40 µl of Sigma anti-FLAG M2 affinity gel suspension (corresponding to ~20 µl of packed gel volume) were used for each mg of total protein extract. Prior to use, the resin was washed 5 times with 1X Wash buffer (50 mM Tris HCl pH 8, 150 mM NaCl), to remove any residual storing solution. Cell lysates were incubated with the resin and the final volume in each reaction tube was brought to 1 ml by adding suitable amounts of IP lysis buffer. Samples were incubated 2 h on a roller shaker in gentle rotation. Then, the resin was centrifuged 3 min at 1500 g and the supernatant (unbound fraction) transferred to a fresh tube. Three washes were performed using the IP lysis buffer and finally the 3xFLAG-fusion protein(s) was/were eluted by incubating the resin with a 3xFLAG elution buffer (Sigma 3xFLAG-peptide 200 µg/µl in 1X Wash buffer) for 30 min at 4°C. After centrifugation, the supernatant containing the

immunoprecipitated fraction was transferred to a fresh tube and stored at -80°C until it was analyzed. Preparative immunoprecipitations for mass spectrometry analysis were performed starting from 4 mg of total protein extract whereas analytical immunoprecipitations for western blot assays were performed starting from 1 mg of total protein extract. In the last case, 1/6-1/10 of the total immunoprecipitated fraction was resolved by denaturing electrophoresis and then transferred to a nitrocellulose or PVDF membrane to perform the immunoblot analysis.

2.19 SDS-PAGE and In situ hydrolysis of proteins.

The immunoprecipitated fractions obtained by the anti-FLAG immunoprecipitations performed on cells transfected with the 3xFLAG-AldoC expressing vector or mock transfected were resuspended in 1X protein sample buffer for one-dimensional electrophoresis. Protein mixtures were fractionated by 10% SDS-PAGE (sodium dodecyl sulfate-polyacrylamide gel electrophoresis). Gels were run at 100-130 V or 30-40 mA in 1X Tris-Glycine-SDS running buffer (25 mM Tris, 192 mM glycine, 0.1% w/v SDS). Molecular masses of protein bands were estimated by comparison, using Precision Plus All Blue protein standards (Bio-Rad). Electrophoretic patterns of proteins were visualized using GelCode Blue Stain Reagent (Pierce). Both the sample and control gel lanes were cut into 25 thin slices. Each slice was broken into little pieces that were repeatedly washed alternating 50 mM ammonium bicarbonate to 100% acetonitrile. Subsequently, protein samples were reduced by incubation in 10 mM DTT for 45 min at 56°C and alkylated with 55 mM iodoacetamide in 50 mM ammonium bicarbonate for 30 min at RT in the dark. The gel particles were repeatedly washed with 50 mM ammonium bicarbonate and 100% acetonitrile as before. A modified porcine trypsin (Sigma) solution (10 ng/ μl) in 50 mM ammonium bicarbonate pH 8.5 was

added to each sample and incubated at 4°C for 45 min. The exceeding enzymatic solution was then removed and a new aliquot of the ammonium bicarbonate buffer solution was added to the samples to complete hydrate and cover the gel particles. Samples were incubated at 37°C for 18 h to allow the enzymatic digestion to proceed. Finally, supernatants were collected and the gel particles were further incubated in acetonitrile at 37°C for 15 min to maximize peptide extraction. The resulting samples were dried in a vacuum centrifuge and stored at -20°C until they were analyzed.

2.20 Protein identification by mass spectrometry and bioinformatics.

The tryptic peptide mixtures were resuspended in 0.2% formic acid (HCOOH) and were analyzed by nanoLC-ESI-MS/MS using the LC/MSD Trap XCT Ultra (Agilent Technologies, Palo Alto, CA, USA) equipped with a 1100 HPLC system and a chip cube (Agilent Technologies). After loading, the peptide mixture (7 µl in 0.2% HCOOH) was first concentrated and washed at 4 µl/min in a 40-nl enrichment column (Agilent Technologies chip) with 0.1% formic acid as the eluent. The sample was then fractionated on a C18 reverse-phase capillary column (75 µm × 43 mm) at a flow rate of 200 nl/min with a linear gradient of eluent B (2% formic acid in acetonitrile) in A (2% formic acid) from 5 to 60% in 50 min. Elution was monitored on the mass spectrometer without any splitting device. Peptide analysis was performed using data-dependent acquisition of one MS scan (mass range from 400 to 2000 m/z) followed by MS/MS scans of the three most abundant ions in each MS scan. Dynamic exclusion was used to acquire a more complete survey of the peptides by automatic recognition and temporary exclusion (2 min) of ions from which definitive mass spectral data had been acquired previously. Moreover a permanent exclusion list of the most frequent peptide contaminants (keratins and trypsin doubly and triply charged peptides: 403.20, 517.00, 519.32, 525.00,

532.90, 559.32, 577.30, 587.86, 616.85, 618.23, 721.75, 745.90, 747.32, 758.43, 854.30, 858.43, 896.30, and 1082.06) was included in the acquisition method to focus the analyses on significant data. Data Analysis was performed using the Mascot software (<http://www.matrixscience.com>) and the LC-MS/MS analyses were converted into a Mascot format text. The protein search was performed using the NCBI database (www.ncbi.nlm.nih.gov) and was governed by the following parameters: specificity of the proteolytic enzyme used for the hydrolysis (trypsin), taxonomic category of the sample, no protein molecular weight was considered, up to one missed cleavage, cysteines as S-carbamidomethylcysteines, unmodified N- and C-terminal ends, methionines both unmodified and oxidized, putative pyro-Glu formation by Gln, precursor peptide maximum mass tolerance of 600 ppm, and a maximum fragment mass tolerance of 0.6 Da. Mascot uses probability based scoring. This enables a simple rule to be used to judge whether a result is significant or not. According to the probability-based Mowse (MOlecular Weight SEarch) score, the ion score is $-10 \times \log_{10}(P)$, where P is the probability that the observed match is a random event. Individual scores >41 indicate identity or extensive homology ($p \leq 0.05$). All the MS/MS spectra displaying a Mascot score higher than 41 had a good signal/noise ratio leading to an unambiguous interpretation of the data.

2.21 Protein extraction from cells or tissues.

Cells or tissues were washed twice with cold PBS and lysed for 30 min on ice in Lysis Buffer (50mM Tris-HCl pH 7.5, 150 mM NaCl, 0.1-1% Triton X-100, 0.5 mM PMSF). When tissues were used, prior to the lysis step they were mechanically grind into cells using a dounce homogenizer with a tight-fitting glass pestle. Lysates were clarified by centrifugation at 16000xg for 30 min at 4°C in a Eppendorf microcentrifuge and the total protein concentration was determined with

classical Bradford's or Lowry's methods, depending on the percentage of detergents used in the lysis step.

2.22 Western blotting (immunoblotting).

Protein extracts were resolved on SDS-PAGE gels (ranging in concentration from 8% to 15% depending on the molecular weight of the protein(s) of interest) and transferred onto nitrocellulose or PVDF membranes (GE Healthcare) at 200 mA for 90 min in 1X Transfer Buffer (25 mM Tris, 192 mM Glycine, 10-20% methanol). Following transfer, membranes were stained using Ponceau solution (5% glacial acetic acid, 0.1% Ponceau powder Sigma P3504 in ddH₂O), to verify the efficiency of the blotting process, and subsequently incubated for 1 h in blocking solution (5% nonfat dry milk (Biorad, Hercules, CA) in PBS pH 7.6 containing 0.1% Tween-20 (T-PBS)) to prevent non specific binding. After blocking, membranes were incubated from 1 h (RT) to overnight (4°C) with specific primary antibodies (see table C) diluted in blocking solution. After three washes with T-PBS, membranes were incubated 45 min at RT with a suitable horseradish peroxidase-conjugated secondary antibody (anti-mouse 1:5000; anti-rabbit 1:5000; anti-goat 1:20000; GE Healthcare). A mouse anti- β -actin or anti- α -tubulin primary antibody was always used as loading control. Immunoblots were developed by chemiluminescence using Amersham ECL Western Blotting Detection Reagents (GE Healthcare). Protein bands on X-ray films were quantified using the Quantity One 4.5 tool (Biorad).

Table C. Primary antibodies.

Antibody	Dilution	Clonality	Ab-producing company
β -actin	1:5000	Mouse monoclonal	Sigma-Aldrich
α -Tubulin	1:2000	Mouse monoclonal	Santa Cruz Biotechnology
Aldolase C, 9F mAb	1:1000	Mouse monoclonal	Promab
Aldolase C, 2A mAb	1:1000	Mouse monoclonal	Promab
Aldolase A	1:1000	Goat polyclonal	Abnova
14-3-3 γ	1:1000	Rabbit polyclonal	Cell Signaling Technology
FLAG	1:1000	Mouse monoclonal	Sigma
GFP	1:1000	Rabbit polyclonal	Santa Cruz Biotechnology

2.23 *In vitro* transcription.

A nucleotide segment of the light neurofilament mRNA, spanning the translation termination signal (-75; +91 from the TGA), was *in vitro* transcribed in both a cold and a radiolabeled form to perform protein-RNA co-immunoprecipitation assays, in the first case, and EMSA and UV cross-linking experiments, in the second case. To this aim, the nucleotide sequence of interest was amplified from mouse genomic cDNA, using a suitable primer pair (Table D) that allowed the incorporation of the T7 promoter sequence in the PCR product.

Table D. Primers used to amplify the NF-L mRNA fragment (-75; +91 from TGA) from mouse genomic cDNA.

Primer Name	Primer Sequence
mouse NFL-75s T7 promoter	5'-aagtccTAATACGACTCACTATAGGGccaaagaatctgaagaggaagaga-3'
mouse NFL+91as	5'-ATTTGTATAGGATCTGGAACTCAACTG-3'

For non-radioactive RNA transcription, 500-1000 ng of purified PCR product were mixed with 0.5 μ l of T7 RNA polymerase enzyme (50 U/ μ l, Stratagene), 6 μ l of 5X Transcription Buffer (Stratagene), 3 μ l DTT 100 mM, 3 μ l of rNTP 15 mM, 0.5 μ l of RNase inhibitor (40 U/ μ l, Ambion) in a final reaction volume of 30 μ l, and the sample was incubated for 2 h at 37°C. Following transcription, 1 μ l of DNase (Roche) was added in the reaction tube and incubated 15 min at 37°C to remove any residual DNA. Finally, the resulting RNA was purified using the Trifast reagent, following the standard protocol described for RNA extraction. For radioactive RNA transcription, a mix of cold adenine-guanine-cytosine rNTPs and a radioactive α -³²P-UTP were used instead of the cold complete 4-rNTP mix. The RNA purification was performed using the illustra Nick column Sephadex G-50 DNA Grade (GE Healthcare) following the manufacturer's instruction.

2.24 Protein-RNA co-immunoprecipitation assay.

HEK293T cells, transfected with the 3xFLAG-AldoC expressing vector or mock transfected, were lysed in HEGN buffer (20 mM Hepes pH 7.7, 150 mM NaCl, 0.5 mM EDTA, 10% glycerol, 0.1% Triton X-100, 1 mM DDT, 1X Protease Inhibitors Cocktail(Roche)). 100 µg of each total protein extract were incubated with equal amounts of cold NF-L RNA (0.2 ng). Each sample was subsequently split in equal parts into two fresh tubes: one was stored at -20°C as the input reference sample and the second one was incubated with 5 µg of a mouse anti-FLAG antibody (Sigma), to test for protein-RNA co-immunoprecipitation. Its final volume was brought to 500 µl by adding further HEGN buffer. After 2 h of incubation at 4°C on a rotating wheel, 30 µl of A/G plus agarose-beads (Santa Cruz Biotechnology) were added to the reaction tube and the sample was incubated again for 2 h at 4°C on a rotating wheel. Subsequently, the beads were washed extensively with HEGN buffer supplemented with 0.1% sodium deoxycholate to avoid non-specific binding and the RNA was finally extracted from the immunoprecipitated fraction as well as from the input sample. The RNA was retro-transcribed using the mouse NFL+91as primer (Table E) and the resulting cDNA was diluted 1:40 in sterile ultrapure water and used to evaluate the NF-L mRNA enrichment fold by Real Time PCR using the primer pair specified in Table E.

Table E. Real Time PCR primers.

Primer Name	Primer Sequence
mouse NFL-75s	5'-ACCAAAGAATCTGAAGAGGAAGAGA-3'
mouse NFL+91as	5'-ATTTGTATAGGATCTGGA ACTCAACTG-3'

2.25 Real Time PCR.

Real-time quantitative PCR, also known as qPCR, combines PCR amplification and detection into a single step. This enables the method to be truly quantitative. Fluorescent dyes are used to label PCR products during thermal cycling. Real-time PCR instruments measure the accumulation of fluorescent signal during the exponential phase of the amplification reaction (the dye emits fluorescence only when bound to double-stranded DNA). In this study, reactions were run in the CFX96 Real-Time System (Biorad), a real-time PCR instruments with thermal cycling and fluorescence detection capabilities. The amplification conditions used are recapitulated in the following protocol:

Step 1. 95°C for 2 min

Step 2. 95°C for 15 sec.

Step 3. 58°C for 30 sec.

Plate Read.

Step 4. Go to 2, 48 more times.

Step 5. 95°C for 10 sec.

Step 6. Melt Curve 65°C to 95°C; increment 0.5°C for 0:01.

Plate Read.

Samples were loaded in appropriate optical 96-well plates, specific for real time PCR instruments. In each well, the sample volume was 15 μ l. Particularly, they were dispensed 10 μ l of Master MIX (containing 7.5 μ l of iQ SYBR Green Supermix, Biorad and 0.3 μ l of each specific sense and antisense primer (20 μ M stock; Table E) in sterile and ultrapure water) and 5 μ l of cDNA sample (1:40 dilution of the cDNA derived from protein-RNA co-immunoprecipitation experiments). It was always included in the analysis a negative control sample (containing water instead of cDNA). Each sample was always assayed in duplicate. Before running, the plate was briefly centrifuged to expel air bubbles.

2.26 Expression and purification of fusion proteins.

The mouse aldolase C and the human TDP43 wild type proteins were previously cloned into the pGEX-4T-3 and pGEX-3 vectors respectively (Amersham Biosciences) and used, in this study, to produce the recombinant GST-aldolase C, and GST-TDP43 fusion proteins. To this purpose, *E. coli* cells (strain BL21 or DH5 α) were separately transformed with the GST, GST-aldolase C or GST-TDP43 expressing vectors and used to obtain large amounts of transformed bacteria culture (400 ml). Once reached an OD₆₀₀ of 0.5, the recombinant protein expression was induced by adding 0.1 mM IPTG. Following an overnight static incubation at RT, bacteria cultures were harvested, centrifuged and the resulting bacteria pellets were resuspended in 40 ml PBS containing 0.1% Tween-20 and 1X Complete Protease Inhibitors cocktail (Roche). Cell suspensions were sonicated 10 times for 20 sec (32W/cm²) and subsequently centrifuged 20 min at 4000 rpm to remove cell debris. GST proteins were affinity purified with a GST-BindTM resin (Novagen, Madison, WI). 500 μ l of such resin were used for each 40 ml of bacterial extract and incubated 2 h at 4°C on a rotating wheel. Then the unbound fraction was removed and the resin washed 3 times with 40 ml of PBS containing 0.1% Triton X-100 (each washing step was performed incubating the resin 15 min on a roller shaker). Finally the recombinant proteins were eluted by incubating the resin 15 min with gentle rotation in 1 ml of Elution Buffer (5 mM reduced glutathione, 1 mM DTT, 1X complete protease inhibitor cocktail in 100 mM Tris pH 8.8). Three consecutive elutions were performed to maximize the purification of the recombinant proteins. The quality of purified proteins was checked on SDS-PAGE. After staining with Coomassie Brilliant Blue (Biorad), protein concentration was assessed by comparison with bovine serum albumin (BSA) standard samples (Fig. 3.10b).

2.27 RNA EMSA.

The Electrophoretic Mobility Shift Assay (EMSA) method is schematized in Fig. 2.1. It is a common electrophoretic technique used to study protein–DNA or protein–RNA interactions. The EMSA technique is based on the observation that protein-DNA or protein-RNA complexes migrate more slowly than free linear DNA or RNA fragments, when subjected to non-denaturing electrophoresis. Briefly, 15 µg of total protein extracts or 0-10 µg of purified recombinant proteins were incubated with the ³²P-labeled NF-L RNA probe (1:100 dilution in ultrapure water of the T7 *in vitro* transcribed product) in a final reaction volume of 15 µl containing 1.5 µl of 10X Binding Buffer (400 mM KCl, 150 mM HEPES pH 7.9, 10 mM EDTA, 5 mM DTT, 50% glycerol), 1 µl of BSA 1mg/ml, 1.5 µl Heparin 20 µg/µl. When required for supershift-tests on tissue extracts, 1 µg of anti-aldolase C antibody (anti-aldolase C 9F mAb, ProMab Biotechnologies, Inc., Richmond, CA) was added to the sample. The reaction mix was incubated 20 min on ice and subsequently loaded onto a native 6% polyacrylamide gel after addition of 5 µl of DNA Loading Buffer (0.25% bromophenol blue, 20% sucrose in Tris 10 mM, EDTA 1 mM). The native electrophoretic separation was run at 100 V constant for about 1 h and half at 4°C in 0.5 X TBE. Gels were dried and exposed to X-OMAT AR films (Kodak) for 1-3 h. A control lane (containing only the labeled RNA fragment, without the addition of any purified protein or protein extract) was always included in the gel, resulting in a fast-migrating band corresponding to the unbound probe.

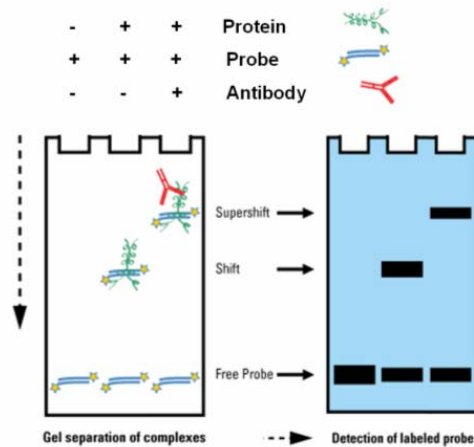


Fig. 2.1. Schematization of the Electrophoretic Mobility Shift Assay (EMSA) method.

2.28 UV cross-linking experiments.

UV-irradiation of protein-nucleic acid complexes causes the formation of covalent bonds between the nucleic acid and proteins that are in close contact with it. The UV cross-linking assay was performed as following: the ^{32}P -labeled NF-L mRNA probe was incubated 15 min at RT with purified GST-aldolase C or GST-TDP43 (3 μg) in a reaction volume of 20 μl (final binding conditions were 15 mM Hepes, pH 7.9, 40 mM KCl, 0.5 mM dithiothreitol, 5% glycerol, and heparin at a 5 $\mu\text{g}/\mu\text{l}$ final concentration as a nonspecific competitor). Subsequently, samples were transferred in the wells of an HLA plate (Nunc) and irradiated with UV light on ice (0.8 J for 5 min). After UV irradiation, the unbound RNA was digested at 37°C for 30 min with 30 μg of RNase A (Sigma) and the complex formation was verified by 10% SDS-PAGE (30 mA run, RT) followed by autoradiography (X-OMAT AR films, Kodak).

2.29 Elisa assay of biotinylated peptides.

For the ELISA assays (enzyme-linked immunosorbent assay), aldolase C peptides of interest were synthesized with a biotin coupled to their N-terminus (Table F), and immobilized on a solid phase by streptavidin capture. To this end, each well of a Nunc-Immuno MaxiSorb plate was coated with 100 μ l of a streptavidin solution (5 μ g/ml in 10 mM Na₂CO₃ pH 9.6) by leaving the plate exposed to the air for 12-16 h at 37°C to allow the solution to evaporate to dryness. The day after, non-specific absorption was blocked by dispensing 200 μ l of blocking buffer (10 mg/ml BSA in 1X PBS, 0.05% Tween-20) and incubating the plate 1 h at RT on a shaker. After three washes with wash buffer (1X PBS, 0.05% Tween-20), 100 μ l of the appropriate peptide solution (1 μ M peptide in wash buffer) were added to the corresponding well position and incubated 1 h at RT on a shaker. Subsequently, the peptide solution was removed and the washing procedure was repeated as previously specified. The monoclonal antibodies to be tested (anti-aldolase C 9F and 2A mAbs, ProMab Biotechnologies, Inc., Richmond, CA) were diluted, from 1:5000 to 1:40000, in 1X PBS, 0.5% BSA, 0.05% Tween-20 and 100 μ l of such primary antibody solution were added to each well and incubated at RT on a shaker for 1 h. Following three washes, 100 μ l/well of an horseradish peroxidase-conjugated anti-mouse IgG solution (1:2000 secondary antibody dilution in 1X PBS, 0.5% BSA, 0.05% Tween-20) were added to each well and incubated 45 min at RT on a shaker. Five final washes were performed using the wash buffer. Subsequently 100 μ l of a 3,3',5,5' Tetramethylbenzidine substrate solution (TMB, Sigma T4444) were added to each well and the enzymatic reaction was stopped using 1N sulphuric acid. The results were spectrophotometrically analyzed at 450 nm using an appropriate plate reader.

The peptides used in this study were chemically synthesized by the “Protein Structure and Bioinformatics Group” at ICGEB, Area Science Park, Padriciano 99, Trieste (Italy). Each peptide was synthesized including a GSGSG spacer sequence between the biotin and the aldolase C peptide.

Table F. *Biotinylated human aldolase C peptides.*

aldolase C aa residues included in the peptide	Complete peptide sequence
2-17	Biotin-GSGSG-PHSYPALSAEQKKELS
41-58	Biotin-GSGSG-AKRLSQIGVENTEENRRL
60-75	Biotin-GSGSG-RQVLFSADDRVKKCIG
85-102	Biotin-GSGSG-YQKDDNGVFPVRTIQDKG

2.30 Aldolase C immunoprecipitation using the 9F mAb.

When the immunoprecipitation experiment was performed to isolate the endogenous aldolase C protein, the input sample consisted of adult mouse brain total protein extract (1 mg) and was pre-cleared using 2 µg of mouse control IgG (sc-2025, Santa Cruz Biotechnology, CA, USA) to reduce non-specific binding of proteins to agarose beads and to remove proteins that binds immunoglobulins non-specifically. Lysate pre-clearing was performed incubating samples for 1h at 4°C on a rotating wheel. The solution was then incubated with 50 µl of slurry Protein A/G plus-Agarose beads (sc-2003, Santa Cruz Biotechnology, CA, USA) for 1h at 4°C on a rotating wheel and subsequently centrifuged at 4000xg for 5 min at 4°C. The supernatant was then incubated with 10 µg of the anti-aldolase C 9F primary antibody for 1h on a rotating wheel at 4°C. Subsequently, 50 µl of fresh Protein A/G plus-Agarose beads were added to the test tube and incubated 2h or overnight at 4°C. After extensive washing of the pellet beads, the resulting immunoprecipitated complex was eluted incubating the resin at 99°C for 5 min in 40 µl of 2X protein sample buffer. The IP lysis buffer, the washing conditions and the amount of immunoprecipitated fraction analysed by western blot were the same specified in paragraph 2.18.

Chapter 3

RESULTS AND DISCUSSION

PART A

A functional proteomics approach to identify novel molecular interactors of the aldolase C protein: from a new binding partner of aldolase C to the study of its putative RNA-binding ability.

3A.1 Immunoprecipitation of 3xFLAG-tagged aldolase C protein in Neuro2a cells.

To gain insights into the physiological roles of aldolase C in the CNS a functional proteomic strategy was applied: aiming to identify proteins interacting with the aldolase C isozyme *in vivo*, multi-protein complexes containing this neuronal isozyme were isolated by performing an affinity-based approach. A commercial system for the purification of proteins expressed in fusion with the peptidic tag 3xFLAG was used. The overall strategy is schematized in Fig.3.1. Briefly, the mouse aldolase C ORF sequence was cloned in the p3xFLAG CMV 7.1 vector and the resulting plasmid was transfected into host Neuro2a cells. At 48 h post-transfection, cells were collected, lysed and the whole protein extract, enriched in the 3xFLAG-tagged form of aldolase C protein (3xFLAG-aldoc), was incubated with a resin functionalized with a specific anti-FLAG antibody. Following the procedures described in the “Anti-FLAG immunoprecipitation” section, the bait (3xFLAG-aldoc) was isolated and its putative molecular partners were pulled down in turn. In parallel, as control experiment, the anti-FLAG immunoprecipitation was performed on Neuro2a cells transfected with the empty p3xFLAG CMV 7.1 vector (mock transfected).

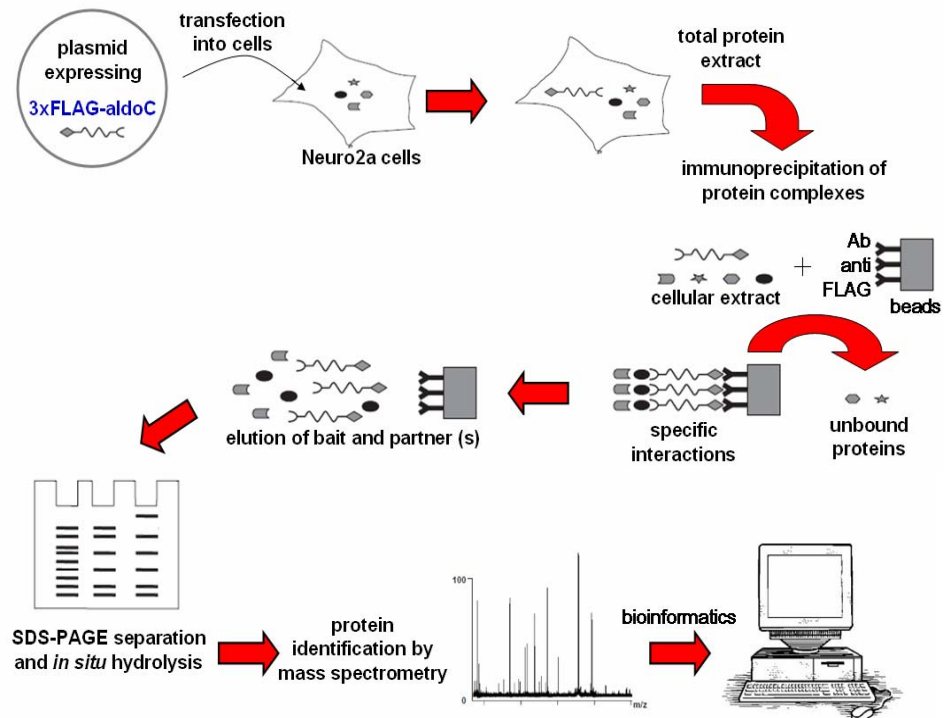


Fig. 3.1. Workflow of the functional proteomic strategy used in this study.

Aiming to verify the success in bait isolation, a small aliquot (1/30) of the total immunoprecipitated (IP) fractions was saved to be analyzed by western blot, before proceeding to analyze the IP complexes by mass spectrometry. The immunoblot analysis of the IP fractions was performed using an anti-aldolase C antibody. As shown in Fig. 3.2 (p3xFLAG-AldoC panel) the anti-FLAG immunoprecipitation approach was very efficient in capturing the 3xFLAG-aldolase C protein: in fact no residual bait signal was observed in the unbound (U) fraction whereas it was strong in the IP fraction. Moreover, the immunoprecipitation occurred specifically, since no immunoreactive signal was observed in the negative control IP lane (Fig. 3.2, p3xFLAG panel, lane 3 “IP”).

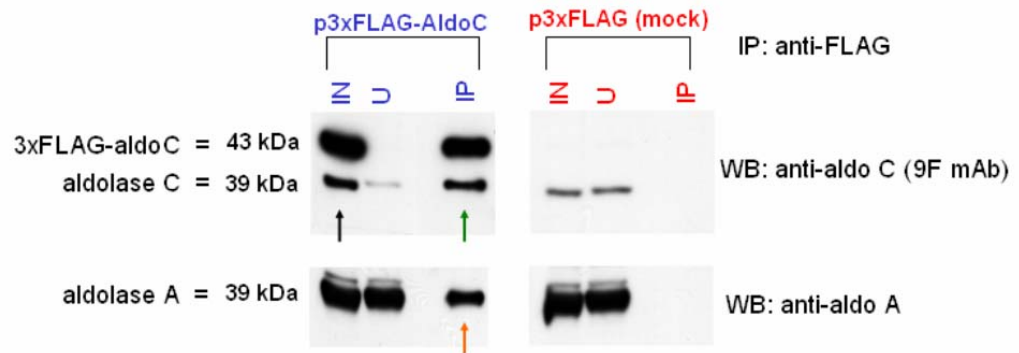


Fig. 3.2. Immunoblot analysis of anti-FLAG immunoprecipitation. The anti-FLAG immunoprecipitation (IP lane) was performed on whole protein extracts (IN lane) obtained from Neuro2a cells transfected with the p3xFLAG-AldoC plasmid (left panel) or mock transfected (right panel; negative control). The IP fractions were separated by 12% SDS-PAGE and analysed by immunoblotting using an anti-aldolase C monoclonal antibody (9F mAb) and an anti-aldolase A polyclonal antibody, as indicated. U = unbound; IP = immunoprecipitate; IN = input.

Interestingly, the immunoblot assay highlighted also that the endogenous aldolase C protein (39 kDa) co-immunoprecipitated with the transfected 3xFLAG-aldolase C (43 kDa) (Fig. 3.2, green arrow). To clearly explain this result, it is necessary to remind that Neuro2a cells, according to their brain origin, express endogenously the aldolase C protein. Consequently, their transfection with the p3xFLAG-AldoC plasmid results in the co-expression of both the endogenous (39 kDa) and the 3xFLAG-tagged form (43 kDa) of aldolase C (Fig. 3.2, black arrow). This result demonstrated the occurrence of subunit-subunit interactions between exogenous and endogenous aldolase C monomers: this finding is supported by the scientific literature where it is reported that, at the structural level, aldolase exists as a very stable hetero- or homo- tetramer, whose inter-subunit interactions are very strong and stable (Lebherz, 1972, 1975; Swain and Lebherz, 1986) (Fig. 3.3).

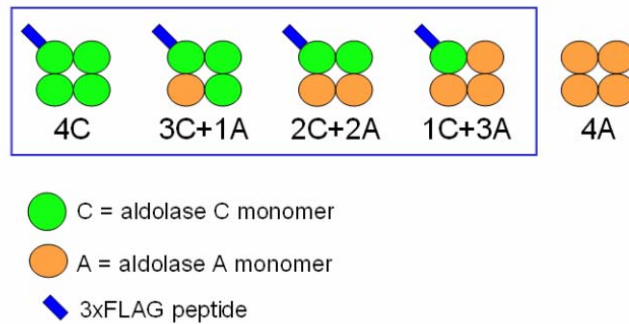


Fig. 3.3. Aldolase tetramers in the CNS. All the possible hetero- and homo- tetramers formed by aldolase C and A monomers. Blue box includes the putative tetramers assembled in vitro upon the exogenous 3xFLAG-tagged form of aldolase C.

Since in the CNS aldolase C is always expressed together with aldolase A, we asked whether the aldolase A isoform was also present in the immunoprecipitate. To address this question, we performed a second immunoblot analysis of the IP fractions using an anti-aldolase A primary antibody. The assay revealed the presence of this ubiquitous form of the isozyme in the 3xFLAG-aldolase C immunocomplex, demonstrating that also the endogenous aldolase A isoform was pulled down by the transfected bait (Fig. 3.2, orange arrow). Taken together, these results provided an internal positive control of the experiment, demonstrating that the recombinant 3xFLAG-aldolase C retained its ability to properly fold and to interact with other aldolase monomers.

The formation of oligomers containing aldolase isoforms is intriguing. The ability of two protein isoforms to interact with each other and generate both homo- and hetero- oligomeric versions have also been observed for other structural as well as enzymatic proteins, such as beta-crystallin in lens (Hejtmancik et al., 1997), alpha-actinines in skeletal muscles (Chan et al., 1998), and Pho1-type phosphorylase in plants (Albrecht et al., 1998). Of course, the formation of homo- and hetero- tetramers might simply mirror the high degree of structural similarity between aldolase isoforms. However, it should be considered that aldolase A and

C genes are localized on different loci, and that their transcripts are differently regulated. Therefore, spatial/temporal/developmental differences in their expression might play a critical role in the final composition of the aldolase tetramers, that could have different *in vivo* stability. There are a number of possible reasons why it might be advantageous for neurons and other cell types to form different kind of aldolase homo- and hetero-tetramers. The different composition of the oligomers might change the enzymatic properties of aldolase and further modulate its glycolytic role. Moreover, it might increase the complexity of the network of protein-protein aldolase associations and help in coupling the glycolytic pathway to ATP-hydrolyzing processes as suggested, for instance, for the vacuolar H⁺pump (Lu et al., 2004).

3A.2 Mass spectrometry identification of aldolase C interacting proteins.

To identify the proteins belonging to the aldolase C interactome, the two independent IP fractions (sample and control), were resolved by SDS-PAGE and revealed using colloidal Coomassie stain (Fig. 3.4): two major bands were observed in the sample lane (IP p3xFLAG-AldoC) at about 43 and 39 kDa, but not in the negative control IP (IP p3xFLAG). They were consistent with the expected immunoprecipitation of the 3xFLAG-aldoc bait (43 kDa) and the concomitant co-immunoprecipitation of endogenous aldolase monomers (39 kDa) (Fig. 3.4, thick arrows).

The sample and control lanes of the gel were cut into 25 thin slices and each slice was subsequently *in situ* hydrolysed with trypsin, to digest proteins into peptides. The resulting peptide mixtures were finally analyzed using tandem mass spectrometry (nanoLC-MS/MS) and the proteins identified using the Mascot software, following the procedures described in paragraph 2.20.

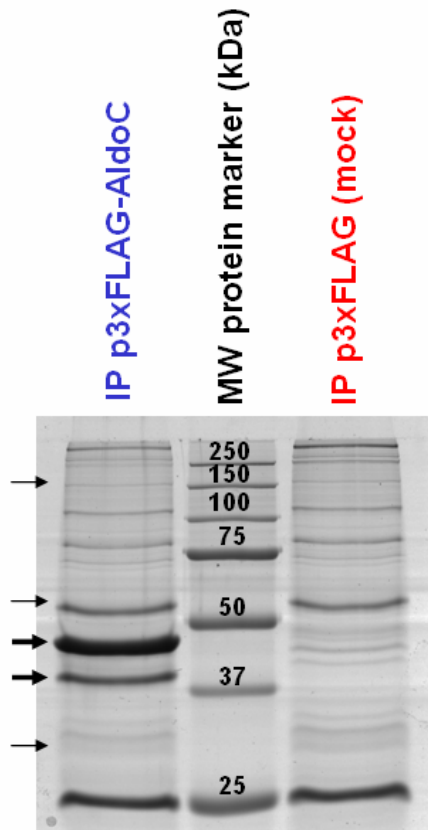


Fig. 3.4.

Preparative anti-FLAG immunoprecipitation for mass spectrometry analysis.

Sample (p3xFLAG-AldoC) and control (p3xFLAG) IP fractions were resolved by 10% SDS-PAGE and stained with colloidal Coomassie. Thick arrows indicate the two major bands corresponding to the expected molecular weights of the 3xFLAG-aldoc bait (upper arrow) and endogenous aldolase monomers (lower arrow). Thin arrows indicate the gel regions from which the four novel aldolase C putative interactors were identified in this study (from top to bottom: SAP155 (155 kDa), PRP31 (55 kDa), 14-3-3 γ and 14-3-3 θ (both isoforms 28 kDa)); see text and Table G for additional details.

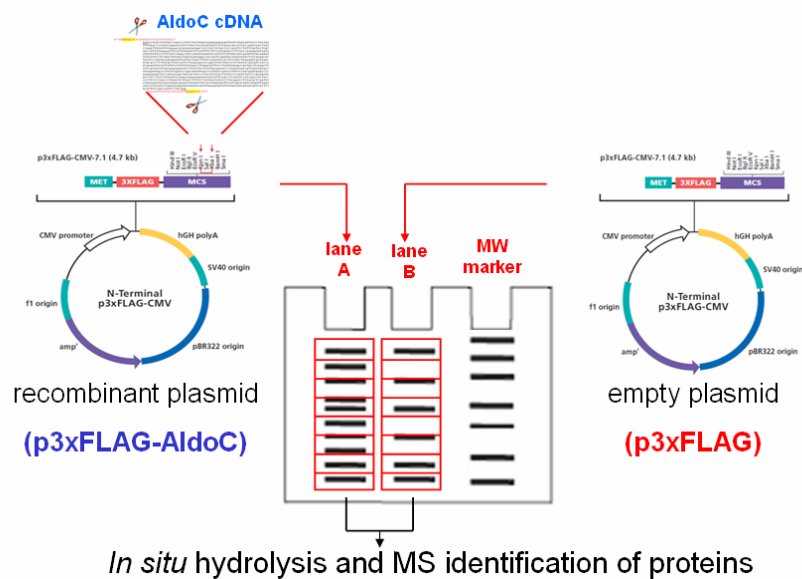


Fig. 3.5. Selection of specific bait-interactors. Species common to the control (p3xFLAG) and sample (p3xFLAG-AldoC) lanes were subtracted to select aldolase C-specific binding partners.

Since the peptides deriving from the lane referred to as IP p3xFLAG constituted our negative control, they were always injected in the mass spectrometer before those deriving from the IP p3xFLAG-AldoC lane. To select those proteins that interacted specifically with aldolase C, we subtracted species common to the control and sample lanes (Fig. 3.5).

This approach allowed the identification of 4 novel putative molecular interactors of the 3xFLAG-aldolase C protein, in addition to the endogenous aldolase monomers (Table G).

Table G. Identification of aldolase C interactors by LC-MS/MS.

Protein Name (M.W.)	Peptides identified by LC-MS/MS	Mascot peptide score	Number of peptides identified	Total score
Aldolase C (39 kDa)	ALQASALNAWR	61	11	758
	DNAGAATEEFIK	65		
	GILAADESVGSMK	88		
	LSQIGVENTEENR	64		
	TPSALAIENANVLAR	90		
	YSPEEIAMATVTALR	70		
	YEGSGDGGAAQSLYIANHAY	80		
	ISDRTPSALAIENANVLAR	85		
	GVVPLAGTDGETTTQGLDGLLER	71		
	TVPPAVPGVTFLSGGQSEEEASLNLNAINR	41		
	YASICQQNGIVPIVEPEILPDGDHDLKR	43		
Aldolase A (39 kDa)	QLLLTADDR	51	11	682
	ALANSLACQGK	60		
	GILAADESVGSIK	76		
	ADDGRFPQVIK	49		
	PHPYPALTPEQK	46		
	LQSIGTENTEENR	77		
	FSNEEIAMATVTALR	81		
	CPLLKPWALTFSYGR	46		
	IGEHTPSALAIMENANVLAR	85		
	YTPSGQSGAAASESLFISNHAY	61		
	VDKGVVPLAGTNGETTTQGLDGLSER	50		
Prp31 (55 kDa) (U4/U6 small nuclear ribonucleoprotein Prp31)	LGLTEIR	42	3	139
	IMGVAGGLTNLSK	46		
	VGVELKDEIER	51		
SAP155 (155 kDa) (Splicing factor 3B subunit 1)	VGAAEIIISR	47	2	89
	IWDPTPSHTPAGAATPGR	42		
14-3-3 θ (28 kDa)	YLAEVACGDDR	45	2	135
	AVTEQGAELSNEER	90		
14-3-3 γ (28 kDa)	YLAEVATGEK	52	3	188
	DSTLIMQLLR	53		
	NVTELNEPLSNEER	83		

Among the four novel putative aldolase C protein partners, two of them, namely 14-3-3 γ and 14-3-3 θ , belonged to a family of adapter proteins implicated in the regulation of a broad spectrum of cellular processes (Sluchanko and Gusev, 2010); the other two, identified as Prp31 and Sap155, were classified as splicing factors. Particularly, Prp31 and Sap155 proteins are components of spliceosome structures involved in per-mRNA splicing. Concerning 14-3-3 proteins, they are a family of acidic regulatory proteins that function as molecular scaffolds by modulating the conformation of their binding partners; consequently, they are involved in many processes, including cell cycle regulation, metabolism control, apoptosis, modulation of gene transcription, functioning of ion channels and NGF-cell signalling (Aitken, 2006; Fu et al., 2000; Hermeking and Benzinger, 2006; MacNicol et al., 2000). Recent data implicate them also in carcinogenesis and neurodegenerative diseases (Ge et al., 2007; Sluchanko and Gusev, 2010). Interestingly, previous studies have shown that aldolase can localize not only in the cytosolic fluid phase but also associated to cytoskeletal components (Pagliaro and Taylor, 1992). Similarly to what observed for other glycolytic enzymes (Vertessy et al., 1997), it has been shown that aldolase, in addition to its role in glycolysis, can interact with different cytoskeletal (Carr and Knull, 1993; O'Reilly and Clarke, 1993; Schindler et al., 2001; Wang et al., 1996), structural and enzymatic proteins (Campanella et al., 2005; Hatakeyama et al., 2004; Kao et al., 1999; Kim et al., 2002; Lu et al., 2001; Lu et al., 2004; Lundmark and Carlsson, 2004; Reddy and Suleman, 2004). It has been proposed that this intricate network of aldolase interactions might support the coupling of glycolysis to ATP-hydrolyzing processes (Lu et al., 2004); however, aldolase seems to be targeted for structural rather than enzymatic purposes in most of cases. In this context, our finding further support this hypothesis.

By investigating the scientific literature, we found a possible functional link between aldolase C and the 14-3-3 protein family, since independent publications reported that both neuronal aldolases and 14-3-3 proteins share the ability to interact with and regulate the stability of light neurofilament (NF-L) mRNA (Canete-Soler et al., 2005; Ge et al., 2007). Neurofilaments (NF) are major cytoskeletal components of large neurons and are instrumental in maintaining their asymmetrical differentiated shape. They are heteropolymers constituted by three types of subunits defined, on the basis of their molecular weight, as low (NF-L), intermediate (NF-M) and high (NF-H) molecular weight neurofilament subunits. NF assembly is orchestrated by NF-L subunits and alterations in NF-L expression are often associated to neurodegeneration (Bergeron et al., 1994; Canete-Soler et al., 1999; Ge et al., 2005; Strong et al., 2005; Xu et al., 1993). Consequently, the fine regulation of NF-L mRNA stability and expression is essential in maintaining neuronal homeostasis. Such a functional link between aldolase C and 14-3-3 proteins suggested us to focus on verify their interaction by independent experiments and on further investigating the aldolase C interaction with the NF-L mRNA.

3A.3 Validation of the interaction between aldolase C and the 14-3-3 γ protein by Western Blotting.

To validate the interaction between aldolase C and the 14-3-3 proteins, the immunoprecipitation assay was repeated on an analytical scale, and western-blot analyses of the IP fractions were performed, using primary antibodies directed against the two 14-3-3 isoforms of interest (γ and θ). As shown in Fig. 3.6, the co-immunoprecipitation of 14-3-3 γ protein with aldolase C was confirmed by western blot (purple circle) and the interaction was specific, as it was not observed in the negative control (Fig. 3.6, IP p3xFLAG lane). This independent experiment confirmed the occurrence of a protein-protein interaction between aldolase C and the 14-3-3 γ protein. On the contrary it was not possible to confirm by immunoblot the interaction between aldolase C and the 14-3-3 θ protein, probably due to a lower sensitivity of the commercial antibody available to this isoform (data not shown).

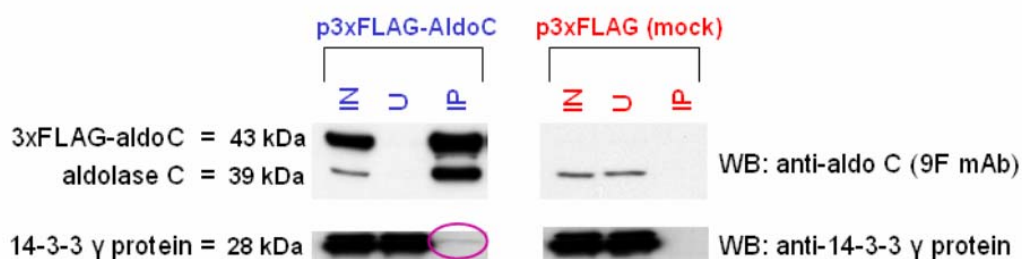


Fig. 3.6. Co-immunoprecipitation of the 14-3-3 γ protein with 3xFLAG-aldolase C. Sample (p3xFLAG-AldoC) and control (p3xFLAG) IP fractions, obtained from analytical anti-FLAG immunoprecipitations, were analysed by immunoblotting: the bait immunoprecipitation was verified using an anti-aldolase C antibody (9F mAb); 14-3-3 γ protein co-immunoprecipitation was assayed using a specific anti-14-3-3 γ antibody. U = unbound; IP = immunoprecipitate; IN = input.

3A.4 The NF-L mRNA: a possible functional link between aldolase C and the 14-3-3 γ protein.

As above cited, different publications reported an RNA-binding ability of aldolase C and 14-3-3 proteins to the 3'UTR of the NF-L mRNA. Interestingly, concerning 14-3-3 proteins, the interaction with this transcript was demonstrated in particular for five isoforms, which included the γ but not the θ one (Ge et al., 2007). In the attempt to find clues as to the biological relevance of the novel interaction between aldolase C and the 14-3-3 γ protein, it was considered noteworthy their shared ability to interact with and regulate the NF-L mRNA, for two main reasons:

- 1) according to the above mentioned publications, a destabilizing effect is exerted by both aldolase C and 14-3-3 proteins on the transcript, thus implicating that the two proteins could work in the same direction;
- 2) the scaffolding function of 14-3-3 proteins is well documented but the molecules they recruit in the context of the NF-L mRNA-binding complex are yet to be defined; our finding of an *in vivo* interaction between aldolase C and the 14-3-3 γ protein suggests the possibility that the last may recruit the first within a larger NF-L mRNA-binding complex.

In this context, it is also important to recall that the ability to interact with the NF-L mRNA, reported in 2005 and 2007 by Canete-Soler and colleagues (Canete-Soler et al., 2005; Stefanizzi and Canete-Soler, 2007), arose for the first time the hypothesis of a novel RNA-binding function of the aldolase C protein. This ability to bind RNA has not yet been verified by other investigators and represent an intriguing finding since aldolase C is mainly a glycolytic enzyme. Interestingly, our proteomic studies have evidenced a possible association of aldolase C with the mRNA processing pathway also through its putative interaction with Prp31 and Sap155 proteins (Table G). For all these reasons, we decided to further

investigate this unconventional RNA-binding activity of aldolase C. Particularly, to explore its interaction with the NF-L mRNA, we carried out a threefold strategy:

- protein-RNA co-immunoprecipitation
- EMSA
- protein-RNA UV cross-linking

To perform these experiments, a nucleotide segment of the NF-L mRNA, spanning the translation termination signal (-75; +91 from the TGA) and including the minimal aldolase C binding domain (-23; +45 from TGA) described by Canete-Soler and colleagues (Canete-Soler et al., 2005), was *in vitro* transcribed in both a cold and a radiolabeled form (Fig. 3.7).

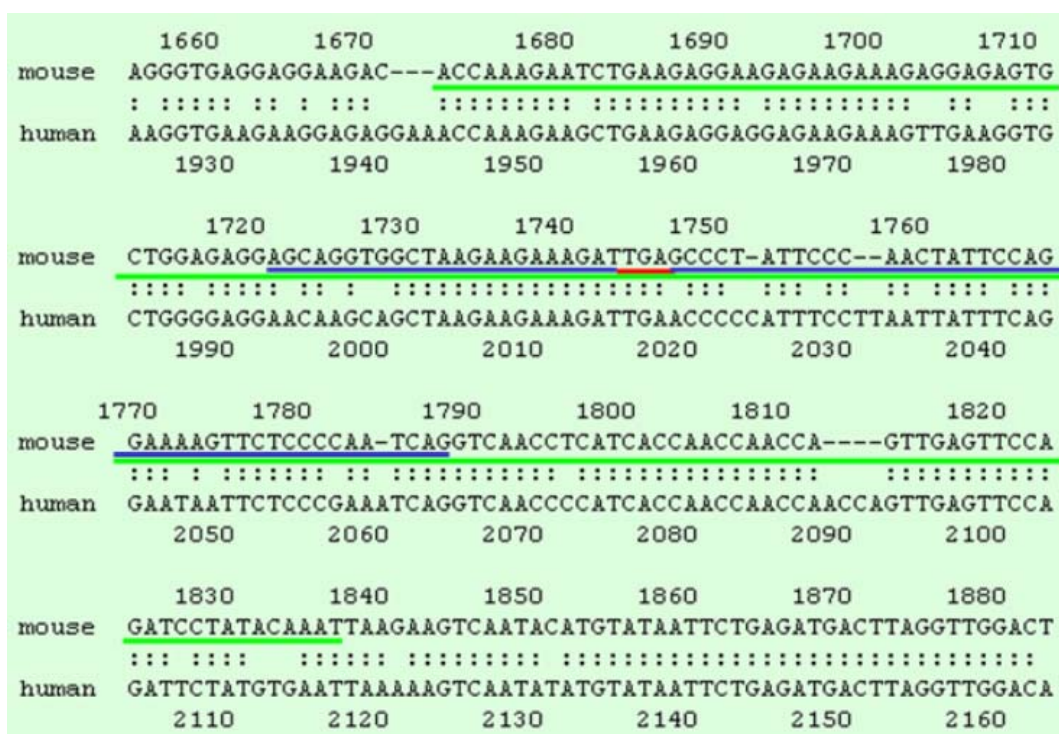
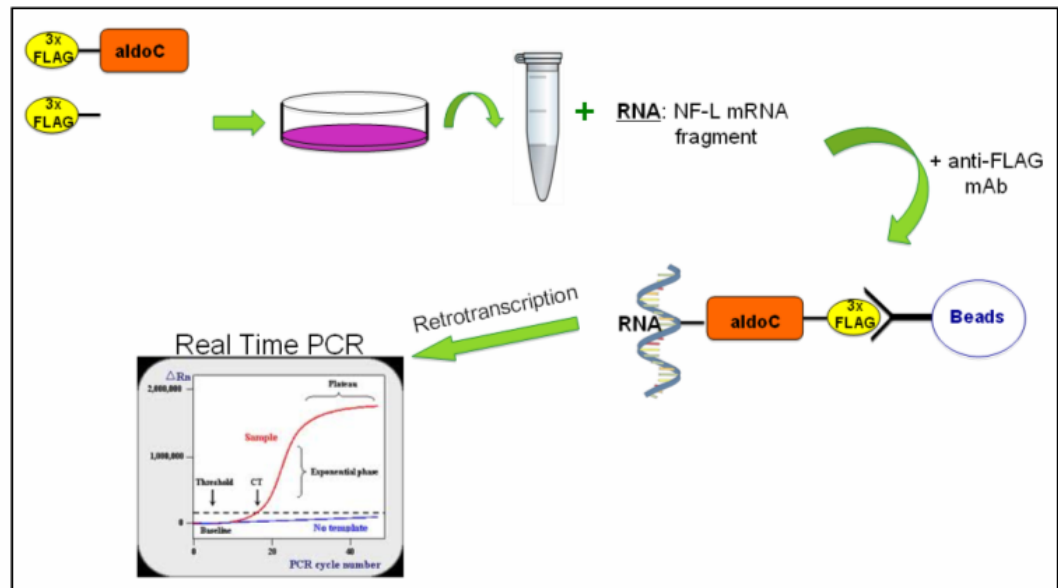


Fig. 3.7. Detail of the sequence alignment between mouse and human NF-L mRNA transcripts, using the LALIGN software. The *in vitro*-transcribed NF-L fragment (-75; +91 from TGA) is underlined in green and includes the minimal aldolase C binding sequence (-23; +45 from TGA) described by Canete-Soler (underlined in blue). Red line indicates the TGA codon.

3A.4.1 The NF-L RNA co-immunoprecipitates with aldolase C.

The first strategy applied in this study to verify the RNA-binding ability of aldolase C to the NF-L mRNA was the protein-RNA co-immunoprecipitation (co-IP) approach. Briefly, total protein extracts from HEK293T cells, transfected with the p3xFLAG-AldoC construct or mock transfected (p3xFLAG), were incubated with equal amounts of the cold NF-L mRNA fragment and with an anti-FLAG antibody. Using the standard procedures described in the “protein-RNA co-immunoprecipitation” section, the IP fractions were isolated. Subsequently they were processed with classical methods for RNA extraction and the resulting RNA was retro-transcribed to evaluate the NF-L mRNA enrichment fold (Fig. 3.8a). Real Time PCR experiments revealed a two-fold increase in NF-L mRNA immunoprecipitation in the p3xFLAG-AldoC transfected sample versus the mock transfected one (Fig. 3.8b), demonstrating a moderate but statistically significant enrichment of NF-L mRNA within the 3xFLAG-aldoc immunoprecipitated complex. This result provided evidence supporting the presence of the aldolase C protein within an NF-L mRNA-binding complex.

a)



b)

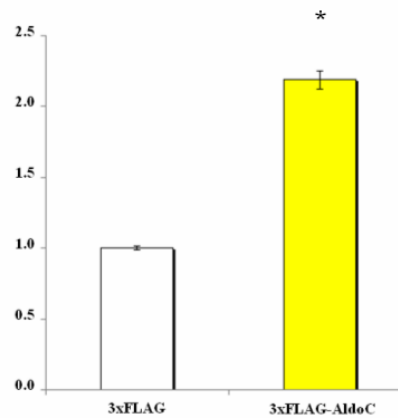


Fig. 3.8. Aldolase C-NF-L RNA co-immunoprecipitation. a) protein-RNA co-IP workflow.

b) qPCR analysis of NF-L RNA immunoprecipitated by 3xFLAG-tagged aldolase C. The enrichment-fold is referred to HEK293T cells transfected with the p3xFLAG empty vector. Results are means±S.D. from three independent experiments in duplicate. * $P < 0.05$ versus 3xFLAG.

3A.4.2 EMSA and supershift tests confirm the presence of aldolase C within an NF-L mRNA-binding complex but demonstrate that no direct binding occurs between aldolase C and this RNA target.

To further study the possible binding of aldolase C to NF-L mRNA, we performed EMSA (electrophoretic mobility shift assay) experiments, by incubating the ³²P-labeled NF-L mRNA fragment with total protein extracts obtained from brain, kidney, liver or heart tissues, respectively. Particularly, these protein extracts were incubated with the probe of interest in the absence or in the presence of a specific anti-aldolase C monoclonal antibody (9F mAb) (Fig. 3.9a). The formation of the NF-L mRNA-protein(s) complex was observed only within the brain (lanes 2,3), as expected for the specific neuronal nature of this tissue. Moreover, in the presence of the anti-aldolase C antibody, the formation of a sharper band (lane 3) suggested the brain-specific presence of the aldolase C protein within the complex interacting with the NF-L mRNA. It is important to note the high recognition specificity of the anti-aldolase C monoclonal antibody used in the assay. Indeed, immunoblot analysis showed a specific positive signal, corresponding to the molecular weight of aldolase C, only in the brain whereas no cross-reactivity was demonstrated with any other aldolase isoform (aldolase A and aldolase B) as proven by the absence of ECL detection in liver, kidney and heart tissues (Fig. 3.9b; see also Fig. 3.15).

This result, together with the one obtained from the protein-RNA co-immunoprecipitation approach, confirmed the presence of aldolase C in a complex interacting with the NF-L mRNA and supported the hypothesis of an involvement of aldolase C in neurofilaments physiology.

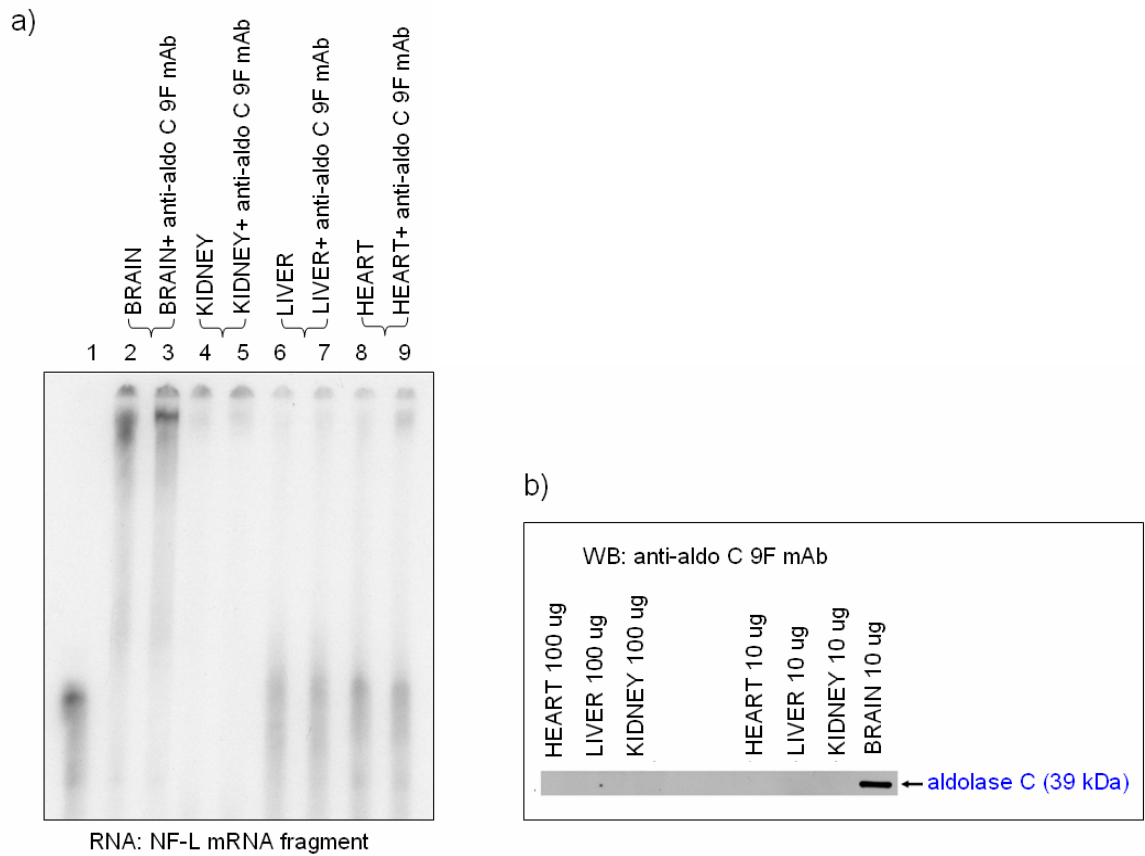
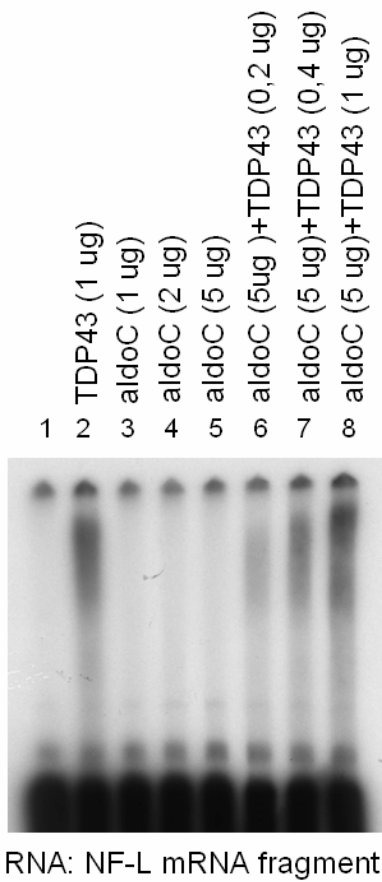


Fig. 3.9. EMSA and supershift assay with the ^{32}P -labeled NF-L RNA probe. a) Autoradiogram of EMSA run on a 4% non-denaturing PAGE: the ^{32}P NF-L mRNA probe was incubated with mouse brain, kidney, liver or heart tissue extracts in the absence or in the presence of a specific anti-aldolase C monoclonal antibody (9F mAb). b) Western blot with the anti-aldolase C 9F mAb in mouse heart, liver, kidney and brain tissue extracts.

Importantly, although the co-IP and EMSA experiments supported the interaction between aldolase C and the NF-L mRNA, no indication was available about the possibility that the aldolase C-RNA interaction occurred directly. In order to shed light on this point, additional EMSA experiments were performed (Fig. 3.10a) by incubating *in vitro* the ³²P NF-L mRNA probe with a recombinant GST-aldolase C protein (Fig. 3.10b). As a positive control of the experiment, the same probe was incubated with a second protein, namely TDP43, an actual RNA-binding protein that preferentially binds UG repeats but that has also been found to interact with the NF-L mRNA by recognizing a non-UG repeat sequence (Strong et al., 2007). Whereas the interaction with the NF-L mRNA was confirmed for the positive control, the TDP43 protein (Fig. 3.10a lane 2), this *in vitro* approach did not reveal any direct binding between aldolase C and the NF-L mRNA (Fig. 3.10a lanes 3,4,5) since no retarded band was observed when the probe was incubated with this protein.

Provided that TDP43 binds directly to the NF-L mRNA and that aldolase C is involved in the complex interacting with the NF-L mRNA, it was also investigated if aldolase C and TDP43 proteins interact with each other. To this aim, an EMSA supershift test was performed by simultaneously incubating the two proteins with the ³²P-labeled NF-L mRNA probe: as shown in Fig. 3.10a (lanes 6,7,8), no supershift was observed in comparison to the retarded band that was generated by the single incubation of TDP43 with the probe. This result indicated that aldolase C and TDP43 proteins do not interact with each other and suggested that the aldolase C recruitment in the context of an NF-L mRNA-binding complex could not be mediated by TDP43.

a)



b)

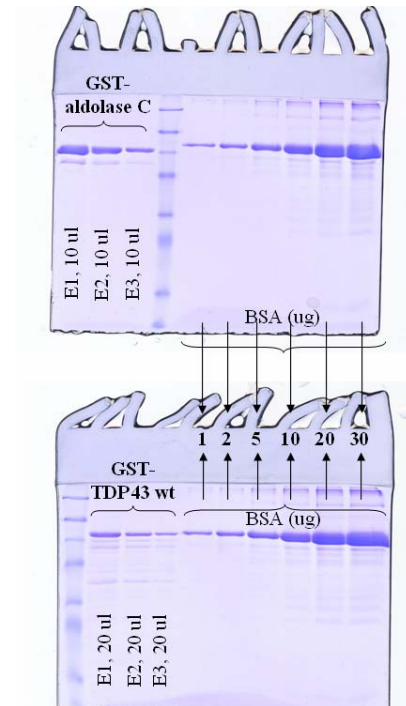


Fig. 3.10. EMSA with the ³²P-labeled NF-L RNA probe and recombinant GST-aldolase C and GST-TDP43 proteins. a) autoradiogram of EMSA run on a 4% non-denaturing PAGE; b) expression of GST-aldolase C and GST-TDP43 in *E. coli* (see paragraph 2.26 for details).

The absence of detectable protein-protein interaction between aldolase C and TDP43 was further demonstrated using a second different probe: these proteins were simultaneously incubated with a 20-nt ³²P-labeled RNA molecule containing (UG)₆ repeats, which is the sequence motif bound by TDP43 with higher affinity. Even using this probe, it was not possible to reveal a supershifted band (Fig. 3.11), thus confirming the results obtained with the ³²P-labeled NF-L mRNA probe.

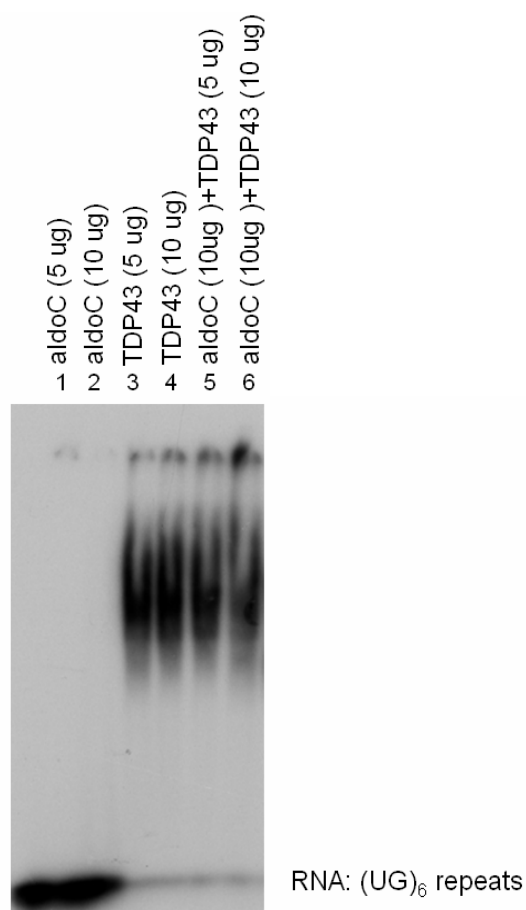


Fig. 3.11. EMSA with (UG)₆ repeats RNA probe and recombinant GST-aldolase C and GST-TDP43 proteins. Autoradiogram of EMSA run on a 6% non-denaturing PAGE.

3A.4.3 The protein-RNA UV cross-linking assay confirm the absence of direct binding between aldolase C and the NF-L mRNA.

To definitively rule out the direct binding between aldolase C and the NF-L mRNA, this interaction was further investigated by performing a protein-RNA UV cross-linking assay. The rationale behind the choice of this approach was that irradiation with UV light causes the formation of covalent bonds between the radiolabeled nucleic acid and the interacting proteins: consequently, even weak interactions are easily detectable, since the binding is stabilized through the formation of irreversible bonds. Briefly, the assay was performed by incubating the ³²P-labeled NF-L mRNA probe with purified GST-aldolase C or GST-TDP43 and by irradiating the samples with UV light. The unbound RNA was digested with RNase A and the complex formation was verified by 10% SDS-PAGE gel electrophoresis followed by autoradiography. As shown in Fig. 3.12, the assay confirmed the absence of direct binding between aldolase C and the NF-L mRNA, since it was not possible to reveal any radioactive signal when this protein was incubated with the probe (lane 2), whereas the ability to bind the NF-L mRNA was confirmed again for TDP43 (lane 1).

An explanation for the different data obtained by Canete-Soler and colleagues relies on the possibility that the observed interaction between aldolase C and the NF-L mRNA might be not direct, but could be mediated by one or more binding partners within the NF-L mRNA-binding complex.

In conclusion, these data allowed to confirm the hypothesis of an involvement of aldolase C in the NF-L mRNA physiology but led us to consider more carefully the RNA-binding ability as a novel activity of aldolase C. How the aldolase C is recruited in an NF-L mRNA-binding complex needs to be clarified but the absence of a direct interaction between aldolase C and TDP43 proteins demonstrates that it is not even mediated by TDP43. Our finding of an *in vivo*

interaction between aldolase C and the 14-3-3 γ protein suggests the possibility that the 14-3-3 γ protein, through its well known scaffolding function, might tether aldolase C on the transcript. Additional approaches, such as EMSA experiments performed incubating simultaneously the aldolase C and the 14-3-3 γ proteins with the NF-L mRNA probe or immunofluorescence assays designed to *in vivo* verify their co-localization on the transcript, will help to address this hypothesis. However, it is also important to consider that additional biological reasons could exist behind this novel protein-protein interaction, as 14-3-3 proteins participates in a very broad spectrum of biological processes, including a second neuronal specific process in which also aldolase C seems to be involved: the NGF-induced neuronal differentiation.

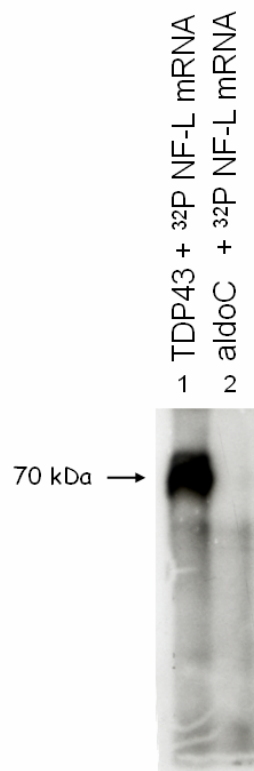


Fig. 3.12. UV-crosslinking using ³²P-labeled NF-L mRNA fragment and recombinant GST-aldolase C and GST-TDP43 proteins.

3A.5 Evaluation of aldolase C expression response after NGF administration in the PC12 cell line.

The PC12 cell line, established in 1976 from rat adrenal pheochromocytoma, is worldwide considered a useful model system for neurobiological studies, because of its ability to reversibly differentiate into a neuronal-like phenotype when exposed to nerve growth factor (NGF). It has been extensively demonstrated that NGF-treatment of PC12 cells results in the extension of long and branching neuronal-like processes, that progressively degenerate if NGF is removed (Greene and Tischler, 1976). At the molecular level, it has been presented evidence that NGF, through Trk receptors, lead to neurite outgrowth and cell cycle exit, by activating rap1 and its signalling kinase effector B-raf (Kao et al., 2001). Interestingly, literature data report that the transcriptional changes promoted by NGF in PC12 cells, includes a significant increase in 14-3-3 γ transcript (Angelastro et al., 2000; Greene and Angelastro, 2005) and that 14-3-3 proteins are critical regulators of B-raf activity (Dougherty and Morrison, 2004; Qiu et al., 2000). Particularly, it has been demonstrated that a point mutation in B-raf, compromising its capacity to interact with 14-3-3 proteins, affects NFG-induced differentiation of PC12 cells (MacNicol et al., 2000), thus ascribing a dominant role to 14-3-3 proteins in a so crucial biological process. An involvement in neuronal differentiation was also proposed for aldolase C, as a consequence of its heterogeneous expression in different cell types of neonatal rat forebrain: it was proposed that aldolase C expressing cells provide support to stimulate maturation and migration of other cells during cerebellar development (Staugaitis et al., 2001). Given these evidences, preliminary experiments were performed in the present study to investigate the possible involvement of aldolase C in the NGF-induced neuronal differentiation process. To this aim, the PC12 model system was used to evaluate the specific cellular response to the NGF-stimulation, with regard to aldolase C

protein expression. Cells were cultured for three days (72 h) in the absence or presence of this neurotrophin (100 ng/ml), respectively. They responded to the NGF-treatment showing the expected neuronal-like phenotypic modification, in contrast to the classical roundish shape presented by the not-treated cells (Fig. 3.13). Interestingly, immunoblot assays demonstrated a significantly higher expression of the aldolase C protein in the NGF-treated PC12 cells versus the not stimulated ones: densitometry analysis revealed an increase higher than two-fold in protein levels, compared to the not-treated condition that was considered as the basal point (Fig. 3.14).

The increased aldolase C expression in response to NGF-stimulation is consistent with the hypothesis of an involvement of this protein in the NGF-mediated differentiation process. Indeed, it is believed that they are the changes in gene transcription and protein expression promoted by neurotrophins that influence, in turn, the ways that cells respond to trophic factors. Our results represent only preliminary data supporting the possible implication of aldolase C in neuronal differentiation. Of course, the higher aldolase C expression in response to NGF-stimulation might simply reflect a boost of glycolysis during neuronal differentiation. However, the concomitant increase in aldolase C and 14-3-3 γ expression after NGF-stimulation in PC12 cells, considered together with the corroborated importance of 14-3-3 proteins in neuronal development and differentiation, also introduces the possibility that an additional functional role for the protein-protein interaction between aldolase C and 14-3-3 γ proteins could arise from this neuronal specific process.

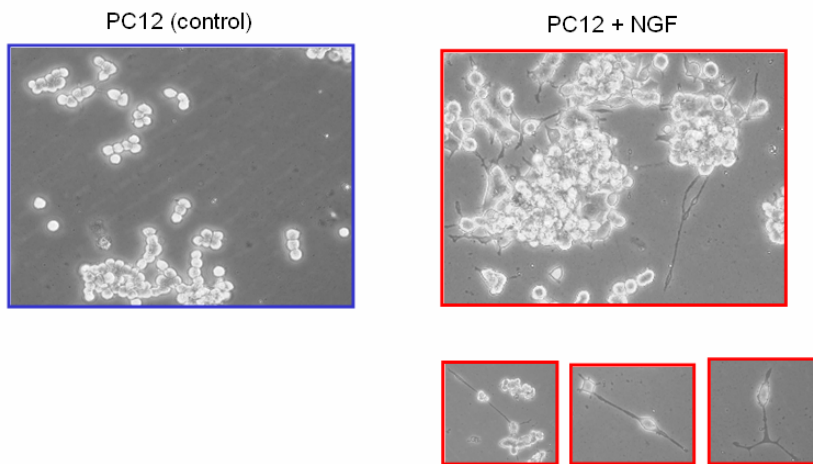


Fig. 3.13. NGF promotes the formation of neurite-like processes in PC12 cells.

Left: negative control. Right: neurite outgrowth in PC12 cells stimulated for 3 days with 100 ng/ml NGF.

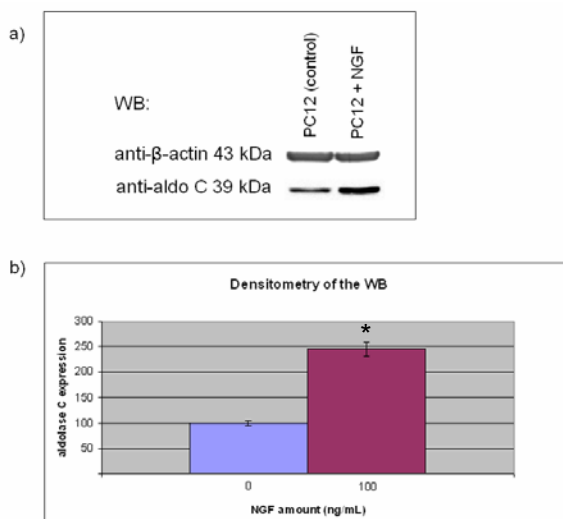


Fig. 3.14. NGF increases the levels of aldolase C in PC12 cells.

a) anti-aldolase C immunoblot analysis of total protein extracts obtained from control and NGF-stimulated (72h) PC12 cells. β -actin served as loading control. b) Densitometry analysis of the immunoblot: results represent the average of three independent experiments. * $P < 0.05$ versus PC12 (control).

PART B

Antigenic characterization of monoclonal anti-human aldolase C antibodies.

Only a few anti-aldolase C antibodies are commercially available and, all of them are polyclonal. As discussed in the introductory section (paragraph 1.9), the quality of results obtained with monoclonal antibodies (mAbs) is generally more consistent of those derived from polyclonal antibodies (pAbs) and, consequently, their use is strongly suggested, particularly while working with proteins (like aldolase C) for which paralogs exist. Therefore, during this PhD program, our research group commissioned the ProMab Biotechnologies, Inc. (Richmond, CA) to produce specific monoclonal anti-human aldolase C antibodies. The American company was able to provide two anti-aldolase C mAbs, whose antigenic characterization constituted a task of this PhD project.

3B.1 Monoclonal antibodies preparation.

The anti-aldolase C mAbs were produced, in mouse, using as immunogen the full length human protein expressed in fusion with an His₇-tag at the N-terminus.

To this aim, the human cDNA encoding the full length aldolase C protein was cloned in the pET16b+ vector and subsequently expressed and affinity purified in *E. coli* BL21DE3 cells. The resulting recombinant product was shipped to the ProMab company where it was used first as immunogen to achieve monoclonal antibodies production and, subsequently, as test antigen to verify the immunoreactivity of the primary antibodies obtained. All the clones derived from the immunization procedure were identified by a distinctive alpha-numeric code. Two of these, showing the stronger immunoreactive signals, were selected within the whole set and the corresponding monoclonal antibodies were finally purified from the company. The identity codes of these two lastly chosen clones were 9F1B5 and 2A3E8, hereinafter indicated as 9F and 2A mAbs, respectively. The specificity of these mAbs for aldolase C was investigated and a complete epitope-mapping was performed. Moreover the antibodies were tested for use in applications including immunoblotting, ELISA and immunoprecipitation. A detailed description of the experimental strategy carried out is reported.

3B.2 Isozyme specificity of the 9F and 2A mAbs.

As already discussed in the introductory section, aldolases isoforms share a very high percentage of sequence identity and similarity. Starting from this evidence, the possible cross-reactivity of the generated mAbs was taken into consideration. So, first of all, the 9F and 2A mAbs were tested to assess their specificity for the recognition of the aldolase C isozyme. To this aim, immunoblot experiments were performed on total protein extracts obtained from mouse brain, kidney, liver and heart tissues. As shown in Fig. 3.15, a specific positive signal, corresponding to

the molecular weight of aldolase C (39 kDa), was observed only in the brain tissue extract. On the contrary, no cross-reactivity was demonstrated by these mAbs with any other aldolase isoform, as proven by the absence of ECL detection in liver, kidney and heart tissues, where aldolases A and/or B but not C are expressed. These results demonstrated the high specificity of the 9F and 2A mAbs for the aldolase C isozyme.

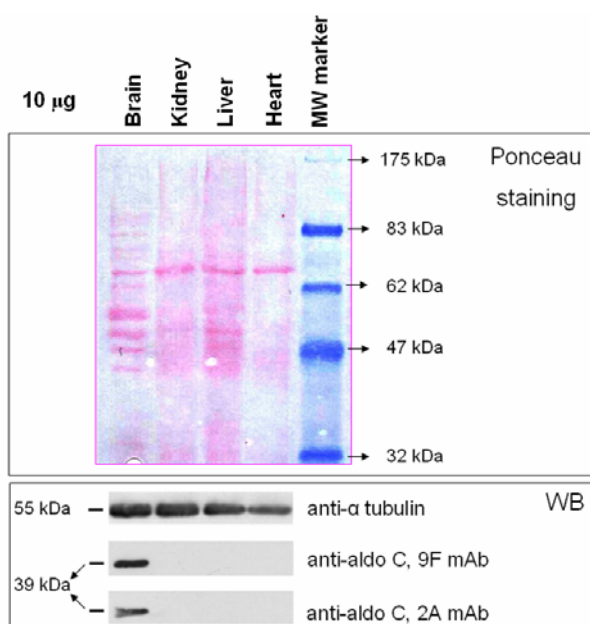


Fig. 3.15. Western blot with the anti-aldolase C 9F and 2A mAbs. ECL detection of aldolase C protein expression in heart, liver, kidney and brain tissue extracts. Proteins were separated by 12% SDS-PAGE and probed with the anti-aldolase C 9F and 2A mAbs. α -tubulin immunoblot and Ponceau staining served as loading controls.

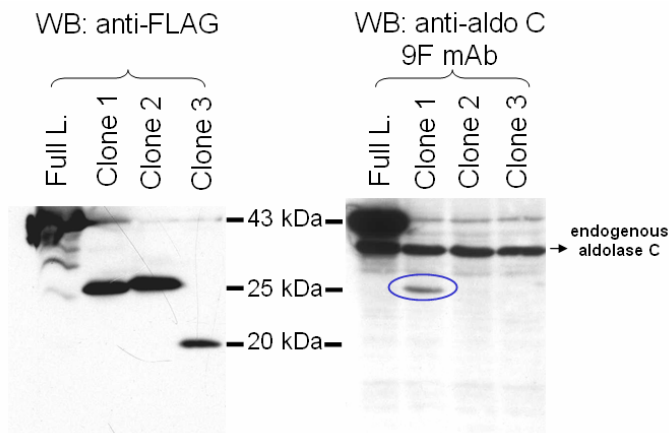


Fig. 3.17. Western blot analysis, using the 9F mAb, of total protein lysates from Neuro2a cells alternatively transfected with the 3xFLAG tagged full length (Full. L.), clone 1, clone 2 or clone 3 fusion products. Proteins were separated by 15% SDS-PAGE and probed with an anti-FLAG antibody (left panel) and with the anti-aldolase C 9F mAb (right panel).

As observed in the immunoblot panel (Fig. 3.17), the 9F mAb was able to detect 3 proteins of different molecular weights. The intermediate-molecular-weight band (corresponding to 39 kDa), was present in all the four tested lanes, as expected because of the expression of endogenous aldolase C in Neuro2a cells. On the contrary, among the 3xFLAG-tagged aldolase C products, only the exogenous full length (43 kDa; Fig. 3.17, lane 1 of the right panel) and clone 1 proteins (26 kDa; Fig. 3.17, lane 2 of the right panel) were recognized by the 9F mAb, whereas those encoded by clone 2 and clone 3 were not. This experiment clearly showed that the epitope recognized by the 9F mAb was included in the clone 1 macrodomain (spanning from aa 1 to aa 210 of the human aldolase C protein); moreover, it also demonstrated that the epitope was specifically localized within the 1-100 aa region, as proven by the absence of ECL detection toward clone 2 that overlaps clone 1 from aa 101 to aa 210. To confirm this finding, we further split the clone 1 macrodomain into two additional sub-clones, namely clone 1A

(including amino acids from 1 to 100) and clone 1B (including amino acids from 101 to 210) (Fig. 3.18; Table A).

Immunoblot assays, performed after transfection of these two additional sub-clones, confirmed that the epitope recognized by the 9F mAb was localized within the N-term region of the aldolase C protein spanning from aa 1 to aa 100. Indeed, the 9F mAb detected the sub-clone 1A (15 kDa) but not the sub-clone 1B (16 kDa) (Fig. 3.19).

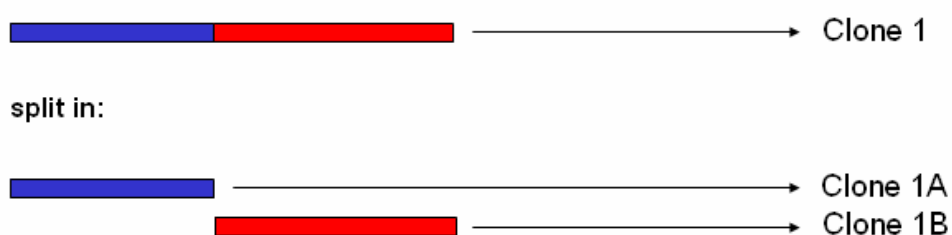


Fig. 3.18. Scheme of the two additional sub-clones, namely clones 1A and 1B, produced in the 3xFLAG CMV 7.1 vector. The corresponding clone names are reported on the right. The amino acidic limits of each sub-domain have been previously specified in Fig. 3.16 and Table A.

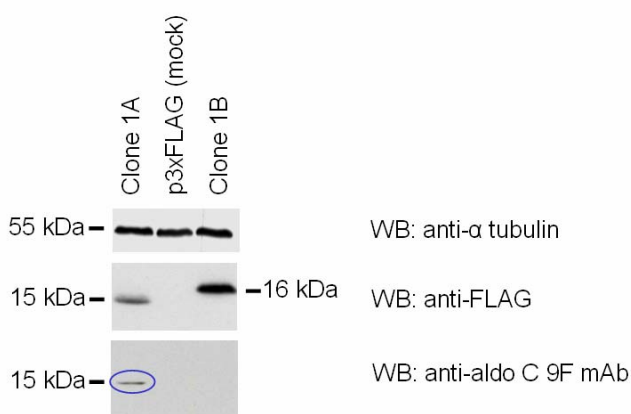


Fig. 3.19. Western blot analysis, using the 9F mAb, of total protein lysates from Neuro2a cells alternatively transfected with the 3xFLAG tagged clone 1A and clone 1B fusion products or mock transfected. Proteins were separated by 15% SDS-PAGE and probed with an anti-FLAG antibody (to verify transfection) and with the anti-aldo C 9F mAb (lower panel). α-tubulin served as loading control.

Once identified the aldolase C protein macrodomain targeted by the 9F mAb, we repeated the same immunoblot approach using the second antibody obtained from ProMab, the 2A mAb. Particularly, the five clones produced and just introduced (clone1, clone2, clone3, clone 1A, clone 1B) were examined again, aiming to understand if the epitope targeted by the 2A mAb was included in the same macrodomain targeted by the 9F mAb or it was, otherwise, located in a different region of the protein. Interestingly, the 2A mAb detected the endogenous aldolase C protein and the 3xFLAG-tagged products full length, clone1 and clone 1A (Fig. 3.20) thus revealing the same pattern of immunoreactive signals observed using the 9F mAb.

This experiment demonstrated that also the 2A mAb target an epitope localized within the region spanning from aa 1 to aa 100 of the human aldolase C protein, prompting to focalize on this discrete N-terminal macrodomain of the enzyme in the following steps of the work.

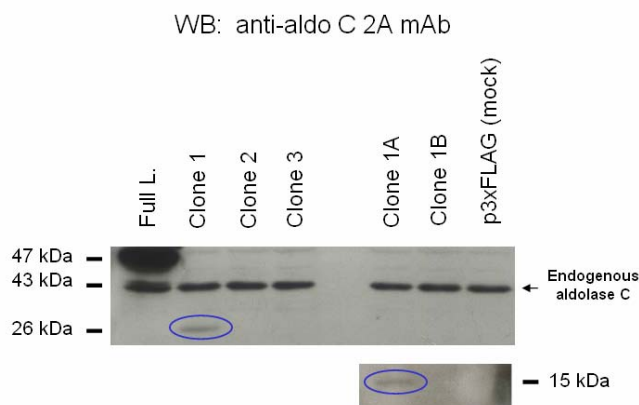


Fig. 3.20. Western blot analysis, using the 2A mAb, of total protein lysates from Neuro2a cells alternatively transfected with the 3xFLAG tagged full length, clone 1, clone 2, clone 3, clone 1A, clone 1B fusion products or mock transfected. Proteins were separated by 15% SDS-PAGE and probed using the anti-aldolase C 2A mAb.

3B.4 Aldolase A vs aldolase C: sequence alignment of residues 1-100.

Once identified the protein macrodomain retaining immunoreactive properties, the real goal was to achieve a fine antigenic characterization of the two monoclonal antibodies by restricting the localization of the target epitopes to a small peptidic sequence of the human aldolase C protein.

Considering the high recognition specificity demonstrated by the 9F and 2A mAbs toward the aldolase C isozyme, we deduced that an amino acidic stretch including some aldolase C isozyme-specific residues and located inside the 1-100 aa macrodomain of the protein, should have been responsible of the epitope specificity. In order to identify the putative minimal epitope-containing regions within this N-terminal macrodomain, we decided to select those 16-mer/18-mer peptides containing the aldolase C-specific-residues (as compared to aldolase A). To this aim, we first compared the N-term 100 amino acids primary sequence of the human aldolase C protein with the corresponding region of the human aldolase A isoform, the ubiquitous form of the isozyme that shares the higher percentage of sequence identity to aldolase C. The sequence alignment was performed using the "ClustalW2-Multiple Sequence Alignment" software, available on the EMBL-EBI website (www.ebi.ac.uk/Tools/msa/clustalw2). Fig. 3.21 shows the visual identification of four main regions containing most of the aldolase C isozyme-specific residues (blue boxes): one of these regions had to be related, in our opinion, to the epitope-specificity demonstrated by the 9F and 2A mAbs.

ClustalW2 Results

[Alignments](#)[Result Summary](#)[Guide Tree](#)[Submission Details](#)[Submit Another Job](#)

Alignment

MUSCLE (3.8) multiple sequence alignment

```
1 60
AldoA  MPYQYPALTPEQKKEKELSDIAHRIVAPGKGILAADESTGSI AKRLQSIGTENT EENRRFYR
AldoC  MPHYPALSAEQKKEKELSDIALRIVAPGKGILAADESVGSM AKRLSQIGVENT EENRRLYR
**:.****:..***** ***** ..**:.****. **.*****: **
61 120
AldoA  QLLLTADDRVNPCIGGVILFHETLYQKADDGRPF P QVIKSKGGVVG IKV DKG VVPLAGTN
AldoC  QVLF SADDRVKKCIGGVIF FHETLYQKDDNGV PFV RTIQDRG I VVG IKV DKG VVPLAGTD
*.:.:****: ***** *:* ** ..:.* *****:*****:
```

Fig. 3.21 Sequence alignment between residues 1-100 of the human proteins aldolase A and aldolase C. The sequences were aligned using the “ClustalW2-Multiple Sequence Alignment” software. The blue boxes highlight the four main regions where they are localized most of the aldolase C isozyme specific residues.

3B.5 “ElliPro” analysis of the tertiary structure of the human aldolase C protein.

Aiming to find additional support for this hypothesis and to better set the limits of the peptidic sequences to be tested as the putative epitope-containing regions in the following steps of the study, the aldolase C 1-100 aa macrodomain was further analyzed by using a second bioinformatic tool, the ElliPro software. This software is a new structure-based tool that predicts antibody epitopes in protein antigens (Ponomarenko et al., 2008). Particularly, ElliPro is a web accessible application, available at <http://tools.immuneepitope.org/tools/ElliPro>, that predicts and visualizes putative antibody epitopes in a given protein sequence or structure, considering the demonstrated correlation between antigenicity, solvent accessibility and flexibility in proteins (Novotny et al., 1986). This software accepts two types of input data: protein sequence or structure. Indeed, when the protein

structure of interest is not available, a modeller method included in the software predicts the 3D structure of the protein starting from the knowledge of its primary sequence. ElliPro implements three algorithms performing the following tasks: i) approximation of the protein shape as an ellipsoid; ii) calculation of the residue protrusion index (PI) and iii) clustering of neighbouring residues based on their PI values. Remarkably, for each residue the PI value indicates the percentage of the aa mass that lies outside the ellipsoid. This PI value can vary between 0 and 1 and the higher it is, the higher is the percentage of the residue's mass lying outside the ellipsoid, being therefore exposed on the protein surface. A PI score equal or higher than 0.7 is generally associated to a very pronounced residue exposition on the protein surface. ElliPro suggests the user to never set the minimum residue score (protrusion index, PI value) lower than 0.5. The output score for each predicted epitope is then defined as a PI value averaged over epitope residues. Taking advance of the availability of the aldolase C crystal structure (Arakaki et al., 2004), we performed the ElliPro analysis using as input data the four-character PDB ID of the aldolase C protein, 1XFB, and fixing the PI value 0.5 as the threshold residue score for epitope prediction. The software highlighted 12 putative antibody epitopes distributed throughout the whole protein. We focused our attention on the 4 epitopes localized within the first N-term 100 amino acids of our interest (Fig. 3.22 a, red arrows). A molecular viewer, included in the ElliPro software, allowed the visualization of the predicted epitopes on the 3D protein structure. As shown in Fig. 3.22 b, they were obviously all located on the protein surface, being accessible for putative antibody binding.

Fig. 3.22 a)

EliPro: Antibody Epitope Prediction Results

Protein Sequence(s):

Chain	Sequence
A	1 HSYPALSAEQ KKELSDIALR IVAPGKGILA ADESVGSMAS RLSQIGVENT EENRRLYRQV 61 LFSADDRVKK CIGGVIFHE TLYQKDDNGV PFVRTIQDKG IVVGKVDKG WVPLAGTDGE 121 TTTQGLDGLS ERCAQYKKG ADFAKWRCVL KISERTPSAL AILEMANVLA RYASICQNG 181 IVPIVEPEIL PDGDHDLKRC QYVTEKVLAA VYKALSDHHV YLEGTLLKPN MVTPGHACPI 241 KYTPEEIAMA TVTALRRTVP PAVPGVTFLS GGQSEEEASF NLNAINRCPL PRPWALTFYSY 301 GRALQASALN AWRGQRDNAG AATEEFIKRA EVNGLAAQ GK YE

Predicted Linear Epitope(s):

No.	Chain	Start Position	End Position	Peptide	Number of Residues	Score	3D Structure
1	A	114	122	VPLAGTDGE	9	0.851	View
2	A	3	18	HSYPALSAEQKKELSD	16	0.832	View
3	A	85	93	YQKDDNGVP	9	0.800	View
4	A	312	327	NAWRGQRDNAGAATEE	16	0.792	View
5	A	41	58	AKRLSQIGVENTEENRRL	18	0.751	View
6	A	340	344	QGKYE	5	0.750	View
7	A	235	251	TPGHACPIKYTPEEIAM	17	0.739	View
8	A	153	166	KISERTPSALAILE	14	0.716	View
9	A	289	296	RCPLRPW	8	0.704	View
10	A	193	204	PDGDHDLKRCQY	12	0.668	View
11	A	126	133	QGLDGLSE	8	0.631	View
12	A	65	73	SADDRVKKC	9	0.561	View

Fig. 3.22 b)

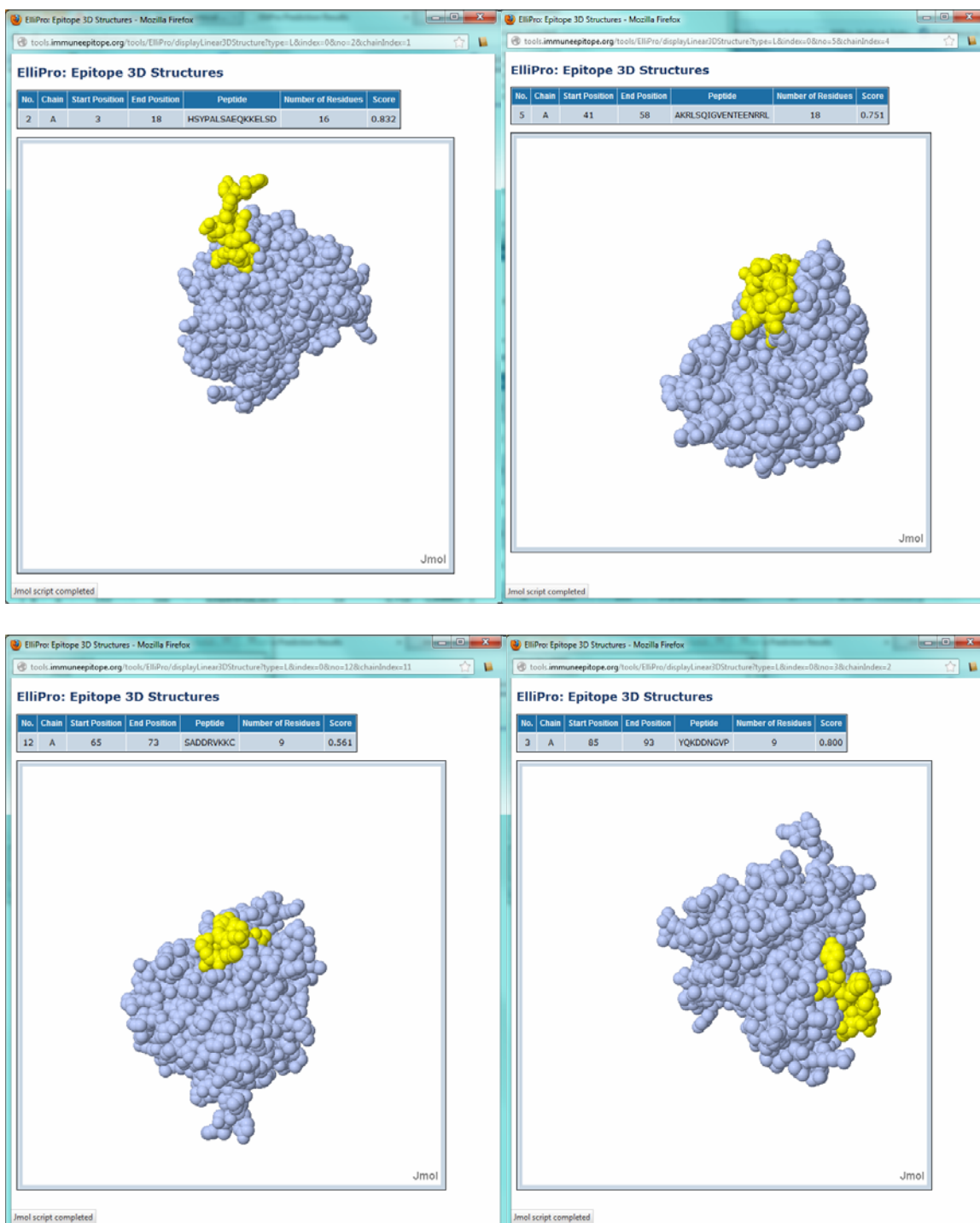


Fig. 3.22. “ElliPro” analysis of the human aldolase C protein.

a) 12 putative antibody epitopes were predicted throughout the whole protein: 4 of these (red arrows) were localized within the first 100 N-term amino acids.

b) Visualization of the four predicted epitopes of interest on the 3D protein structure.

Interestingly, the four peptides highlighted by ElliPro as putative antibody epitopes all overlapped, at least partially, those selected through the ClustalW2 analysis of the protein primary structure (Fig. 3.23 red lines vs blue boxes). Therefore, the data obtained using the two independent bioinformatic approaches were compared and partially merged, leading to the final definition of 4 peptide sequences of 16-18 amino acids each (Fig. 3.23 green lines) to be further tested as the putative epitope-containing regions in the next steps of the antibodies characterization.

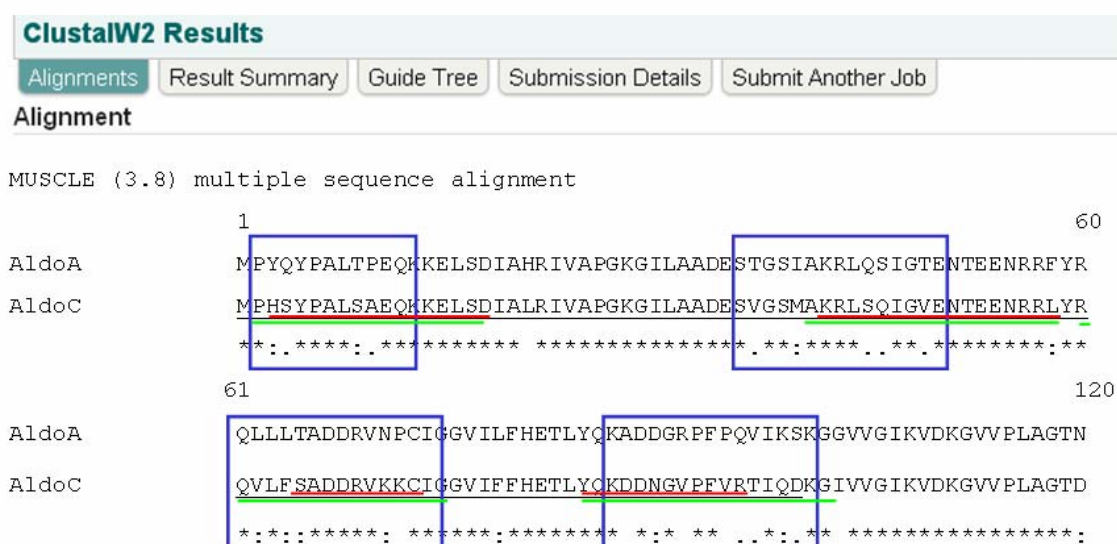


Fig. 3.23. Selection of the 4 putative epitope-containing peptides of the human aldolase C protein. The four peptides highlighted by ElliPro as putative antibody epitopes (red lines) all overlapped, at least partially, those selected through the ClustalW2 analysis of the protein primary structure (blue boxes). The four peptides finally chosen to be tested as the putative epitope containing regions (green lines) were defined also by taking into account technical problems of peptide synthesis.

The four chosen peptides are recapitulated in the table below (Table H): their precise lengths (and amino acidic sequences) were defined also taking into account technical problems associated with peptides syntheses (i.e. the need to reach a minimal peptide length compatible with the proper native folding and/or the necessity to avoid the presence of negatively charged residues in terminal positions). As described in the materials and methods section, these four peptidic sequences were produced in both a biotinylated form (see Table F) to perform ELISA assays, and fused to a GFP-tag (see Table B) to perform immunoblot experiments.

Table H. *Human aldolase C peptides.*

Amino acidic limits of aldolase C peptides	peptide sequence
2-17	PHSYPALSAEQKKELS
41-58	AKRLSQIGVENTEENRRL
60-75	RQVLFSADDRVKKCIG
85-102	YQKDDNGVPPFVRTIQDKG

3B.6 ELISA screening of biotinylated aldolase C peptides.

To test whether and which one of the four aldolase C peptides demonstrated immunoreactive properties, we first performed an enzyme-linked immunosorbent assay (ELISA). The ELISA test was performed by spotting the 4 different biotinylated aldolase C peptides in specific positions of a 96 well plate. The plate wells were coated with streptavidin; so peptides immobilization was achieved through biotin-streptavidin capture (Fig. 3.24).

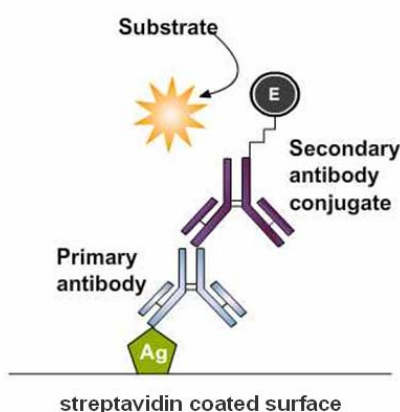


Fig. 3.24. Indirect-ELISA method used in this study. The biotinylated aldolase C peptides were immobilized through streptavidin capture. The unlabeled primary antibodies of interest (9F or 2A mAbs) were used in conjunction with a labeled secondary antibody, as described in the text.

After peptides immobilization, the 9F and 2A mAbs were added as test samples to investigate their ability to detect the immobilized peptides. In particular, four different mAbs dilutions (1:5000; 1:10000; 1:20000; 1:40000) were tested in the experiment. For both mAbs, they were prepared starting from stock solutions characterized by the same value of antibody concentration (1.8 mg/ml); each different dilution was always assayed in duplicate. Following primary antibody binding, an anti-mouse HRP conjugated secondary antibody and an appropriate substrate solution (3,3',5,5' tetramethylbenzidine) were added to each well, allowing the development of a yellow colorimetric reaction only whether a specific

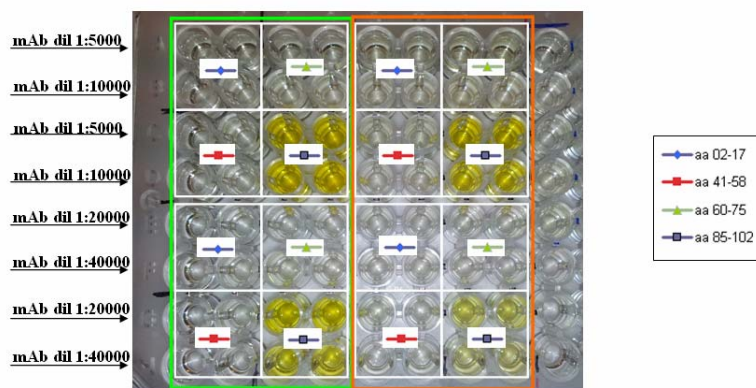
peptide-antibody interaction occurred. With both antibodies, the colorimetric reaction was observed only in the wells containing the peptide 85-102 (Fig. 3.25 a). This result unequivocally demonstrated that the specific epitope recognized by both the 9F and the 2A mAbs was located within the short peptidic region of the human aldolase C protein encompassing amino acids 85-102. Moreover, both the antibodies showed an high immunoreactive sensitivity toward this peptide: indeed, the colorimetric reaction developed in all the four condition tested, even when the antibodies were strongly diluted. The specific enzymatic response, occurred in each well of the ELISA plate, was recorded and spectrophotometrically measured at 450 nm, using an appropriate plate reader. The resulting data were analyzed and plotted on a graph, relating the measured absorbance values to the corresponding mAb dilution factors (Fig. 3.25 b). These data revealed an almost perfect reproducibility between the duplicate samples (as demonstrated by the small and sometimes not visible error bars), and further demonstrated the high detection sensitivity of both the tested mAbs, also at very low antibodies concentrations (1:40000 dilution). Furthermore, this ELISA assay allowed us to reveal a slightly higher sensitivity of the 9F clone over the 2A one. Indeed, the absorbance values measured with the 9F mAb in the wells containing the 85-102 aa peptide were always higher than those observed with the 2A mAb, in all the dilution conditions tested.

Taken together these results allowed us:

- to drastically narrow the position of the epitope targeted by the 9F and 2A mAbs to a small region consisting of 18 amino acids and spanning residues 85-102 of the aldolase C protein.
- to demonstrate that the two antibodies are very sensitive in detecting their target antigens.
- to verify that they are suitable to be used in ELISA applications.

- to prove that they are able to bind the target epitope when the immunogen is free to fold in its tertiary structure (ELISA assay), as well as when the immunoreactivity is tested in denaturing conditions (Immunoblotting).

a)



b)

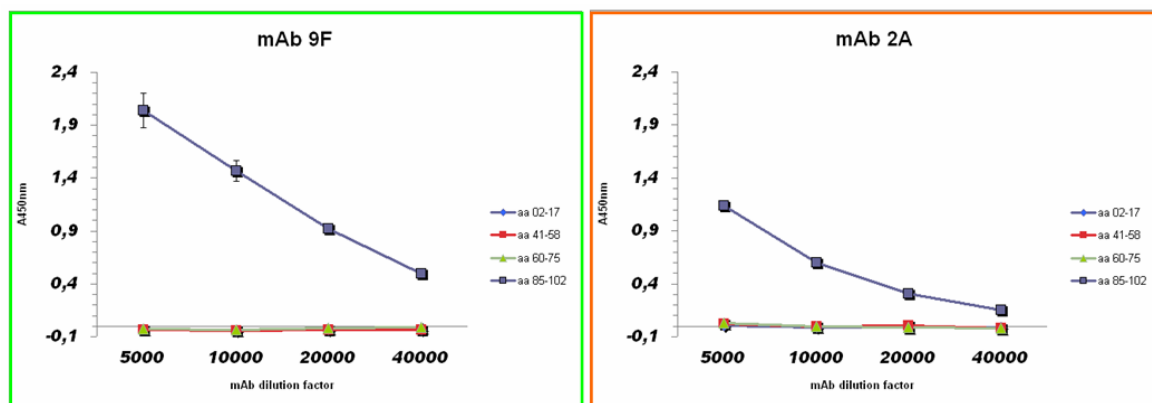


Fig. 3.25. ELISA screening of biotinylated aldolase C peptides. The four test peptides are differentially represented as reviewed in the figure. Four different dilution factors for each one of the two antibodies were tested in the experiment (1:5000; 1:10000; 1:20000; 1:40000).

a) development of colorimetric reaction when the 9F and 2A mAbs are incubated with the 85-102 aa aldolase C peptide. b) spectrophotometric quantification of the specific enzymatic response: x axis, mAb dilution factors; y axis, absorbance values measured at 450 nm.

3B.7 Epitope mapping in eukaryotic cells confirms specificity of the 9F and 2A mAbs for peptide 85-102.

A complementary strategy was applied to test and confirm the epitope mapping results obtained with the ELISA assay. To this aim, the cDNA sequences encoding for the 4 selected peptides of interest were cloned in the pEGFP-C2 vector, to express them with a GFP tag fused to their N-terminus (Table B). The four pEGFP-C2 clones were transfected in Neuro2a cells and, 48 h after transfection, the resulting total protein extracts were assayed by immunoblots. When the membrane was probed with an anti-GFP antibody, comparable expression levels of all clones were observed (Fig. 3.26, anti-GFP immunoblot). Then, when the membrane was probed with the 9F or the 2A mAbs, it was possible to reveal the occurrence of ECL detection only toward the fusion protein GFP+aldolase C aa 85-102 (Fig. 3.26, 9F and 2A mAb immunoblots). Therefore, the assay definitively confirmed the epitope localization within residues 85-102 of the human aldolase C protein. For a complete overview of the constructs that allowed the progressive identification of the epitope-containing region targeted by the 9F and 2A mAbs, the 3xFLAG-tagged full length aldolase C protein and the clone 1A fusion product (containing the 1-100 aa aldolase C macrodomain) were also included in the immunoblot panel of Fig. 3.26.

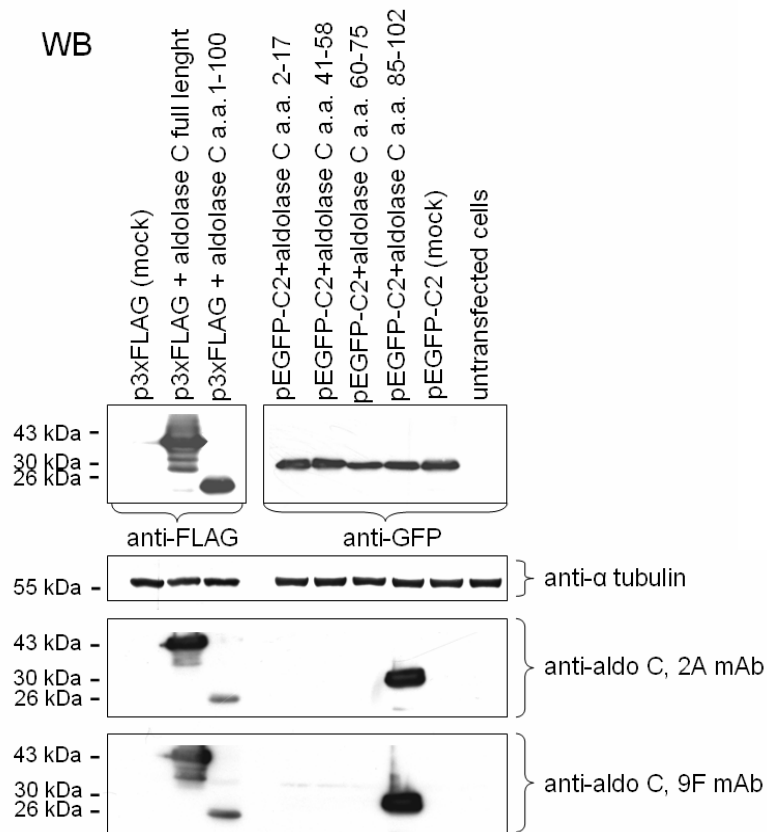


Fig. 3.26. Western blot analysis of aldolase C peptides expressed in fusion with a GFP tag at the N-term. Total protein extracts obtained from Neuro2a cells alternatively transfected with the four pEGFP-C2 recombinant clones (see Table B for details), mock transfected or not transfected were separated by 12% SDS-PAGE and probed using the anti-aldolase C 9F and 2A mAbs. To have a complete overview of the epitope-mapping, the 3xFLAG-tagged full length aldolase C and clone1A fusion proteins were included in the immunoblot panel. α -tubulin served as loading control; anti-FLAG and anti-GFP antibodies were used to verify the transfections.

3B.8 Evaluation of the anti-aldolase C 9F mAb efficiency in the immunoprecipitation application.

The experimental strategy described above successfully led to map the epitope targeted by the 9F and 2A mAbs but also revealed that the two antibodies were directed against epitopes localized within the same punctual region of the aldolase C protein. Therefore, 9F and 2A mAbs should be considered as “equivalent tools”. Starting from this finding, only the 9F mAb was tested for immunoprecipitation protocols. To this aim, the total protein extract obtained from adult mouse brain was used as input sample, because of the specific expression of the aldolase C protein in the CNS. The 9F mAb was used for both the immunoprecipitation step and for the following immunoblot analysis of the IP result. As shown in Fig. 3.27, the assay revealed that the 9F mAb performs very efficiently also in the immunoprecipitation application. Indeed, the immunoreactive aldolase C signal was observed in the IP fraction whereas no ECL detection occurred in the negative control lane, demonstrating a high specificity of the 9F mAb in immunoprecipitating the aldolase C isozyme.

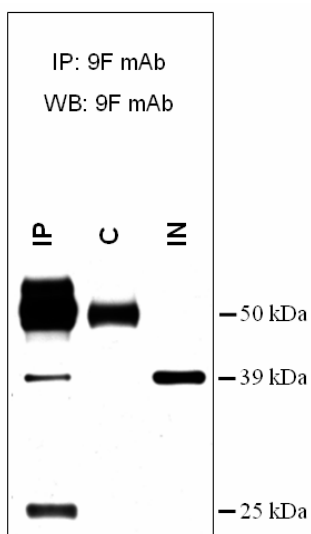


Fig. 3.27. Aldolase C immunoprecipitation using the anti-aldolase C 9F mAb. The endogenous aldolase C (39 kDa) was immunoprecipitated using the 9F mAb (IP) from adult mouse brain total protein extract (IN). Mouse IgG were used in the negative control (C). Immunoblot analysis of the IP result was performed using the anti-aldo C 9F mAb.

3B.9 Epitope mapping of 9F and 2A mAbs: discussion and conclusions.

Epitope mapping involves the definition of the binding site of an antibody to its target protein. The multiple methodologies applied in this work allowed to precisely localize the epitope targeted by the 9F and 2A mAbs to a short peptidic region of the aldolase C protein, consisting of eighteen amino acids and spanning residues 85 and 102 of the enzyme sequence.

It is important to recall that the 9F and 2A mAbs were initially selected within a broader group of mAbs-producing clones that were developed by ProMab using as immunogen the full length isozyme and not against a discrete region of the human aldolase C protein. The finding that both the 9F and 2A mAbs targeted an epitope localized exactly in the same region of the aldolase C protein should not go unnoticed, suggesting that a very strong immunogenicity may be associated to this epitope-containing region.

The peptidic region 85-102 of the human aldolase C protein is localized on the protein surface and is characterized by the presence of aldolase C isozyme-specific residues. Particularly, it would be possible to speculate that a key role in determining the specific immunogenicity associated to this sequence is played by the following amino acids: Asn 90, Val 92, Arg 96, Asp 100. In fact, these residues are specifically present in the aldolase C isozyme, being never observed in the corresponding amino acidic positions of the human aldolase A and/or aldolase B enzymes. Moreover, as calculated by the ElliPro software, these residues represent four out of the nine amino acids of the 85-102 peptide possessing a protrusion index higher than 0.7 (Fig. 3.28 a and b), thus resulting particularly exposed on the protein surface. The presence of a Pro residue in position 93, lying exactly in the middle of the minimal sequence containing the four aldolase C isozyme-specific residues (Fig. 3.28 b), further support the possible key role of these amino acids in determining the specific immunogenicity. In fact, the

distinctive cyclic structure of proline's side chain confers an exceptional conformational rigidity to this aa, potentially contributing to determine the surface exposure of the short amino acidic stretch including the 4 above mentioned residues. Taken together, these considerations suggest that a core aa sequence, included within the 85-102 peptide and consisting of about 10 amino acids (spanning from residue 90 to residue 100) could be crucial in determining the recognition specificity demonstrated by the 9F and 2A mAbs toward the aldolase C protein.

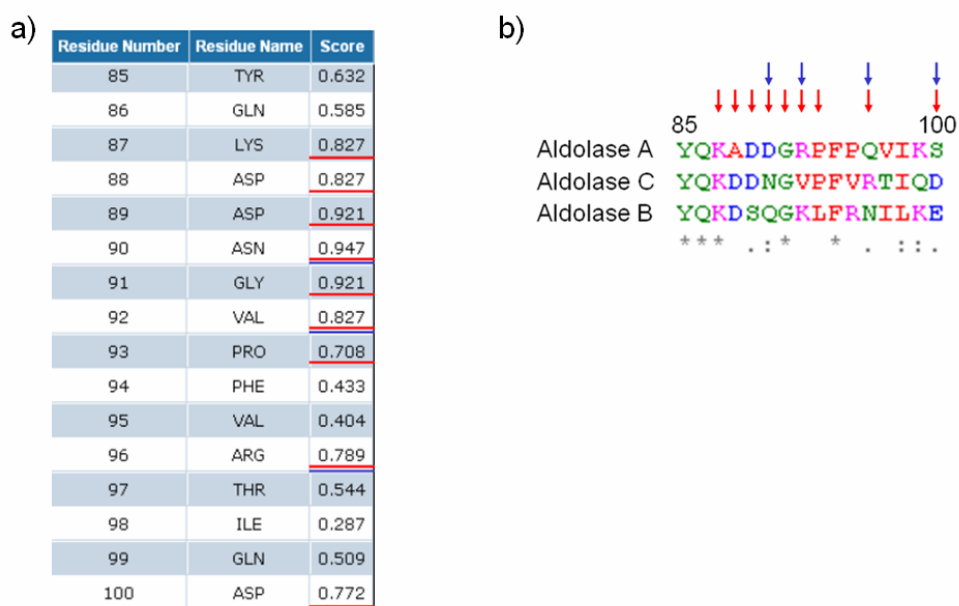


Fig. 3.28. a) *Protrusion Index* scores assigned by *ElliPro* to each aa included between residues 85 and 100 of the human aldolase C protein. b) sequence alignment between residues 85-100 of the three human aldolase isoforms. Red lines and arrows indicate residues with a protrusion index higher than 0.7. Blue lines and arrows highlight aldolase C specific residues.

Although the 85-102 aa region of the aldolase C protein contains these isozyme-specific residues, the epitope localization within an N-terminal region of the protein was surprising since most of the aldolase C isozyme-specific residues are located in the C-tail of the protein. Considering that the isozyme-specific residues are believed to determine the specific functions of each isoform, the availability of these novel antibodies to investigate the physiological functions of aldolase C may also provide important clues on its isozyme-specific roles, since the C-tail of aldolase C is not involved, in this case, in the antibody binding. On the other hand, the presence of the four aldolase C isozyme-specific residues (Asn 90, Val 92, Arg 96, Asp 100) in the epitope-containing region 85-102 also suggests the intriguing possibility that this N-terminal region of the protein may contribute to determine the aldolase C isozyme-specific functions. Future studies involving this specific protein region will help to clarify this aspect.

From a reactivity point of view, it is also important to point out that, although the 9F and 2A mAbs were raised against the human protein, they were found to recognize also the aldolase C enzyme of mouse and rat origin, as demonstrated by immunoblot experiments performed on Neuro2a and PC12 cell lysates and on mouse tissues protein extracts (Figures: 3.2; 3.14 a; 3.15). Consequently, they specifically target multiple aldolase C orthologs without showing undesired cross-reactivity to aldolase A and B paralogs.

The overall data obtained from the multi-disciplinary approach applied in this study to characterize the 9F and 2A mAbs can be reviewed in the following main points:

- i) The two antibodies specifically recognize the aldolase C isozyme and do not show any cross-reactivity with the other aldolase isoforms (aldolase A and aldolase B).

- ii) Both the antibodies recognize an epitope localized within amino acids 85-102 of the protein.
- iii) They perform efficiently in immunoblots and ELISA applications and are able to recognize the aldolase C protein in the denatured form as well as in the native one.
- iv) They detect the aldolase C protein of at least human, mouse and rat origin.
- v) The 9F mAb demonstrate a very good efficiency also in the immunoprecipitation application.
- vi) The presence of four aldolase C isozyme-specific residues within the epitope-containing region 85-102 suggests the intriguing hypothesis that this N-terminal peptide stretch might be involved in the isozyme-specific functions of the protein.

In conclusion, two novel, non-commercial anti-human aldolase C monoclonal antibodies were characterized. Their high specificity and broad range of application make them suitable as tools for research involving this emblematic brain-specific isozyme, potentially contributing to increase our knowledge about its physiological roles in the CNS.

Chapter 4

CONCLUSIONS

Fructose 1,6-bisphosphate aldolase is a constitutive glycolytic enzyme. It plays a central role in the pathway since it catalyzes the reversible cleavage of Fru 1,6-P2 to G3P and DHAP. Vertebrates express three tissue-specific isoforms of aldolase, namely: aldolase A, which is the ubiquitous form of the enzyme predominantly expressed in muscle; aldolase B, which is expressed mainly in the liver, where it is involved in the utilization of exogenous fructose; and aldolase C, which is selectively expressed in the CNS and in tissues of neuronal origin.

The aim of this study was to gain insights into the physiological functions of aldolase C in the CNS, since it is still far from being completely understood.

The aldolase C protein is always expressed together with aldolase A in the CNS but, unlike the latter, it shows a peculiar stripe-like distribution pattern in different areas of the human, mouse and rat brain. The glycolytic role of aldolase C is not considered sufficient to explain its peculiar expression in well delimited regions of the CNS nor to justify its co-expression with aldolase A, since the two isoforms catalyze the same glycolytic reaction with comparable kinetics.

This scenario suggests that, besides its glycolytic function, aldolase C might play additional roles in the CNS (i.e., it may “moonlight”). However, only a few hypotheses have been proposed regarding these possible additional roles (Buono et al., 2001; Canete-Soler et al., 2005; Slemmer et al., 2007; Staugaitis et al., 2001), and they need to be validated through studies of independent groups.

In addition, the lack of suitable tools hampers the study of the “moonlight” properties of aldolase C.

In this context, the present PhD study was designed to: A) identify new aldolase C interactors, in the attempt to find clues as to its physiological role in the

CNS; B) characterize new, non-commercial anti-human aldolase C monoclonal antibodies (mAbs), since no specific anti-aldolase C mAbs were available when this study began.

By applying a functional proteomic approach, a novel molecular interactor of aldolase C was identified: the 14-3-3 γ protein. The interaction was first found through a mass spectrometry-based approach and, subsequently, validated by immunoblotting analysis. The 14-3-3 γ protein belongs to the 14-3-3 protein family, which is a family of ubiquitous proteins abundant in the brain. They are adapter proteins involved in the modulation of many biological processes including cell cycle, apoptosis, ion channel localization and activity, and they are intimately involved in mediating neuronal differentiation (Aitken, 2006; Fu et al., 2000; Hermeking and Benzinger, 2006; MacNicol et al., 2000). Interestingly, both 14-3-3 proteins and neuronal aldolases were found to bind the 3' UTR NF-L mRNA and affect the stability of the transcript (Canete-Soler et al., 2005; Ge et al., 2007). These observations suggested that the interaction between aldolase C and the 14-3-3 γ protein might serve a functional purpose in NF-L mRNA physiology, and also raised the possibility that these proteins are involved in the complex pathogenesis of neurodegeneration. Indeed, the fine regulation of NF-L mRNA expression, stability and turnover is essential in maintaining neuronal homeostasis and alterations in these processes are often associated to altered neurofilament assembly and neurodegeneration (Bergeron et al., 1994; Canete-Soler et al., 1999; Ge et al., 2005; Strong et al., 2005; Xu et al., 1993).

Since the ability to bind RNA was an unexpected activity of aldolase C and considering that it has been reported in two studies carried out by the same research group (Canete-Soler et al., 2005; Stefanizzi and Canete-Soler, 2007) but not yet verified by others, we investigated the interaction between this brain-

specific isozyme and the NF-L mRNA to further explore this unconventional RNA-binding ability of aldolase C.

Both our *in vivo* protein-RNA co-immunoprecipitations and *in vitro* protein-RNA binding tests supported the presence of aldolase C within a complex interacting with the NF-L mRNA. However, importantly, our results of UV cross-linking and EMSA experiments, performed by incubating the recombinant GST-aldolase C protein with a radiolabeled NF-L mRNA probe, suggested that no direct interaction occurs between this brain-specific isozyme and the transcript. Therefore, the interaction between aldolase C and the NF-L mRNA might be indirect and possibly mediated by one or more binding partner(s) (e.g. the 14-3-3 γ protein). Additional experiments will help to address this point and also to clarify the possible functional role of aldolase C in the NF-L mRNA physiology.

Nevertheless, the presence of aldolase C within a complex interacting with the NF-L mRNA supports its involvement in processes underlying the complex pathogenesis of neurodegeneration. As yet there are no data that suggest aberrant aldolase C expression or accumulation in pathological aggregates in neurodegenerative disorders. Consequently, further investigation might provide important insights into the aldolase C protein physiopathology.

Concerning the interaction between aldolase C and the 14-3-3 γ protein, it is important to consider that this protein-protein interaction may exert additional biological roles other than its possible function in NF-L mRNA physiology. Indeed, the involvement of 14-3-3 proteins in a broad spectrum of cellular functions is well recognized. Interestingly, preliminary results obtained in this PhD project suggest a possible role of aldolase C in NGF-induced neuronal differentiation, in which 14-3-3 proteins are also implicated. In particular, the response of aldolase C protein expression after NGF-stimulation of PC12 cells was investigated in this study. The experiments revealed that aldolase C was significantly upregulated after the

addition of NGF to cells, which implicates aldolase C in NGF-induced differentiation. This finding might reflect a boost of glycolysis during neuronal differentiation, thus indicating that aldolase C might represent a marker of differentiation. However, intriguingly, the 14-3-3 protein family is also intimately involved in mediating the NGF-stimulated response (MacNicol et al., 2000) and, in particular, the 14-3-3 γ isoform is strongly upregulated after NGF-induced differentiation in PC12 cells (Angelastro et al., 2000; Greene and Angelastro, 2005). Consequently, given the aldolase C-14-3-3 γ interaction and the concomitant upregulation of the two proteins after NGF-administration in PC12 cells, we are tempted to speculate that they might also cooperate in modulating the cellular response to this trophic factor.

The role of aldolase C in both NF-L mRNA physiology and NGF-stimulated neuronal differentiation remains to be clarified, but the results obtained in this project provide evidence of the involvement of this brain-specific enzyme in processes different than glycolysis and lay the ground for further investigations of the role of aldolase C in these neuronal specific processes.

The recent availability of novel, non-commercial anti-aldolase C monoclonal antibodies will hopefully contribute to the advance of research on aldolase C. These antibodies, which were not available when this study begun, were subsequently obtained and fully characterized in the second part of this project. A specialized company (ProMab Biotechnologies, Inc.) was commissioned to produce them and provided two anti-human aldolase C mAbs. In this study, the specificity of these antibodies for the aldolase C isozyme was investigated and a complete epitope-mapping was performed. The experiments demonstrated that the two novel anti-aldolase C mAbs specifically recognize the aldolase C isoform and both target an epitope localized between residues 85 and 102 of the human protein. Notably, the epitope localization between residues 85-102 was surprising,

since most of the aldolase C isozyme-specific residues are located in the C-tail of the protein. On the other hand, the presence of 4 conserved aldolase C isozyme-specific residues (Asn-90, Val-92, Arg-96, Asp-100) within the 85-102 aa region raised the intriguing hypothesis that this N-terminal peptide stretch of aldolase C might also be involved in the isozyme-specific functions of the protein; it will be interesting to further investigate this possibility in the future.

Importantly, beside not showing cross-reactivity with the two paralogs, aldolases A and B, these antibodies recognize not only the human aldolase C protein but also the mouse and rat orthologs. Moreover, the antibodies were validated for use in multiple applications including western blot, immunoassay (ELISA) and immunoprecipitation.

Given these results, it is conceivable that the two novel anti-aldolase C mAbs will help to gain insights into the pathophysiology of this brain-specific isozyme.

In conclusion, this study revealed a novel molecular interactor of aldolase C, produced evidence supporting the involvement of this brain-specific isozyme in the context of two neuronal-specific processes (the NF-L mRNA physiology and the NGF-induced neuronal differentiation), and resulted in novel specific anti-aldolase C mAbs to be used as tools for investigations on this brain protein.

BIBLIOGRAPHY

- Ahn, A.H., Dziennis, S., Hawkes, R., and Herrup, K. (1994). The cloning of zebrin II reveals its identity with aldolase C. *Development* 120, 2081-2090.
- Aitken, A. (2006). 14-3-3 proteins: a historic overview. *Seminars in cancer biology* 16, 162-172.
- Albrecht, T., Greve, B., Pusch, K., Kossmann, J., Buchner, P., Wobus, U., and Steup, M. (1998). Homodimers and heterodimers of Pho1-type phosphorylase isoforms in *Solanum tuberosum* L. as revealed by sequence-specific antibodies. *European journal of biochemistry / FEBS* 251, 343-352.
- Angelastro, J.M., Klimaschewski, L., Tang, S., Vitolo, O.V., Weissman, T.A., Donlin, L.T., Shelanski, M.L., and Greene, L.A. (2000). Identification of diverse nerve growth factor-regulated genes by serial analysis of gene expression (SAGE) profiling. *Proceedings of the National Academy of Sciences of the United States of America* 97, 10424-10429.
- Arai, T., Hasegawa, M., Akiyama, H., Ikeda, K., Nonaka, T., Mori, H., Mann, D., Tsuchiya, K., Yoshida, M., Hashizume, Y., *et al.* (2006). TDP-43 is a component of ubiquitin-positive tau-negative inclusions in frontotemporal lobar degeneration and amyotrophic lateral sclerosis. *Biochemical and biophysical research communications* 351, 602-611.
- Arakaki, T.L., Pezza, J.A., Cronin, M.A., Hopkins, C.E., Zimmer, D.B., Tolan, D.R., and Allen, K.N. (2004). Structure of human brain fructose 1,6-(bis)phosphate aldolase: linking isozyme structure with function. *Protein science : a publication of the Protein Society* 13, 3077-3084.
- Beernink, P.T., and Tolan, D.R. (1994). Subunit interface mutants of rabbit muscle aldolase form active dimers. *Protein science : a publication of the Protein Society* 3, 1383-1391.
- Bergeron, C., Beric-Maskarel, K., Muntasser, S., Weyer, L., Somerville, M.J., and Percy, M.E. (1994). Neurofilament light and polyadenylated mRNA levels are decreased in amyotrophic lateral sclerosis motor neurons. *Journal of neuropathology and experimental neurology* 53, 221-230.
- Berthiaume, L., Tolan, D.R., and Sygusch, J. (1993). Differential usage of the carboxyl-terminal region among aldolase isozymes. *The Journal of biological chemistry* 268, 10826-10835.
- Buono, P., Conciliis, L.D., Izzo, P., and Salvatore, F. (1997). The transcription of the human fructose-bisphosphate aldolase C gene is activated by nerve-growth-factor-induced B factor in human neuroblastoma cells. *The Biochemical journal* 323 (Pt 1), 245-250.
- Buono, P., D'Armiento, F.P., Terzi, G., Alfieri, A., and Salvatore, F. (2001). Differential distribution of aldolase A and C in the human central nervous system. *Journal of neurocytology* 30, 957-965.
- Buono, P., Mancini, F.P., Izzo, P., and Salvatore, F. (1990). Characterization of the transcription-initiation site and of the promoter region within the 5' flanking region of the human aldolase C gene. *European journal of biochemistry / FEBS* 192, 805-811.
- Burd, C.G., and Dreyfuss, G. (1994). Conserved structures and diversity of functions of RNA-binding proteins. *Science* 265, 615-621.
- Buscaglia, C.A., Penesetti, D., Tao, M., and Nussenzweig, V. (2006). Characterization of an aldolase-binding site in the Wiskott-Aldrich syndrome protein. *The Journal of biological chemistry* 281, 1324-1331.

- Campanella, M.E., Chu, H., and Low, P.S. (2005). Assembly and regulation of a glycolytic enzyme complex on the human erythrocyte membrane. *Proceedings of the National Academy of Sciences of the United States of America* *102*, 2402-2407.
- Canete-Soler, R., Reddy, K.S., Tolan, D.R., and Zhai, J. (2005). Aldolases a and C are ribonucleolytic components of a neuronal complex that regulates the stability of the light-neurofilament mRNA. *The Journal of neuroscience : the official journal of the Society for Neuroscience* *25*, 4353-4364.
- Canete-Soler, R., Schwartz, M.L., Hua, Y., and Schlaepfer, W.W. (1998). Stability determinants are localized to the 3'-untranslated region and 3'-coding region of the neurofilament light subunit mRNA using a tetracycline-inducible promoter. *The Journal of biological chemistry* *273*, 12650-12654.
- Canete-Soler, R., Silberg, D.G., Gershon, M.D., and Schlaepfer, W.W. (1999). Mutation in neurofilament transgene implicates RNA processing in the pathogenesis of neurodegenerative disease. *The Journal of neuroscience : the official journal of the Society for Neuroscience* *19*, 1273-1283.
- Carr, D., and Knull, H. (1993). Aldolase-tubulin interactions: removal of tubulin C-terminals impairs interactions. *Biochemical and biophysical research communications* *195*, 289-293.
- Chan, Y., Tong, H.Q., Beggs, A.H., and Kunkel, L.M. (1998). Human skeletal muscle-specific alpha-actinin-2 and -3 isoforms form homodimers and heterodimers in vitro and in vivo. *Biochemical and biophysical research communications* *248*, 134-139.
- Choi, K.H., Lai, V., Foster, C.E., Morris, A.J., Tolan, D.R., and Allen, K.N. (2006). New superfamily members identified for Schiff-base enzymes based on verification of catalytically essential residues. *Biochemistry* *45*, 8546-8555.
- Choi, K.H., Shi, J., Hopkins, C.E., Tolan, D.R., and Allen, K.N. (2001). Snapshots of catalysis: the structure of fructose-1,6-(bis)phosphate aldolase covalently bound to the substrate dihydroxyacetone phosphate. *Biochemistry* *40*, 13868-13875.
- Chung, C.T., Niemela, S.L., and Miller, R.H. (1989). One-step preparation of competent *Escherichia coli*: transformation and storage of bacterial cells in the same solution. *Proceedings of the National Academy of Sciences of the United States of America* *86*, 2172-2175.
- Coffee, E.M., and Tolan, D.R. (2010). Mutations in the promoter region of the aldolase B gene that cause hereditary fructose intolerance. *Journal of inherited metabolic disease* *33*, 715-725.
- Copley, S.D. (2003). Enzymes with extra talents: moonlighting functions and catalytic promiscuity. *Current opinion in chemical biology* *7*, 265-272.
- Davit-Spraul, A., Costa, C., Zater, M., Habes, D., Berthelot, J., Broue, P., Feillet, F., Bernard, O., Labrune, P., and Baussan, C. (2008). Hereditary fructose intolerance: frequency and spectrum mutations of the aldolase B gene in a large patients cohort from France--identification of eight new mutations. *Molecular genetics and metabolism* *94*, 443-447.
- Dougherty, M.K., and Morrison, D.K. (2004). Unlocking the code of 14-3-3. *Journal of cell science* *117*, 1875-1884.
- Droppelmann, C.A., Keller, B.A., Campos-Melo, D., Volkening, K., and Strong, M.J. (2013). Rho guanine nucleotide exchange factor is an NFL mRNA destabilizing factor that forms cytoplasmic inclusions in amyotrophic lateral sclerosis. *Neurobiology of aging* *34*, 248-262.
- Eichele, G. (1989). Retinoic acid induces a pattern of digits in anterior half wing buds that lack the zone of polarizing activity. *Development* *107*, 863-867.

- Esposito, G., Imperato, M.R., Ieno, L., Sorvillo, R., Benigno, V., Parenti, G., Parini, R., Vitagliano, L., Zagari, A., and Salvatore, F. (2010). Hereditary fructose intolerance: functional study of two novel ALDOB natural variants and characterization of a partial gene deletion. *Human mutation* **31**, 1294-1303.
- Esposito, G., Vitagliano, L., Costanzo, P., Borrelli, L., Barone, R., Pavone, L., Izzo, P., Zagari, A., and Salvatore, F. (2004). Human aldolase A natural mutants: relationship between flexibility of the C-terminal region and enzyme function. *The Biochemical journal* **380**, 51-56.
- Faik, P., Walker, J.I., Redmill, A.A., and Morgan, M.J. (1988). Mouse glucose-6-phosphate isomerase and neuroleukin have identical 3' sequences. *Nature* **332**, 455-457.
- Fernandez-Canon, J.M., Hejna, J., Reifsteck, C., Olson, S., and Grompe, M. (1999). Gene structure, chromosomal location, and expression pattern of maleylacetoacetate isomerase. *Genomics* **58**, 263-269.
- Fu, H., Subramanian, R.R., and Masters, S.C. (2000). 14-3-3 proteins: structure, function, and regulation. *Annual review of pharmacology and toxicology* **40**, 617-647.
- Gavin, A.C., Bosche, M., Krause, R., Grandi, P., Marzioch, M., Bauer, A., Schultz, J., Rick, J.M., Michon, A.M., Cruciat, C.M., *et al.* (2002). Functional organization of the yeast proteome by systematic analysis of protein complexes. *Nature* **415**, 141-147.
- Ge, W.W., Volkening, K., Leystra-Lantz, C., Jaffe, H., and Strong, M.J. (2007). 14-3-3 protein binds to the low molecular weight neurofilament (NFL) mRNA 3' UTR. *Molecular and cellular neurosciences* **34**, 80-87.
- Ge, W.W., Wen, W., Strong, W., Leystra-Lantz, C., and Strong, M.J. (2005). Mutant copper-zinc superoxide dismutase binds to and destabilizes human low molecular weight neurofilament mRNA. *The Journal of biological chemistry* **280**, 118-124.
- Greene, L.A., and Angelastro, J.M. (2005). You can't go home again: transcriptionally driven alteration of cell signaling by NGF. *Neurochemical research* **30**, 1347-1352.
- Greene, L.A., and Tischler, A.S. (1976). Establishment of a noradrenergic clonal line of rat adrenal pheochromocytoma cells which respond to nerve growth factor. *Proceedings of the National Academy of Sciences of the United States of America* **73**, 2424-2428.
- Hatakeyama, T., Okada, M., Shimamoto, S., Kubota, Y., and Kobayashi, R. (2004). Identification of intracellular target proteins of the calcium-signaling protein S100A12. *European journal of biochemistry / FEBS* **271**, 3765-3775.
- Hawkes, R., and Herrup, K. (1995). Aldolase C/zebrin II and the regionalization of the cerebellum. *Journal of molecular neuroscience : MN* **6**, 147-158.
- Hejtmancik, J.F., Wingfield, P.T., Chambers, C., Russell, P., Chen, H.C., Sergeev, Y.V., and Hope, J.N. (1997). Association properties of betaB2- and betaA3-crystallin: ability to form dimers. *Protein engineering* **10**, 1347-1352.
- Hermeking, H., and Benzinger, A. (2006). 14-3-3 proteins in cell cycle regulation. *Seminars in cancer biology* **16**, 183-192.
- Hess, D.T., and Voogd, J. (1986). Chemoarchitectonic zonation of the monkey cerebellum. *Brain research* **369**, 383-387.
- Ho, Y., Gruhler, A., Heilbut, A., Bader, G.D., Moore, L., Adams, S.L., Millar, A., Taylor, P., Bennett, K., Boutilier, K., *et al.* (2002). Systematic identification of protein complexes in *Saccharomyces cerevisiae* by mass spectrometry. *Nature* **415**, 180-183.
- Izzo, P., Costanzo, P., Lupo, A., Rippa, E., Paoletta, G., and Salvatore, F. (1988). Human aldolase A gene. Structural organization and tissue-specific

- expression by multiple promoters and alternate mRNA processing. *European journal of biochemistry / FEBS* 174, 569-578.
- Kanzaki, M., and Pessin, J.E. (2001). Insulin-stimulated GLUT4 translocation in adipocytes is dependent upon cortical actin remodeling. *The Journal of biological chemistry* 276, 42436-42444.
- Kao, A.W., Noda, Y., Johnson, J.H., Pessin, J.E., and Saltiel, A.R. (1999). Aldolase mediates the association of F-actin with the insulin-responsive glucose transporter GLUT4. *The Journal of biological chemistry* 274, 17742-17747.
- Kao, S., Jaiswal, R.K., Kolch, W., and Landreth, G.E. (2001). Identification of the mechanisms regulating the differential activation of the mapk cascade by epidermal growth factor and nerve growth factor in PC12 cells. *The Journal of biological chemistry* 276, 18169-18177.
- Kawamoto, Y., Akiguchi, I., Nakamura, S., and Budka, H. (2004). 14-3-3 proteins in Lewy body-like hyaline inclusions in patients with sporadic amyotrophic lateral sclerosis. *Acta neuropathologica* 108, 531-537.
- Kim, J.H., Lee, S., Lee, T.G., Hirata, M., Suh, P.G., and Ryu, S.H. (2002). Phospholipase D2 directly interacts with aldolase via its PH domain. *Biochemistry* 41, 3414-3421.
- Kishi, H., Mukai, T., Hirono, A., Fujii, H., Miwa, S., and Hori, K. (1987). Human aldolase A deficiency associated with a hemolytic anemia: thermolabile aldolase due to a single base mutation. *Proceedings of the National Academy of Sciences of the United States of America* 84, 8623-8627.
- Kohler, G., and Milstein, C. (1975). Continuous cultures of fused cells secreting antibody of predefined specificity. *Nature* 256, 495-497.
- Kreuder, J., Borkhardt, A., Repp, R., Pekrun, A., Gottsche, B., Gottschalk, U., Reichmann, H., Schachenmayr, W., Schlegel, K., and Lampert, F. (1996). Brief report: inherited metabolic myopathy and hemolysis due to a mutation in aldolase A. *The New England journal of medicine* 334, 1100-1104.
- Kukita, A., Mukai, T., Miyata, T., and Hori, K. (1988). The structure of brain-specific rat aldolase C mRNA and the evolution of aldolase isozyme genes. *European journal of biochemistry / FEBS* 171, 471-478.
- Kumagai, I., Tsumoto, K. (2001). Antigen-Antibody binding. In *Encyclopedia of life sciences* (Nature Publishing Group).
- Kusakabe, T., Motoki, K., and Hori, K. (1997). Mode of interactions of human aldolase isozymes with cytoskeletons. *Archives of biochemistry and biophysics* 344, 184-193.
- Lameire, N., Mussche, M., Baele, G., Kint, J., and Ringoir, S. (1978). Hereditary fructose intolerance: a difficult diagnosis in the adult. *The American journal of medicine* 65, 416-423.
- Lebherz, H.G. (1972). Stability of quaternary structure of mammalian and avian fructose diphosphate aldolases. *Biochemistry* 11, 2243-2250.
- Lebherz, H.G. (1975). Evidence for the lack of subunit exchange between aldolase tetramers in vivo. *The Journal of biological chemistry* 250, 7388-7391.
- Lebherz, H.G., and Rutter, W.J. (1969). Distribution of fructose diphosphate aldolase variants in biological systems. *Biochemistry* 8, 109-121.
- Leclerc, N., Dore, L., Parent, A., and Hawkes, R. (1990). The compartmentalization of the monkey and rat cerebellar cortex: zebrin I and cytochrome oxidase. *Brain research* 506, 70-78.
- Leclerc, N., Gravel, C., and Hawkes, R. (1988). Development of parasagittal zonation in the rat cerebellar cortex: MabQ113 antigenic bands are created postnatally by the suppression of antigen expression in a subset of Purkinje cells. *The Journal of comparative neurology* 273, 399-420.

- Lim, M.L., Lum, M.G., Hansen, T.M., Roucou, X., and Nagley, P. (2002). On the release of cytochrome c from mitochondria during cell death signaling. *Journal of biomedical science* 9, 488-506.
- Lorenzatto, K.R., Monteiro, K.M., Paredes, R., Paludo, G.P., da Fonseca, M.M., Galanti, N., Zaha, A., and Ferreira, H.B. (2012). Fructose-bisphosphate aldolase and enolase from *Echinococcus granulosus*: genes, expression patterns and protein interactions of two potential moonlighting proteins. *Gene* 506, 76-84.
- Lu, M., Ammar, D., Ives, H., Albrecht, F., and Gluck, S.L. (2007). Physical interaction between aldolase and vacuolar H⁺-ATPase is essential for the assembly and activity of the proton pump. *The Journal of biological chemistry* 282, 24495-24503.
- Lu, M., Holliday, L.S., Zhang, L., Dunn, W.A., Jr., and Gluck, S.L. (2001). Interaction between aldolase and vacuolar H⁺-ATPase: evidence for direct coupling of glycolysis to the ATP-hydrolyzing proton pump. *The Journal of biological chemistry* 276, 30407-30413.
- Lu, M., Sautin, Y.Y., Holliday, L.S., and Gluck, S.L. (2004). The glycolytic enzyme aldolase mediates assembly, expression, and activity of vacuolar H⁺-ATPase. *The Journal of biological chemistry* 279, 8732-8739.
- Lundmark, R., and Carlsson, S.R. (2004). Regulated membrane recruitment of dynamin-2 mediated by sorting nexin 9. *The Journal of biological chemistry* 279, 42694-42702.
- MacNicol, M.C., Muslin, A.J., and MacNicol, A.M. (2000). Disruption of the 14-3-3 binding site within the B-Raf kinase domain uncouples catalytic activity from PC12 cell differentiation. *The Journal of biological chemistry* 275, 3803-3809.
- Makeh, I., Thomas, M., Hardelin, J.P., Briand, P., Kahn, A., and Skala, H. (1994). Analysis of a brain-specific isozyme. Expression and chromatin structure of the rat aldolase C gene and transgenes. *The Journal of biological chemistry* 269, 4194-4200.
- Malaspina, A., Kaushik, N., and de Bellerocche, J. (2000). A 14-3-3 mRNA is up-regulated in amyotrophic lateral sclerosis spinal cord. *Journal of neurochemistry* 75, 2511-2520.
- Malay, A.D., Allen, K.N., and Tolan, D.R. (2005). Structure of the thermolabile mutant aldolase B, A149P: molecular basis of hereditary fructose intolerance. *Journal of molecular biology* 347, 135-144.
- Malay, A.D., Prociuous, S.L., and Tolan, D.R. (2002). The temperature dependence of activity and structure for the most prevalent mutant aldolase B associated with hereditary fructose intolerance. *Archives of biochemistry and biophysics* 408, 295-304.
- Marouga, R., David, S., and Hawkins, E. (2005). The development of the DIGE system: 2D fluorescence difference gel analysis technology. *Analytical and bioanalytical chemistry* 382, 669-678.
- Maughan, D.W., Henkin, J.A., and Vigoreaux, J.O. (2005). Concentrations of glycolytic enzymes and other cytosolic proteins in the diffusible fraction of a vertebrate muscle proteome. *Molecular & cellular proteomics : MCP* 4, 1541-1549.
- Monti, M., Orru, S., Pagnozzi, D., and Pucci, P. (2005). Functional proteomics. *Clinica chimica acta; international journal of clinical chemistry* 357, 140-150.
- Morris, R.C., Jr. (1968). An experimental renal acidification defect in patients with hereditary fructose intolerance. II. Its distinction from classic renal tubular acidosis; its resemblance to the renal acidification defect associated with the Fanconi syndrome of children with cystinosis. *The Journal of clinical investigation* 47, 1648-1663.

- Motoki, K., Kitajima, Y., and Hori, K. (1993). Isozyme-specific modules on human aldolase A molecule. Isozyme group-specific sequences 1 and 4 are required for showing characteristics as aldolase A. *The Journal of biological chemistry* 268, 1677-1683.
- Mukai, T., Yatsuki, H., Masuko, S., Arai, Y., Joh, K., and Hori, K. (1991). The structure of the brain-specific rat aldolase C gene and its regional expression. *Biochemical and biophysical research communications* 174, 1035-1042.
- Neumann, M., Sampathu, D.M., Kwong, L.K., Truax, A.C., Micsenyi, M.C., Chou, T.T., Bruce, J., Schuck, T., Grossman, M., Clark, C.M., *et al.* (2006). Ubiquitinated TDP-43 in frontotemporal lobar degeneration and amyotrophic lateral sclerosis. *Science* 314, 130-133.
- Novotny, J., Handschumacher, M., Haber, E., Bruccoleri, R.E., Carlson, W.B., Fanning, D.W., Smith, J.A., and Rose, G.D. (1986). Antigenic determinants in proteins coincide with surface regions accessible to large probes (antibody domains). *Proceedings of the National Academy of Sciences of the United States of America* 83, 226-230.
- O'Reilly, G., and Clarke, F. (1993). Identification of an actin binding region in aldolase. *FEBS letters* 321, 69-72.
- Obsilova, V., Silhan, J., Boura, E., Teisinger, J., and Obsil, T. (2008). 14-3-3 proteins: a family of versatile molecular regulators. *Physiological research / Academia Scientiarum Bohemoslovaca* 57 Suppl 3, S11-21.
- Odievre, M., Gentil, C., Gautier, M., and Alagille, D. (1978). Hereditary fructose intolerance in childhood. Diagnosis, management, and course in 55 patients. *Am J Dis Child* 132, 605-608.
- Pagliaro, L., and Taylor, D.L. (1992). 2-Deoxyglucose and cytochalasin D modulate aldolase mobility in living 3T3 cells. *The Journal of cell biology* 118, 859-863.
- Paoletta, G., Buono, P., Mancini, F.P., Izzo, P., and Salvatore, F. (1986). Structure and expression of mouse aldolase genes. Brain-specific aldolase C amino acid sequence is closely related to aldolase A. *European journal of biochemistry / FEBS* 156, 229-235.
- Penhoet, E.E., Kochman, M., and Rutter, W.J. (1969). Molecular and catalytic properties of aldolase C. *Biochemistry* 8, 4396-4402.
- Penhoet, E.E., and Rutter, W.J. (1971). Catalytic and immunochemical properties of homomeric and heteromeric combinations of aldolase subunits. *The Journal of biological chemistry* 246, 318-323.
- Penhoet, E.E., and Rutter, W.J. (1975). Detection and isolation of mammalian fructose-diphosphate aldolases. *Methods in enzymology* 42, 240-249.
- Pezza, J.A., Choi, K.H., Berardini, T.Z., Beernink, P.T., Allen, K.N., and Tolan, D.R. (2003). Spatial clustering of isozyme-specific residues reveals unlikely determinants of isozyme specificity in fructose-1,6-bisphosphate aldolase. *The Journal of biological chemistry* 278, 17307-17313.
- Pierce, T.S. *Antibody Production and Purification Technical Handbook*.
- Ponomarenko, J., Bui, H.H., Li, W., Fussedner, N., Bourne, P.E., Sette, A., and Peters, B. (2008). ElliPro: a new structure-based tool for the prediction of antibody epitopes. *BMC bioinformatics* 9, 514.
- Popovici, T., Berwald-Netter, Y., Vibert, M., Kahn, A., and Skala, H. (1990). Localization of aldolase C mRNA in brain cells. *FEBS letters* 268, 189-193.
- Qiu, W., Zhuang, S., von Lintig, F.C., Boss, G.R., and Pilz, R.B. (2000). Cell type-specific regulation of B-Raf kinase by cAMP and 14-3-3 proteins. *The Journal of biological chemistry* 275, 31921-31929.

- Reddy, V.M., and Suleman, F.G. (2004). Mycobacterium avium-superoxide dismutase binds to epithelial cell aldolase, glyceraldehyde-3-phosphate dehydrogenase and cyclophilin A. *Microbial pathogenesis* 36, 67-74.
- Rocchi, M., Vitale, E., Covone, A., Romeo, G., Santamaria, R., Buono, P., Paoletta, G., and Salvatore, F. (1989). Assignment of human aldolase C gene to chromosome 17, region cen----q21.1. *Human genetics* 82, 279-282.
- Rose, I.A., O'Connell, E.L., and Mehler, A.H. (1965). Mechanism of the Aldolase Reaction. *The Journal of biological chemistry* 240, 1758-1765.
- Rottmann, W.H., Deselms, K.R., Niclas, J., Camerato, T., Holman, P.S., Green, C.J., and Tolan, D.R. (1987). The complete amino acid sequence of the human aldolase C isozyme derived from genomic clones. *Biochimie* 69, 137-145.
- Rutter, W.J. (1960). *Aldolase* (Academic Press, N.Y.).
- Rutter, W.J. (1964). Evolution of Aldolase. *Federation proceedings* 23, 1248-1257.
- Sambrook, J., Fritsch, E.F., and Maniatis, T. (1989). *Molecular Cloning - A Laboratory Manual*, 2 edn (Cold Spring Harbor Laboratory Press).
- Santer, R., Rischewski, J., von Weihe, M., Niederhaus, M., Schneppenheim, S., Baerlocher, K., Kohlschutter, A., Muntau, A., Posselt, H.G., Steinmann, B., et al. (2005). The spectrum of aldolase B (ALDOB) mutations and the prevalence of hereditary fructose intolerance in Central Europe. *Human mutation* 25, 594.
- Schindler, R., Weichselsdorfer, E., Wagner, O., and Bereiter-Hahn, J. (2001). Aldolase-localization in cultured cells: cell-type and substrate-specific regulation of cytoskeletal associations. *Biochemistry and cell biology = Biochimie et biologie cellulaire* 79, 719-728.
- Slemmer, J.E., Haasdijk, E.D., Engel, D.C., Plesnila, N., and Weber, J.T. (2007). Aldolase C-positive cerebellar Purkinje cells are resistant to delayed death after cerebral trauma and AMPA-mediated excitotoxicity. *The European journal of neuroscience* 26, 649-656.
- Sluchanko, N.N., and Gusev, N.B. (2010). 14-3-3 proteins and regulation of cytoskeleton. *Biochemistry Biokhimiia* 75, 1528-1546.
- St-Jean, M., Izard, T., and Sygusch, J. (2007). A hydrophobic pocket in the active site of glycolytic aldolase mediates interactions with Wiskott-Aldrich syndrome protein. *The Journal of biological chemistry* 282, 14309-14315.
- Staugaitis, S.M., Zerlin, M., Hawkes, R., Levine, J.M., and Goldman, J.E. (2001). Aldolase C/zebrin II expression in the neonatal rat forebrain reveals cellular heterogeneity within the subventricular zone and early astrocyte differentiation. *The Journal of neuroscience : the official journal of the Society for Neuroscience* 21, 6195-6205.
- Stefanizzi, I., and Canete-Soler, R. (2007). Coregulation of light neurofilament mRNA by poly(A)-binding protein and aldolase C: implications for neurodegeneration. *Brain research* 1139, 15-28.
- Strom, A., Diecke, S., Hunsmann, G., and Stuke, A.W. (2006). Identification of prion protein binding proteins by combined use of far-Western immunoblotting, two dimensional gel electrophoresis and mass spectrometry. *Proteomics* 6, 26-34.
- Strong, M.J., Kesavapany, S., and Pant, H.C. (2005). The pathobiology of amyotrophic lateral sclerosis: a proteinopathy? *Journal of neuropathology and experimental neurology* 64, 649-664.
- Strong, M.J., Volkening, K., Hammond, R., Yang, W., Strong, W., Leystra-Lantz, C., and Shoemith, C. (2007). TDP43 is a human low molecular weight neurofilament (hNFL) mRNA-binding protein. *Molecular and cellular neurosciences* 35, 320-327.

- Swain, M.S., and Lebherz, H.G. (1986). Hybridization between fructose diphosphate aldolase subunits derived from diverse biological systems: anomalous hybridization behavior of some aldolase subunit types. *Archives of biochemistry and biophysics* 244, 35-41.
- Takasaki, Y., Takahashi, I., Mukai, T., and Hori, K. (1990). Human aldolase A of a hemolytic anemia patient with Asp-128----Gly substitution: characteristics of an enzyme generated in *E. coli* transfected with the expression plasmid pHAAD128G. *Journal of biochemistry* 108, 153-157.
- Tano, D., Napieralski, J.A., Eisenman, L.M., Messer, A., Plummer, J., and Hawkes, R. (1992). Novel developmental boundary in the cerebellum revealed by zebrin expression in the *lurcher* (Lc/+) mutant mouse. *The Journal of comparative neurology* 323, 128-136.
- Thaller, C., and Eichele, G. (1990). Isolation of 3,4-didehydroretinoic acid, a novel morphogenetic signal in the chick wing bud. *Nature* 345, 815-819.
- Tolan, D.R., and Penhoet, E.E. (1986). Characterization of the human aldolase B gene. *Molecular biology & medicine* 3, 245-264.
- Tolan, D.R., Schuler, B., Beernink, P.T., and Jaenicke, R. (2003). Thermodynamic analysis of the dissociation of the aldolase tetramer substituted at one or both of the subunit interfaces. *Biological chemistry* 384, 1463-1471.
- Vertessy, B.G., Orosz, F., Kovacs, J., and Ovadi, J. (1997). Alternative binding of two sequential glycolytic enzymes to microtubules. *Molecular studies in the phosphofructokinase/aldolase/microtubule system*. *The Journal of biological chemistry* 272, 25542-25546.
- Volkening, K., Leystra-Lantz, C., Yang, W., Jaffee, H., and Strong, M.J. (2009). Tar DNA binding protein of 43 kDa (TDP-43), 14-3-3 proteins and copper/zinc superoxide dismutase (SOD1) interact to modulate NFL mRNA stability. Implications for altered RNA processing in amyotrophic lateral sclerosis (ALS). *Brain research* 1305, 168-182.
- Wang, J., Morris, A.J., Tolan, D.R., and Pagliaro, L. (1996). The molecular nature of the F-actin binding activity of aldolase revealed with site-directed mutants. *The Journal of biological chemistry* 271, 6861-6865.
- Ward, P.A. (1999). *Monoclonal Antibody Production: A Report of the Committee on Methods of Producing Monoclonal Antibodies*, Institute for Laboratory Animal Research, National Research Council.
- Watanabe, H., Takehana, K., Date, M., Shinozaki, T., and Raz, A. (1996). Tumor cell autocrine motility factor is the neuroleukin/phosphohexose isomerase polypeptide. *Cancer research* 56, 2960-2963.
- Xu, W., Seiter, K., Feldman, E., Ahmed, T., and Chiao, J.W. (1996). The differentiation and maturation mediator for human myeloid leukemia cells shares homology with neuroleukin or phosphoglucose isomerase. *Blood* 87, 4502-4506.
- Xu, Z., Cork, L.C., Griffin, J.W., and Cleveland, D.W. (1993). Increased expression of neurofilament subunit NF-L produces morphological alterations that resemble the pathology of human motor neuron disease. *Cell* 73, 23-33.
- Yao, D.C., Tolan, D.R., Murray, M.F., Harris, D.J., Darras, B.T., Geva, A., and Neufeld, E.J. (2004). Hemolytic anemia and severe rhabdomyolysis caused by compound heterozygous mutations of the gene for erythrocyte/muscle isozyme of aldolase, ALDOA(Arg303X/Cys338Tyr). *Blood* 103, 2401-2403.